ÁN ULTRASTRUCTURAL STUDY OF THE PIG KIDNEY

By

Nahla Fadhil Zynal, BVMS (University of Baghdad)

A thesis submitted to the Faculty of
Veterinary Medicine, University of Glasgow
For the degree of Master of Veterinary Medicine

Department of Veterinary Anatomy,
University of Glasgow.

June, 1986.

C O N T E N T S

ACKNOWLEDGMENTS

I would like to express my gratitude to Professor N.G. Wright, my supervisor, for his guidance, encouragement and helpful discussion throughout the course of this study.

Many thanks to all Technical Staff in the Histology Laboratory (Miss P. Bell, Mr. G. McMillan, Miss K. Leslie and Mr. A. Minto) for their excellent technical assistance.

Thanks are also due to the following :

Dr. D.J. Taylor for providing the initial 38 pigs, Mr. A. Finnie and Mr. A. May for their help concerning photographic matters and Miss P. Hanlon for her secretarial assistance.

Finally, my husband Najat was a constant source of help and sympathy and to him I give a special word of thanks.

S U M M A R Y

Despite intensive research into the structure and function of the mammalian kidney, only a single brief study on the histology of the pig kidney has appeared in the literature. In Chapter 3 of the present work, using 38 pigs of different ages, the basic morphological parameters of the structure of the pig kidney was established. This formed a useful basis for comparison for any future pathological studies in which the pig is used as a model. The kidney specimens used were either perfused with fixative via the renal artery or non-perfused and fixed by immersion. Tissues were then processed for histology, transmission electron microscopy and scanning electron microscopy; throughout the study, particular emphasis was placed on ultrastructure.

The swine kidney was found to be histologically similar to that of other mammals. A most significant finding, however, was the hypercellular mesangium with up to 8, and occasionally as many as 25 contiguous mesangial cells being present within single glomerulus.

The ultrastructural studies of some of these pigs showed electron dense deposits mainly in the mesangial and, in a few cases, subendothelial regions. These mesangial changes warranted further investigation and, in

Chapter 4 of this work, an ultrastructural and immunohistochemical study of 130 clinically normal pigs from different sources (including the initial group of 38 pigs) was carried out. An unexpectedly high number of kidneys (51.5%) showed immunofluorescence deposits of IgA and, to a lesser extent, IgG and IgM. The vast majority of immunofluorescence positive kidneys also showed electron dense deposits in the mesangium. These results indicated a number of distinct similarities with idiopathic mesangial IgA nephropathy (Berger's disease) in man.

KEY TO TABLES

KEY TO ABBREVIATIONS

TEM : Transmission electron microscope (or microscopy).

SEM : Scanning electron microscope (or microscopy).

GBM : Glomerular basement membrane.

GN : Glomerulonephritis.

HE : Haematoxylin and eosin.

KEY TO FIGURES

C H A P T E R 1

INTRODUCTION AND REVIEW OF THE LITERATURE

The mammalian kidneys are paired excretory organs in which waste products are continuously eliminated from the blood. They regulate the fluid and salt balance of the body and thus maintain normal osmotic pressure in the blood and tissues. The kidneys, therefore, have considerable controlling regulatory influence over the blood; they receive approximately 25% of the total cardiac output and convert 20% of the plasma to primitive urine, yet at the same time retaining blood cells and protein in the circulation (Michell, 1983).

The kidneys also have other important functions such as the elimination from the body of foreign chemicals (e.g., drugs, pesticides and food additives), the control of blood pressure and blood sodium through the release of renin by the juxtaglomerular apparatus and the control of erythrocyte production by means of release of erythropoietin.

It is now well accepted that all mammalian kidneys are usually situated retroperitonealy in the sublumber region of the dorsal abdominal wall to the right and left of the median plane; the right kidney is usually somewhat more cranial than the left, more so in the dog and horse and less so in the cat and pig (Nickel et al, 1979).

The colour of the kidneys varies from brownish red to dark bluish red depending upon the amount of blood they contain. They are basically bean-shaped. The carnivores and small ruminants have thick, smooth-surfaced kidneys. Exception to this basic shape is the right kidney of the horse, which is heart-shaped and both kidneys of the ox which are divided into 15-25 lobes by deep fissures.

Depending on the species and the condition of the animal, the kidneys are embedded in a mass of perirenal fat of varying thickness. This is well developed in ruminants, less so in the carnivores, and is least evident in the horse. Each kidney is covered with a tough fibrous capsule which consists of bundles of collagenous, and to a lesser extent, elastic fibres.

The parenchyma of the kidney is divided into an outer, dark cortex and an inner, pale medulla. The cortex is brownish red in colour and has a granular appearance. The external part of the medulla, i.e., the portion nearest the cortex is dark red, almost purple; the internal part of the medulla is lighter, greyish red and shows distinct radial striations. Narrow spikes of medullary tissue radiating into the cortex are known as medullary rays.

The basic architecture of the kidneys of the domestic mammals consists of a varying number of radially arranged lobes, which are not readily apparent, except in the ox. Each separate unit, or renal lobe, comprises a cap-like cortex enclosing the base and sides of a pyramid-shaped medulla. The apex of the pyramid, the renal papilla, is inserted into a cup-shaped end-piece (calyx) of a branch of the ureter.

In the domestic mammals, the cortical and medullary portions of each lobe are fused to varying degree; complete fusion of the cortical tissue of neighbouring lobes results in a kidney with a smooth external surface. Examples include the dog, cat and horse.

Incomplete cortical fusion results in a kidney that is superficially divided by fissures of varying depths as in the ox and marine mammals such as the seal. Likewise, complete fusion of the medullary pyramids occurs in the dog, cat and sheep. Thus in these species there are no calyces, only an expanded end of the ureter, the renal pelvis. In the ox and aquatic mammals the medullary pyramids remain separate, each projecting into its own calyx.

The kidneys receive their blood supply through

the renal arteries, which are short but remarkably large branches of the abdominal aorta. As the main artery approaches the hilus of the kidney different arterial patterns may occur. Thus in the horse, for example, each renal artery gives rise to a number of branches which course over the surface of the kidney before plunging into the deep hilus. From the branches of the renal artery originate the interlobar arteries, which enter the parenchyma between adjacent lobes and radiate towards the cortex. At the corticomedullary junction, each interlobar artery gives rise to a number of arcuate arteries which follow the curvature of the base of the medullary pyramids. From the arcuate arteries arise the small radially disposed interlobular arteries which enter the cortex. In the cortex, the straight interlobular arteries give off afferent arterioles to the renal corpuscles. Each afferent arteriole enters the corpuscle at the vascular pole and breaks up into a spherical network of capillary loops, the renal glomerulus. The smaller (in diameter) efferent arteriole leaves the corpuscle also at the vascular pole (Smith, 1956) and immediately breaks down into a network of peritubular capillaries which drain eventually into the interlobular vein.

The blood supply to the renal medulla demands

special consideration. The arteriolar supply derives from the efferent arterioles of the juxtamedullary glomeruli in the inner cortical zone of the cortex and descends as long straight loops (vasa recta) deep into the medulla; these vessels are in intimate contact with the loops of Henle and eventually empty into the arcuate veins. Various inter-connecting branches exist between the ascending and descending limbs of the vasa recta. It has been found that the only tubules to be supplied entirely by efferent vessels arising from their own glomerulus are the outer cortical subcapsular proximal convoluted tubules (Beeuwkes and Bonventre, 1975).

The kidney of the mammal has fascinated anatomists, clinicians and pathologists for decades. Since the introduction of the modern light microscope and more recently of the transmission and scanning electron microscopes, a vast literature dealing with many diverse aspects of kidney structure has accumulated. It is not possible to review all the histological and ultrastructural features of the mammalian kidney, the literature is now so extensive that this would not be possible; only a brief summary of the major morphologic characteristics of the kidney are now given.

The functional unit of the kidney is the nephron,

an expression first coined by Braus (1929). The essential components of the nephron are the renal or Malpighian corpuscle (glomerulus and Bowman's capsule), the proximal tubule, the loop of the nephron (loop of Henle) and the distal tubule. Collecting tubules and papillary ducts, derived from the embryologically distinct ureteric bud, then deliver the glomerular filtrate to the renal pelvis and/or calyces. Depending on the species, familiarity with the anatomy of the renal corpuscle is an essential prerequisite to the understanding of its pathophysiology and the interpretation of abnormalities detected by light and electron microscopy.

The renal corpuscle has been the subject of considerable anatomic and functional interest since its discovery by the great Italian anatomist Marcello Malpighi (1669) who described it as a curious spherical tufted arrangement of capillaries confined to the renal cortex. From the earliest days of its discovery, increasing knowledge of its structure has been paralleled by changing concepts of structural composition and function. It was not until 200 years later in 1842 that William Bowman showed each corpuscle was enveloped by the expanded end of a renal tubule to form a capsule (Bowman's capsule) around the capillary tuft. The space between the glomerulus and Bowman's capsule that collects the glomerular

filtrate is termed the urinary or, in honour of its discoverer, Bowman's space. Bowman also described the course of the afferent vessel into the glomerulus where it breaks up into two, three, four or even eight branches. Moore (1931) reported that the efferent arteriole of those glomeruli adjacent to the medulla, so called juxtamedullary glomeruli, is larger than that draining the other glomeruli. Later Ljungqvist (1963), in a study of the renal vasculature of man, reported a direct vascular continuity between afferent and efferent arterioles in some of these juxtamedullary glomeruli.

As techniques in light microscopy improved, Gerlach as early as 1845 described cells covering the outer surface of the glomerular capillaries, the visceral epithelium. The currently-held view of the structural complexity of these cells had, however, to await the introduction of electron microscopy. In 1933, Zimmerman introduced the term "mesangium" to denote the supporting tissue for the glomerular capillaries.

Since these early steps in our understanding of mammalian kidney morphology, there have been extensive pioneer investigations of its normal histology and ultrastructure (McGregor, 1929; McManus, 1948; Pease and Baker, 1950; Trabucco and Marquez, 1952;

Mueller et al, 1955; Pease, 1955; Rhodin, 1955; Mueller and Syracuse, 1958).

Most of the progress made in the 1950's in the study of the morphology of the mammalian kidney was due to the technical possibilities offered by the transmission electron microscope (TEM). Pease and Baker (1950) carried out the first TEM studies on the rat kidney. Vincent Hall (1954), however, used more advanced methods and he is now credited with pioneering many of the basic concepts used today regarding the ultrastructure of the renal corpuscle. The detailed structure of the glomerular capillaries have now been investigated with the electron microscope by many workers (Pease and Baker, 1950; Hall, 1953, 1954; Pease, 1955; Rhodin, 1955; Yamada, 1955; Farquhar et al, 1961; Graham and Karnovsky, 1966; Latta, 1970).

It is now clear from the reports in the literature that, in various mammalian species, there appears to be a remarkable similarity of glomerular structure. In spite of some variation in the arrangement of the glomerular capillaries, a general pattern can easily be distinguished (Boyer, 1956; Elias et al, 1960; Murakami et al, 1971; Murakami, 1972). Thus, the afferent arteriole breaks up at the vascular pole of the

glomerular tuft into several lobular branches which run towards the urinary pole. The returning limbs form the efferent arteriole which emerges from the glomerular tuft at the vascular pole close to the afferent vessel.

The basic components that are organized to form each renal glomerulus include the capillary endothelial cell, the mesangial cell embedded in a fibrillar matrix, the glomerular basement membrane (GBM) and the visceral epithelial cell. The latter cells are continuous with the squamous parietal epithelial cells which line Bowman's capsule. The endothelial cells, together with those of the mesangium, account for the greatest number of cells in the glomerular tuft and often increase in numbers in response to various pathologic conditions. A brief description of the major morphologic characteristics of these glomerular structures is now given.

Glomerular endothelial cells :

These cells line the glomerular capillary, the nucleus and main cytoplasmic mass lying usually on the mesangial or axial side of the capillary. These cells are similar to endothelial cells lining capillaries of other parts of the body, except that their attenuated cytoplasm contains large pores or fenestrae, 500-1000^{o}A in diameter (Hall, 1953; Pease, 1955; Farquhar et al,

1961; Churg and Grishman, 1975). Although 60°A thick diaphragms have been observed bridging the fenestrae of mouse glomerular endothelium (Rhodin, 1962), such diaphragms have not been observed in other mammalian species (Farquhar et al, 1961; Latta, 1970). Of importance with regard to the movement of macromolecules across the glomerular filter is the presence of a negatively charged glycocalyx on the plasma membrane of the endothelial cells. This glycocalyx also lines the walls of the fenestrae and is continuous with glycoproteins in the lamina rara interna (Latta and Johnston, 1976).

In the cytoplasm surrounding the nucleus are a few mitochondria, a poorly developed Golgi apparatus, occasional strands of rough-surfaced endoplasmic reticulum and free ribosomes. Vacuoles of different sizes, dense and hyaline droplets and fibrillar elements are also found.

Mesangium :

Since 1933, when Zimmerman introduced the term mesangium to designate the structure that he assumed served as a supporting mesentery for the renal glomerular capillary tuft, the mesangium has been the subject of considerable ultrastructural definition, functional analysis and pathophysiologic evaluation due to its

importance in various glomerulonephropathies. After years of dispute regarding the structural nature of the glomerular mesangium, it is now known to be distinguishable, even with the light microscope, from visceral epithelial and capillary endothelial cells.

The mesangium consists of a population of cells surrounded by varying amounts of a fibrillar matrix (mesangial matrix) (Suzuki, 1959; Suzuki et al, 1963) located in an intercapillary position between the glomerular capillary loops (Yamada, 1955; Jones et al, 1962).

Mesangial cells are now considered to be of two general types, those resident cells permanently sited between the capillaries and those which are derived from circulating monocytes which migrate into the mesangial region. Mesangial cells which are embryologically derived from the vascular ingrowth into the S-shaped metanephric vesicle are stellate in shape and, in some respects, resmeble morphologically smooth muscle cells. They have peripheral myofilaments and dense bodies, a well-developed rough surfaced endoplasmic reticulum and a small number of lysosomes. The circulating mononuclear cells which have also been identified in the renal glomerulus belong to the macrophage line (Striker et al, 1981) and can therefore be considered to be part of the

mononuclear phagocytic system.

Latta and Fligiel (1985) have reviewed the mesangial region and likened it to a branching tree-shaped structure that supports the glomerular capillary network. Blood plasma flows through the mesangial region, in part contributing to glomerular filtration. Some circulating substances are filtered out by the mesangial matrix and may be taken up rapidly by intrinsic mesangial cells or more slowly by monocytes which have infiltrated from the bloodstream. Mesangial cells can act as myofibroblasts that can contract or swell readily; these actions, supplemented by endothelial swelling seem to account for the cessation of glomerular blood flow in renal ischaemia, toxaemia of pregnancy and acute glomerulonephritis.

The mesangium is separated from the glomerular capillary lumen by endothelial cells and its lateral borders are covered by GBM, on the other side of which lies the visceral epithelium. Mesangial cell cytoplasmic processes may insinuate between overlying endothelial cells to reach the lumen of the capillaries (Farquhar and Palade, 1962; Crowell et al, 1974).

Normally, mesangial matrix consists of an amorphous, fibrillar, dense basement membrane-like material

of unknown origin and biochemical composition (Suzuki et al, 1963). It has been suggested that mesangial matrix is formed in part by deposition of old GBM components swept into the mesangium following turnover and renewal of the GBM lining the capillaries (Walker, 1973). Mesangial matrix is considerably increased in certain pathologic conditions.

The functions attributed to mesangial cells include fibrocytic activity, smooth muscle contractility, phagocytosis, action as receptors for selected hormones and peptides, prostaglandin production, synthesis of new mesangial matrix and proliferation in response to injury (Dunihue and Boldosser, 1963; Jones, 1963; Machielsen and Creemers, 1967; Ausiello et al, 1980; Sraer et al, 1980). Schreiner et al (1981) reported that the normal glomerulus contains a sub-population of mesangial cells bearing Ia antigen; they appear to function as immunocompetent cells capable of presenting antigen to lymphocytes in a genetically restricted fashion. Their ability to induce proliferation to T lymphocytes suggests that the glomerulus may play a more active role than formerly believed in developing an in situ immune response to deposited antigen.

The mesangium can therefore be involved in many

pathologic processes of the renal glomerulus as highly specialised pericapillary tissue which is composed of intrinsic resident mesangial cells, resident Ia antigen bearing cells and transient monocytes - macrophages surrounded by an extracellular matrix (Farquhar and Palade, 1962; Stein et al, 1983; Latta and Fligiel, 1985).

Glomerular basement membrane (GBM) :

Glomerular basement membrane is that portion of the glomerular filtration barrier located between endothelial cells and visceral epithelial cells in peripheral portion of capillaries and between mesangial cells and visceral epithelial cells in other portions of the glomerular tuft. No part of the GBM is inserted between endothelial cells and mesangial cells.

Although the GBM appears as a single layer when viewed with light microscopy, it appears to be composed of three layers when examined by TEM (Crowell et al, 1974; Churg and Grishman, 1975). The inner layer, or lamina rara interna, is of low electron density (Farquhar et al, 1961). The middle layer, or lamina densa, consists of an electron-dense mesh work of fibrils that comprises approximately 50% of the thickness of GBM in the normal dog (Crowell et al, 1974). The outer layer, or lamina rara externa, is electron lucent and contains a few

fibrils which course between the lamina densa and the foot processes of visceral epithelial cells (Jorgensen and Bentzon, 1968).

The GBM is negatively charged (Rennke et al, 1975) and the anionic sites have been shown to be present in the lamina rara interna and externa and to consist of glycosaminoglycans, principally heparin sulphate (Karnovsky and Ryan, 1975; Farquhar and Kanwar, 1980).

It is now known that the glomerular filter acts as a charge selective as well as a size selective barrier to macromolecules. Thus circulating anionic proteins are effectively excluded from the glomerular filter (Brenner et al, 1978; Venkatachalam and Rennke, 1978; Kanwar and Farquhar, 1979).

Visceral epithelial cells :

In 1845, Gerlach described some cells which covered the outer aspect of the glomerular capillary tuft and termed them epithelial cells. Since then, they have been studied by many workers and now are recognized as cells with an elaborate layer of primary, secondary and tertiary cytoplasmic processes which extend to the GBM (Osborne et al, 1977). Tertiary cytoplasmic processes are commonly called foot processes (Pease and Baker, 1950).

Foot processes appear to be embedded in the outer aspect of the lamina rara externa of the GBM (Latta, 1973) and are separated from each other by narrow spaces called filtration slits or slit pores (Yamada, 1955). These spaces are not in fact continuous with the urinary space but are bridged by a fine diaphragm, the slit membrane.

In recent years, scanning electron microscopy (SEM) has, without doubt, been the most useful technique in elucidating the complicated morphology of the visceral epithelial cells or podocytes as they are often termed with their interdigitating arrangement of foot processes (Buss and Kronert, 1969; Arakawa, 1970; Fujita et al, 1970; Arakawa, 1971; Andrews and Porter, 1974; Arakawa and Tokunaga, 1974; Andrews, 1975, 1981). The surface membrane of the foot processes, as well as the cell body of the epithelial cell, have a covering of sialoproteins (glycosaminoglycans) (Jones, 1969; Latta, 1970; Karnovsky and Ainsworth, 1972) which complements and extends the overall negative charge of the glomerular filter.

With the transmission electron microscope, the visceral epithelial cell is found to have numerous ribosomal granules either lying free in the cytoplasm or

associated with the rough-surfaced endoplasmic reticulum (Farquhar et al, 1961). The cisternae of the endoplasmic reticulum sometimes contain secretory bodies, considered by Thoenes (1967) to be concerned in the manufacture of basement membrane material. Mitochondria are present particularly near the nucleus, and both microtubules and microfibrils have been described. The microfibrils may be arranged randomly or in dense bundles that may fill the cytoplasm of the foot process. Vesicles of different sizes, some containing dense bodies may be present.

The glomerular (or Bowman's) capsule :

The glomerular capsule is a double-walled envelope surrounding the glomerulus, and is composed of a collagenous basement membrane lined by a squamous epithelium termed the parietal epithelium which is continuous with the visceral epithelial cells reflected over the glomerular capillaries as well as the proximal tubular epithelium. Normally, parietal epithelial cytoplasm is prominent only around the nucleus. Electron microscopic studies of these cells have revealed that they have few cytoplasmic organelles and, apart from sparse mitochondria scattered throughout the cytoplasm, they do not have the intricate organisation of internal

structure which characterises the cells of the proximal tubule with which they are continuous at the urinary pole (Mueller et al, 1955; Yamada, 1955).

Peripolar cells have recently been described by Ryan et al (1979) as distinctive granular forms of parietal cells encircling the vascular pole of the glomerulus. The function of these cells is still in dispute but they may be involved in juxtaglomerular complex activity or they may have some regulatory role on the glomerular filtrate which flows past these cells on its way to the proximal tubule. Until the discovery of peripolar cells Bowman's capsule had generally been assumed to function as a passive container for glomerular filtrate, which is then passed to the proximal tubule (Osborne et al, 1977). The basement membrane of the capsule is continuous with that of the proximal convoluted tubule at the urinary pole while, at the vascular pole, it is reflected over the tuft and is apparently continuous with the GBM (Mueller and Syracuse, 1958). SEM has shown one or two long cilia to arise from near the nucleated centre of each parietal cell; the remainder of the parietal surface is covered with a sparse population of small microvilli which are most numerous along the cell borders (Andrews and Porter, 1974; Spinelli, 1976).

Juxtaglomerular apparatus or complex :

The juxtaglomerular apparatus situated at the hilus of the glomerulus conventionally is considered to consist of four basic elements: (1) the terminal portion of the afferent arteriole; (2) the macula densa, a specialised segment of the distal tubule; (3) the extraglomerular mesangial region and (4) the efferent arteriole of the glomerulus. To these can possibly now be added a fifth component, the peripolar cells.

The juxtaglomerular apparatus can also be separated into vascular and renal tubular components. The vascular component is composed of the afferent and efferent arterioles and the extraglomerular mesangial region; the tubular component is that portion of the distal tubule in contact with the vascular component and includes the macula densa (Barajas, 1970; Barajas, 1971). The extraglomerular mesangial region which has been referred to as the polar cushion (Polkissen) or the juxtaglomerular cell mass, is bounded by the cells of the macula densa, the afferent and efferent glomerular arterioles and the mesangial cells of the glomerular tuft. Within this region there are two basic cell types; the granular extraglomerular mesangial cells (Lacis cells) (Oberling and Hatt, 1960), also referred to as the

granular cells, lie principally in the centre of the extraglomerular mesangium and represent the major cell component of the region. The granular myoepithelial cells, which appear to represent specialised smooth muscle cells, are located within the wall of the afferent and efferent arterioles (Barajas and Latta, 1963; Tisher et al, 1968). Both cell types possess structural characteristics suggestive of smooth muscle origin (Latta et al, 1962), except for the presence of granules in the myoepitheliod cells. These granules are believed to represent the hormone renin or its precursor. Renin has been demonstrated within the juxtaglomerular apparatus through the use of (Barajas and Latta, 1963; Chandra et al, 1965) immunofluorescence and biochemical techniques (Edelman and Hartroft, 1961; Bing and Kazimierczak, 1962). It is thought that the juxtaglomerular apparatus represents a major structural component of the renin-angiotensin system.

The macula densa is a specialised region of the distal tubule adjacent to the hilus of the glomerulus. The cells in this region of the distal tubule are low columnar and exhibit a dense apically placed nucleus. Most of the cell organelles lie beneath the nucleus toward the basal surface of the cell. The basal cell membrane interdigitates with adjacent extraglomerular mesangial cells.

Ovoid mitochondria are numerous (Barajas and Latta, 1963; Tisher et al, 1968). Other cellular organelles including lysosomes, autophagic vacuoles, ribonucleoprotein granules and profiles of smooth and granular endoplasmic reticulum are located near the cell nucleus.

Proximal tubule :

The proximal tubule begins abruptly at the urinary pole of the glomerulus and initially forms several convolutions in the vicinity of the parent glomerulus before descending towards the medulla as a straight segment.

Under normal in vivo conditions the lumen of the proximal tubule is patent (Walker and Oliver, 1941; Gottschalk and Mylle, 1956). However, with interruption of blood supply during preparation for histological studies, the proximal epithelium quickly swells to produce an apparent occlusion of the lumen. For visualization of tubules in a state comparable to that in life, it is necessary to use perfusion fixation or drip fixation onto the surface of the kidney immediately prior to death.

The initial portion of the proximal tubule, the convoluted segment, is usually referred to as the pars

convoluta and the more distal straight segment extending towards the medulla as the pars recta (Tisher, 1981). The pars convoluta is lined by columnar cells and possesses a well-developed brush border. The brush border is made up of a series of microvilli that project into the lumen, these microvilli increase the cellular surface area some 40 times. The rounded nucleus is in a basal position; large numbers of mitochondria and many ribonucleic protein granules are present. Numerous vesicles are seen, particularly in the apical part of the cell and granules and dense bodies may be found in them. At the base of the cell are large numbers of infoldings of the basal plasma membrane. These represent an intimate interlocking of adjacent cells (Maunsbach, 1973) and a device whereby the surface area is increased. The basement membrane of the proximal tubule is continuous with that of Bowman's capsule at the urinary pole and that of the thin descending limb of Henle. The epithelium of the pars recta is cuboidal; the apical cell surface is convex and is covered by a well-developed brush border composed of elongated microvilli. The pars recta is less complex than the pars convoluta and contains fewer basal infoldings, endocytotic vacuoles and mitochondria. In the pars convoluta the mitochondria are arranged perpendicular to the basement membrane, this is

not so apparent as in the pars recta (Maunsbach, 1973).

SEM studies by Andrews and Porter (1974) have shown that, throughout the course of the proximal tubule, irregularly shaped microvilli are found; also present within the initial segment of proximal convoluted tubules are many long and slender tendrils; these tendrils appear to arise from cells on one side of the lumen and end with their tips expanded into variously sized globular masses on the opposite luminal side.

Thin limb of the loop of the nephron : (Loop of Henle)

The sudden transition from the terminal straight portion of the proximal tubule to the thin descending limb of Henle occurs in the medulla. As early as 1898, Zimmerman studying the thin limb cells of several laboratory animals noted that the cells of the early thin descending limb were irregular in configuration and interdigitated freely with one another. Later ultrastructural studies confirmed Zimmerman's light microscopic finding by demonstrating that the cells of the early thin descending limb of Henle were extremely complex because of extensive interdigitation with one another (Rhodin, 1962; Osvaldo and Latta, 1966; Bulger and Trump, 1966).

Both the descending and ascending part of the thin segment as well as the actual loop have a small diameter and are lined by a flattened type of epithelium. They are found in the medulla and are best seen in the papilla. In the latter they are inclose proximity to capillary loops (vasa recta), being separated from them by a small amount of interstitial substance. The close proximity of thin segments to capillaries is of importance in the mechanism of urine concentration.

Under the electron microscope, the epithelium of the thin limbs has a small number of microvilli and few mitochondria. The cytoplasm is flattened, except where it bulges into the lumen at the site of the nucleus (Bulger and Trump, 1966; Osvaldo and Latta, 1966). Infoldings of the plasma membranes occur in the basal region, but this is not as pronounced as in the proximal convoluted segment. Pinocytotic vacuoles are often plentiful.

SEM studies have shown that the thick brush border characterizing proximal tubules ends along a winding margin at the junction with the loop of the nephron and is replaced by a sparse population of small nub-like microvilli. Occasionally, a single cilium protrudes from the centre of thin loop cells (Andrews and

Porter, 1974).

Distal tubule :

The distal tubule is generally considered to be composed of three morphologically distinct segments, the thick ascending limb of Henle (pars recta), the macula densa and the distal convoluted tubule (pars convoluta).

The pars recta, represents the initial portion of the distal tubule and can be divided into medullary and cortical segments (Allen and Tisher, 1976).

Cells throughout the thick ascending limb of Henle contain numerous elongated mitochondria oriented perpendicularly to the basement membrane and enclosed by invaginations of the basal plasmalemma. Each invagination often extends into two-thirds or more of the cell towards the luminal border. The mitochondria resemble those in the proximal tubule but contain extremely prominent matrical granules (Suzuki and Mostoffi, 1967). Other subcellular organelles in this segment of the nephron include a well-developed Golgi complex and abundant quantities of smooth and rough-surfaced endoplasmic reticulum, multivesicular bodies and lysosomes.

SEM studies of the thick ascending limb of the rat kidney has revealed the existence of two distinctly

different patterns of luminal surface structure among the population of cells forming the epithelium of this segment of the nephron. There are cells with a rough surface due to the presence of extensive microvilli and smooth-surfaced cells largely devoid of microvilli except along the apical cell margins (Allen and Tisher, 1976). This difference in luminal surface structure is also evident using TEM. Most cells possess one, and occasionally two, cilia. Throughout the medullary and cortical segments the rough-surfaced cells possess extensive lateral processes radiating from the main cell body. Lateral processes of smooth-surfaced cells are less common than those of the rough-surfaced cells in the inner strip of the outer medulla, but they do increase in number and complexity in the outer strip of the outer medulla and throughout the cortical segment. A predominance of cells with the smooth-surfaced pattern is observed in the medullary segment, whereas those with a rough-surfaced pattern are predominant in the cortical segment (Tisher, 1981).

Although some investigators choose to refer to the macula densa as a specialised region or initial portion of the pars convoluta (Tisher, 1981), recent studies in the rat (Allen and Tisher, 1976) kidney reveal that the macula densa is more accurately viewed as a specialised segment

of the thick ascending limb since, in many instances, the thick ascending limb extends well beyond the vicinity of the macula densa to form a rather abrupt transition with the pars convoluta. A brief description of the cells of the macula densa has already been given.

The convoluted part of the distal tubule begins at a variable distance beyond the macula densa and extends to the region of transition with the initial collecting tubule. Under the light microscope, the cells are cuboidal and contain abundant quantities of elongated mitochondria that are oriented perpendicular to the basement membrane of the tubule. The cells have a convex luminal surface covered with short and blunt microvilli but they lack the well developed brush border which is characteristic of the proximal tubule.

SEM studies have demonstrated that the luminal surface of the cells of the pars convoluta differs from that of the pars recta. There is a marked absence of lateral interdigitation in the apical region between adjacent cells of the pars convoluta. The rather straight lateral cell margins are accentuated by prominent microvilli. The individual cells possess one and occasionally two centrally placed cilia (Andrews and Porter, 1974).

TEM has shown the mitochondria to be elongated, extending from the basal to the apical cell surface and closely aligned with the lateral cell membrane. Lysosomes are common in the cells of the distal convoluted tubule and include cytosomes and multivesicular bodies (Tisher et al, 1968). The Golgi complex is well developed and located principally lateral to the nucleus. The cells contain numerous microtubules and abundant quantities of granular and smooth-surfaced endoplasmic reticulum as well as free ribosomes. The basement membrane is complex, often multilayered and frequently irregular in configuration.

Collecting tubule :

This is not considered to be part of the nephron and, embryologically, is derived from the ureteric bud. In most mammalian kidneys, the collecting tubule can be divided into at least three regions based primarily on their location in the kidney (Myers et al, 1966). These are the cortical collecting segment, the outer medullary segment and the inner medullary segment. The inner medullary segment terminates as the papillary duct, or duct of Bellini, which opens on the surface of the papilla to form the area cribrosa; here, urine is flushed into the pelvis or calyces. On TEM examination, the cortical

collecting ducts of the rat and mouse are made up of dark and light cells (Novikoff, 1960; Rhodin, 1962; Ericsson and Trump, 1969). Throughout the entire collecting duct, the major cell type is the light cell. Electron microscopy has revealed that the lateral cell margins of the light cells, especially in the inner medullary collecting duct, are interrupted by small interlocking processes with adjacent cells. At the base of the cells, small invaginations of the plasmalemma that are usually too small to contain mitochondria are evident. On the luminal cell surface, short blunt microvilli are present that increase in both size and number and acquire a thin glycocalyx in the medulla. The cytoplasm of these cells contain few ribosomes, mitochondria and no microvesicles: few microvilli are present.

A second less common cell in the collecting duct has been termed the intercalated or dark cell. These cells contain large numbers of mitochondria, numerous ribosomes and large numbers of microvesicles in the apical portion with microvilli frequently present on the luminal surface.

As the collecting duct descends through the medullary ray to the tip of the papilla, the individual cuboidal light cells gradually increase in height, finally

becoming columnar (Myers et al, 1966; Trump and Bulger, 1968; Le Furgey and Tisher, 1979).

With SEM, Andrews and Porter (1974) described two distinct cell types lining the collecting tubules. One cell type is characterized by a lack of surface microprojections and by the presence of one and occasionally two central cilia. The second cell type possesses a cilium, is usually covered with a moderate number of large microprojections and often projects into the collecting tubule lumen more so than the other cell type.

Papillary ducts and renal pelvis or calyces :

As the collecting ducts approach the renal papilla, they are succeeded by larger papillary ducts which open on the surface of the papilla as tiny slit-like openings, the papillary foramina, through which urine enters the renal pelvis. The papillary foramina perforate the surface of the renal papilla forming the area cribrosa. The papillary ducts are lined by columnar epithelium. As they increase in diameter their lining cells become taller and at the renal papilla, in some species, to stratified columnar cells.

It is obvious from the literature that the papillary ducts and their connection with the renal pelvis or calyces

have received scant attention by microscopists. The renal pelvis is a muscular pouch lined with transitional epithelium and in continuity with the ureter below and in some species the calyces above. The calyces are spaces also clothed with transitional epithelium into which the medullary papillae project. The number of calyces is variable and this depends on the number of papillae. The horse, sheep and carnivores do not possess a system of calyces; they do, however, have a renal pelvis (Nickel et al, 1979).

Huker and Frenzel (1975) have concentrated their SEM investigations on the epithelial surface speciatisations of the renal papillae and calyces of the human kidney. They reported a polygonal shaped epithelium covering the surface of the human papillae. Bleb-like microprojections and prominent cell borders were also seen.

Carrol et al (1974), using the rat as a model, observed with the SEM two types of opening on the tip of each renal papillae, either large slits or small pores.

The swine kidney :

Despite intensive research into the structure and function of the mammalian kidney, relatively little

attention has been paid to the anatomy of the swine kidney, despite the fact that, with its internal structure composed of a fused cortex with separate medullary pyramids, it is structurally more similar to that of man than the kidneys of other domesticated or laboratory mammals. The pig kidney, as described in some anatomy text books (Getty, 1975; Nickel et al, 1979) are smooth externally and have several medullary pyramids indicating only partial fusion of their lobes. They are bean-shaped, flattened dorsoventrally and may occasionally have shallow grooves on their surface. They are brown to greyish brown and their average weight is 200-280 gm. Pigs in good condition have a considerable amount of perirenal fat.

The renal cortex in the pig is thick and the medulla is often only one-half to two-thirds the cortical width. The medullary rays are easily seen but the renal columns are not conspicuous. The apices of the medullary pyramids form either single or aggregate papillae. The single papillae are small and conical, the larger aggregate papillae are irregular elevations resulting from the fusion of 2-5 different pyramids. There are 8-12 papillae per kidney (Nickel et al, 1979).

Yadava and Calhoun (1958), reporting a comparative

light microscopic study of the kidneys of domestic animals, described the pig renal corpuscle as pear-shaped and they also stated that the pig juxtamedullary renal corpuscles were larger than their cortical ones.

Regarding the proximal convoluted tubule of the pig, they mentioned that it was lined by simple truncated pyramidal cells whose cytoplasm was coarsely granular. The nuclei usually were basal, the luminal contour irregular and the brush border formed a separate cluster for each cell. They described the loop of Henle as lined by flattened epithelial cells. They went on to report that the cells of the descending limb of Henle's loop were similar to those of the proximal tubule, while the structure of the ascending limb was similar to that of the distal tubule. The distal tubules were lined by cuboidal epithelium, a brush border was absent and the basal striations not distinct. The macula densa was closely associated with the juxtaglomerular cells. The cells forming the macula densa were single-layered and appeared slightly taller than the rest of the cells of the distal tubules. The cytoplasm was faintly stained around the nucleus and contained a few fine granules.

The lumen of the straight collecting tubule of the pig had a regular contour and was lined by a simple

cuboidal epithelium which become somewhat wider and taller towards the papillary duct. Also they reported that the general structure of the papillary duct resembled that of the straight collecting tubule but the diameter and epithelial height were greater in the former. The papillary duct was lined by a simple tall columnar epithelium which become transitional near the opening of the duct at the tip of the papilla. The transitional epithelium of the papillary duct was continuous with the epithelium of the papilla. The epithelium of the papillary duct changed abruptly from a simple to transitional type. The transitional epithelium of the calyx was reflected over the sides of the papilla.

Other reports involving the pig kidney include that of Martin-Dupont and Camber (1981) who affirmed by a sieving method that juxtamedullary glomeruli of the pig are larger than that of the cortical ones. Graham (1953) and Peciffer (1968) described the renal pelvis of pig as being composed of a flattened structure from which two major calyces arise, each subdivided into several smaller branches, the minor calyces, which receive the urine from the renal papillae. There appeared to be eight or more calyces and each calyx may accommodate two or three papillae.

In view of the paucity of literature on the normal structure of the pig kidney, particularly the ultrastructure of the nephron, it was considered worthwhile to carry out a histological and ultrastructural study of the normal pig kidney. In order to add to the existing brief anatomical and histological information, particular attention was placed on its appearance under TEM and more especially the SEM.

As part of this section of the work, an opportunity arose to study, albeit briefly, glomerular morphogenesis in a litter of 10 newborn piglets. This was considered worthwhile as very little reported work in the literature on mammalian glomerular morphogenesis took the pig as a model. A brief review of the literature on the development of the mammalian glomerulus now follows.

Postnatal development of the mammalian glomerulus :

Although the general differentiation of the metanephric nephron in mammals is generally of similar pattern (Schreiner, 1902), there are some differences in the various species concerning the stage of maturation of the nephron at birth. Thus in man, and several other mammals with a long gestatory period, the definitive number of mature nephrons is already present at birth. In mammals such as the rat, mouse and rabbit, on the other

hand (whose intrauterine life is rather short), the kidney of the newborn is still apparently foetal, and nephrogenesis continues for several days (Peter, 1927; Gersh, 1937; Boss et al, 1962; Kazimierczak, 1963).

The formation of the mammalian nephron proceeds in a centrifugal pattern so that the oldest and most mature nephrons are located in the juxtamedullary area and the youngest ones in the superficial cortex. Now, more than 120 years after William Bowman in 1842 described the renal glomerulus as a group of capillary loops lying within the dilated end of a urinary tubule, there is still controversy not only as to the manner in which the glomerulus develops but also as to the source of its capillaries.

In early studies of the development of the mammalian nephron, it was considered that the metanephric vesicle, during its differentiation, first becomes a comma-shaped body with the tail always directed away from the collecting tubule. By further irregular growth in length, the comma forms the S-shaped body, the upper two limbs of which become the convoluted tubules and loop of Henle while the lower limb becomes the Malpighian or renal corpuscle. The lower part of the wall of the lower limb eventually forms the parietal epithelium of the

renal corpuscle or Bowman's capsule. The upper part of the wall of the lower limb contributes to the formation of the glomerulus (Herring, 1900). A somewhat similar description was also given by Ribbert (1900). Reinhoff (1922), however, did not distinguish a metanephric vesicle and regarded the differentiation of the nephrogenic tissue to begin from the S-shaped body.

Edwards (1951) and Trabucco and Marquez (1952) reported that, in the newborn human infant, only a narrow zone of glomeruli at the cortico-medullary junction have a functional blood supply and that the afferent arterioles of all other glomeruli are blindly ending cords of cells. The latter workers reported that the afferent arteriole, on penetrating Bowman's capsule, divided into multiple finger-like capillaries. These elongated and gradually re-converged to form a single vessel, the efferent arteriole, which emerged from the renal corpuscle at the vascular pole.

In most mammals, nephrogenesis is not complete at birth, resulting in a relatively lower functional efficiency of the kidney in newborn animals than in adults (Nash and Edelmann, 1973).

Interest in the structure of the postnatal developing mammalian kidney has received new impetus in

recent years with the development of improved techniques for studying tissues with the TEM. When the development of the electron microscope made it possible to distinguish cell structures not previously possible with light microscope, interest in the pattern of development of the glomerulus gained momentum and several new studies were carried out.

At the ultrastructural level, the development of single nephron segments has been studied to varying extent. Thus, glomerular development has been extensively described in mice (Clark, 1957), rats (Suzuki, 1959), humans (Vernier and Birch-Andersen, 1962, 1963; Aoki, 1966) and dogs (Hay and Evan, 1979). On the other hand, the ultrastructure of the developing proximal tubule has been investigated systematically only in rats (Larsson and Maunsbach, 1975).

The current discussion of the early development of the glomerulus seems to have been largely stimulated by Hall and Roth (1956) and Kurtz (1958). These workers reported that the earliest glomerular structures consist of solid masses of cells with two outer layers arranged concentrically around a central group showing no discernible organization. They also reported that the outer most layer flattened and separated from the inner layer to produce the capsular or urinary space and that

the inner layer gradually forms complex folds and processes which penetrate between the capillaries that have formed in the central mass. They believed, erroneously, that within the cytoplasm of the individual cells of the central mass, vesicles appear which fuse to form mature capillaries.

In a recent ultrastructural (SEM and TEM) study of glomerulogenesis in the rat, Kazimierczak (1980) described five successive arbitrarily selected stages of glomerular differentiation. In stage I, a capillary loop penetrates between the lower limb and the middle segment of the S-shaped body. In stage II, the capillary undergoes a first subdivision, establishing the primitive lobulation of the glomerulus. In stage III, the vascular and urinary poles differentiate. In stage IV, the glomerulus assumes the aspect of a spherical body and the capillaries in each lobule undergo subdivision. In stage V, the glomerular vascular pattern approaches its adult appearance.

The study of mammalian nephrogenesis has received further impetus in recent years with the development of SEM. Spinelli (1976) reported a SEM study on the developing renal glomerulus of rats and he stated that the earliest structure in the development of the glomerulus is

the nephrogenic vesicle which develops through the inductive action of the terminal ampullae of the growing collecting ducts. A group of cells belonging to the blastemal cap of the ampullae separate out and arrange themselves concentrically to form a vesicle. The lateral wall of the vesicle becomes depressed at its lower end to form a transverse cleft which extends upwards inside the vesicular lumen. The cleft is bounded on its upper side by the convexity of the prospective tubular segment and on its lower side by the concavity of the prospective visceral epithelial cell layer. The lower wall of the cleft and the medial wall of the vesicle are separated by the lumen of the vesicle which is reduced to such an extent that both cell layers are almost touching each other. The medial wall of the vesicle soon flattens to become the parietal epithelium of Bowman's capsule. The outer wall of the vesicle consists of cuboidal epithelium of the visceral epithelial layer. Then, in further development, the cuboidal visceral epithelial cells become flattened and start to give off cytoplasmic processes which form a coat around and between the capillaries. The terminal processes of the immature podocytes are normally irregular and of varying thickness.

The only other SEM report is that of Kazimierczak (1980) who described, in the developing rat kidney, the

SEM features of five successive stages starting from the S-shaped to a glomerulus approaching the adult appearance.

Postnatal development of the pig kidney :

Despite the extensive literature on the postnatal development of the mammalian kidney, little work has been done on nephrogenesis in pigs.

The occurrence of transient proteinuria in the newborn piglet within the first 48 hours after onset of colostrum ingestion (Baintner, 1970; Loh, 1970; Loh et al, 1972; Martinsson, 1972; Bergelin and Karlsson, 1973, 1974, 1975; Carlsson et al, 1974) has, however, stimulated some workers to pose the question whether or not neonatal preteinuria in the pig is due to some anomaly of the developing nephron (Bergelin and Karlsson, 1973, 1974). This has led to an investigation of the microscopical structure and ultrastructure of the glomerular filtration barrier and the proximal tubule during development of both foetal and neonatal porcine kidney. In the pig, whose gestation period is about 112 days (Poplewski, 1947), nephrogenesis at birth is not complete though presumably it is in its final stages since only a narrow subcapsular layer of the cortex exhibits signs of immaturity (Bing and Kazimierczak, 1964).

Friis (1980) has also reported that, in the newborn piglet, a thin nephrogenic zone is present in the outer one fourth of the cortex. The nephrons showed a gradient in the degree of development with the mature nephrons in the juxtamedullary area and the immature nephrons towards the capsule. He divided the development of the nephron into five successive stages : stage I comprised the renal vesicle and stage II corresponded to the S-shaped body. Stage III represented the immature renal corpuscle. In stage IV, the corpuscle was larger and contained more patent capillary loops than in stage III. In stage V, the glomerular capillaries were fully developed and patent. He also reported that the formation of nephrons continued up to about 3 weeks of age; after this time the nephrogenic zone had disappeared.

From the available literature it is apparent that most of the studies carried out on postnatal development of the pig glomerulus are rather fragmentary and much information has still to be established. The purpose of this section of the work was to obtain further histological and ultrastructural information about glomerular morphogenesis in the pig kidney and to lay special emphasis on SEM.

CHAPTER 2

GENERAL MATERIALS AND METHODS

Materials and Methods :

1. Source of kidney material :

For the study of normal kidney structure, 38 kidney specimens all from clinically normal pigs and with no macroscopic lesions on visual inspection were used.

The age of the pigs ranged from a litter of 10 newborn piglets to 25 three to five month old animals to three adult sows and they were obtained from two separate sources a) Glasgow University Veterinary School Cochno Farm and b) a commercial pig dealer near Glasgow. Apart from a litter of newborn piglets which were killed at one hour (3 animals), one week (2 animals), two weeks (2 animals), four weeks (2 animals) and six weeks (1 animal) after birth by an intravenous injection of a 20% solution of sodium pentobarbitone (Euthatal, May and Baker, U.K.), all the remaining pigs were destroyed by electrical stunning followed by exsanguination. At necropsy, the kidneys were removed immediately and processed as described below.

In addition, a number of kidneys were fixed by a perfusion method (see below) and arterial and ureteral casts were prepared from others (see Table 2:1).

2. Light microscopic studies :

Small blocks of cortex, medulla, ureter and urinary bladder were fixed in 10% buffered neutral formalin (BNF) for five days and subsequently post-fixed for a maximum of two days in mercuric chloride formal. Samples were then dehydrated, cleared and impregnated with paraffin wax in a histokine automatic processor (Shandon Elliot, Runcorn, Cheshire).

Sections 2-3μm thick were cut and routinely stained with haematoxylin and eosin (HE). The sections were examined using a Leitz Laborlux 12 microscope. Black and white photomicrographs were taken using 35mm Eastman fine grain release positive 5302 film in a wild Mps 51S automatic camera; the film was developed in PQ universal and fixed in Ilford hypam fixer. Prints were made on Agfa-Gavaert Rapitone photographic papers P1 - P4 using an Agfa-Gavaert Rapitone PD 3700 automatic processor.

3. Transmission electron microscopic studies :

Small portions of kidney cortex and medulla were minced in Karnovsky's fixative (paraformaldehyde/ glutaraldehyde) and kept at $4^{o}C$ for a minimum of two hours. The samples were then washed in 0.1 M cacodylate buffer

for one hour and post-fixed in 1% osmium tetroxide. Specimens were then washed with three changes of distilled water. A graded series of acetone (70%, 90%, 100%) were used to dehydrate the tissue which was subsequently placed in propylene oxide/EMix resin (EMscope, Ashford, Kent) (50 : 50) for one hour, EMix resin for four hours; the specimens were then embedded in the resin and polymerised at 60° C overnight.

Using glass knives prepared by an LKB knife maker (LKB, Croydon, Surrey), the blocks were trimmed with an LKB pyramitome and sections of the renal cortex or medulla were cut at one μm. The sections were collected from the knife edge using a pair of fine forceps and placed in a droplet of water on a glass slide. They were then stained with toluidine blue and viewed with a Leitz Laborlux II microscope. Suitable areas were then selected for ultrathin sectioning. Each block was finally trimmed and then transferred to a LKB III ultramicrotome.

Sections of a silver or pale yellow colour 60-90nm thick were gathered by means of a collecting boat containing water. The sections were flattened using trichloroethylene vapour, picked up on polaron 300 copper mesh grids, stained with uranyl acetate and lead citrate and viewed with a Joel 100 CX II electron microscope.

Electron micrographs were taken using Ilford technical EM film plates 3.1/4 x 4.3/4, developed in PQ universal and fixed in Ilford hypam fixer. The prints were developed and fixed as described for light microscopy.

4. Scanning electron microscopic studies :

Slices of cortex and medulla, approximately 10mm x 5mm x 2mm were gently washed in 0.1 M cacodylate buffer in order to remove surface blood and then immersed in Karnovsky's fixative (paraformaldehyde/glutaraldehyde) for 24 hours. The slices were trimmed to expose surfaces to be scanned and then washed in 0.1 M cacodylate buffer for four hours before dehydration with a series of acetone (70%, 90%, 100%), and finally left in 100% acetone overnight. The specimens were then dried in a polaron critical point dryer. Dried specimens were mounted on ½ surface polaron Cambridge type specimen mounts, painted with Agar Aids drying silver paint and coated with gold/palladium for four minutes using an Emscope sputter coater (EMscope, Ashford, Kent). The stubs were viewed in a Philips 501 B scanning electron microscope.

Scanning electron micrographs were taken using Ilford FP4 medium speed black and white film placed in a steinheil trace-recording camera oscillophot M4, attached to the microscope. The film was developed in Ilford

hypam fixer. The prints were developed and fixed as described for light and transmission electron microscopy.

5. Kidney casts :

a) Arterial casts :

Corrosion casts of kidney were prepared by inserting a cannula (12 gauge needle) into the renal artery and flushing out the renal circulation with phosphate buffered saline (PBS, pH 7.3) (approximately 100ml at room temperature at a flow rate of 2ml/min.), 25-40ml of a mixture of tensol cement and No.7 component A and B (I.C.I. Plastics Division, Welwyn Garden City, Herts, England) in a ratio 25/1 was then injected slowly through the cannula (0.1ml cement/gm kidney weight). When filling was complete, the kidney was transferred to an incubator at 37°C for four hours and then placed in 30% solution of potassium hydroxide (KoH) for two days. Once the digestion process was completed, the kidney was placed in a bath of running water in order to remove any crystalized KoH. After drying at 37°C overnight, the kidneys were carefully removed for examination with the SEM as described above.

b) Casts of proximal ureter and calyces :

A cannula (12 gauge needle) was inserted into the

proximal end of the ureter and casting proceeded as for the vascular casts, (0.15ml cement/gm kidney weight was found to be adequate).

6. Kidney perfusion method :

Immediately after death, the kidneys were exposed and any perirenal was removed and the renal artery was identified. A cannula (12 gauge needle) was inserted into the renal artery and, depending on the size of the kidney, 30-35ml of Karnovsky's fixative was slowly injected manually at a flow rate of 2-3ml/min. Prior to the start of perfusion, the renal vein was clamped and when the fixative was seen to emerge from the vein, the clamp was removed and the venous blood and fixative was allowed to escape. The perfusion procedure lasted approximately 5 minutes. At this time, the kidney was blanched and hard to the touch. Selected specimens of cortex and medulla were then removed from the kidney for light or electron microscopy (TEM and SEM).

TABLE 2:1 Number of kidneys cast and amount of tensol cement used

Pig No.	Amount of tensol cement		Kidney Weight
	Left Kidney	Ureter	
PK 1	25 ml	5 ml	170 gm
PK 2	25 ml	5 ml	170 gm
PK 3	25 ml	5 ml	170 gm
PK 4	20 ml	4 ml	110 gm
PK 5	20 ml	4 ml	110 gm
PK 6	40 ml	7 ml	200 gm
PK 7	40 ml	7 ml	200 gm

C H A P T E R 3

A MORPHOLOGIC STUDY OF THE KIDNEYS OF 38 PIGS, WITH PARTICULAR EMPHASIS ON ULTRASTRUCTURE

Introduction :

In Chapter 1, it was pointed out that, despite the voluminous literature on various aspects of mammalian renal architecture, very little information is available pertaining to the pig kidney.

The purpose of the present section of the work was to carry out a combined histological and ultrastructural study of the kidneys of clinically normal pigs. In Part I of the Chapter, the kidneys of young and adult pigs were studied and, in Part II, a sequential investigation of nephrogenesis in ten newborn piglets was carried out.

Materials and methods :

In Part I of the study the kidneys from three adult sows and 25 three to five month old pigs were studied. The animals were killed and exsanguinated and the kidneys processed for histological and ultrastructural examination as detailed in Chapter 2. In addition, arterial and ureteral casts were prepared from seven young adult pig kidneys, again as described in Chapter 2.

In Part II of the work, the kidneys from a litter of 10 newborn piglets were studied.

Results :

a) Part I : Morphologic features of young adult and adult pig kidneys.

Macroscopic features :

The kidneys were pale brown in colour, smooth-surfaced bean-shaped, elongated and flattened dorsoventrally (Fig. 3.1); in a few younger animals shallow clefts were sometimes observed on the surface. They were symmetrically positioned retroperitoneally on each side of the median plane at the level of the first four lumber vertebrae; their average weight was 110-120gm. A considerable amount of perirenal fat was found surrounding each kidney and each was enclosed by a connective tissue capsule.

The renal artery and nerves entered the kidney and the renal vein left at the hilum, a concavity on the medial border. The hilum was continuous with the renal sinus, a large fat filled cavity surrounded by the parenchyma of the kidney. The ureter enlarged within the renal sinus to form the renal pelvis which in turn divided into two major calyces; these gave off 8-12 smaller units, the minor calyces. Each calyx formed a cylindrical attachment around a conical projection of renal medulla, a renal papilla.

Fig. 3.1 Pig kidney showing its smooth-surfaced outline.

Fig. 3.2 Section of pig kidney. Note the fused confluent cortex and separate medullary pyramids.

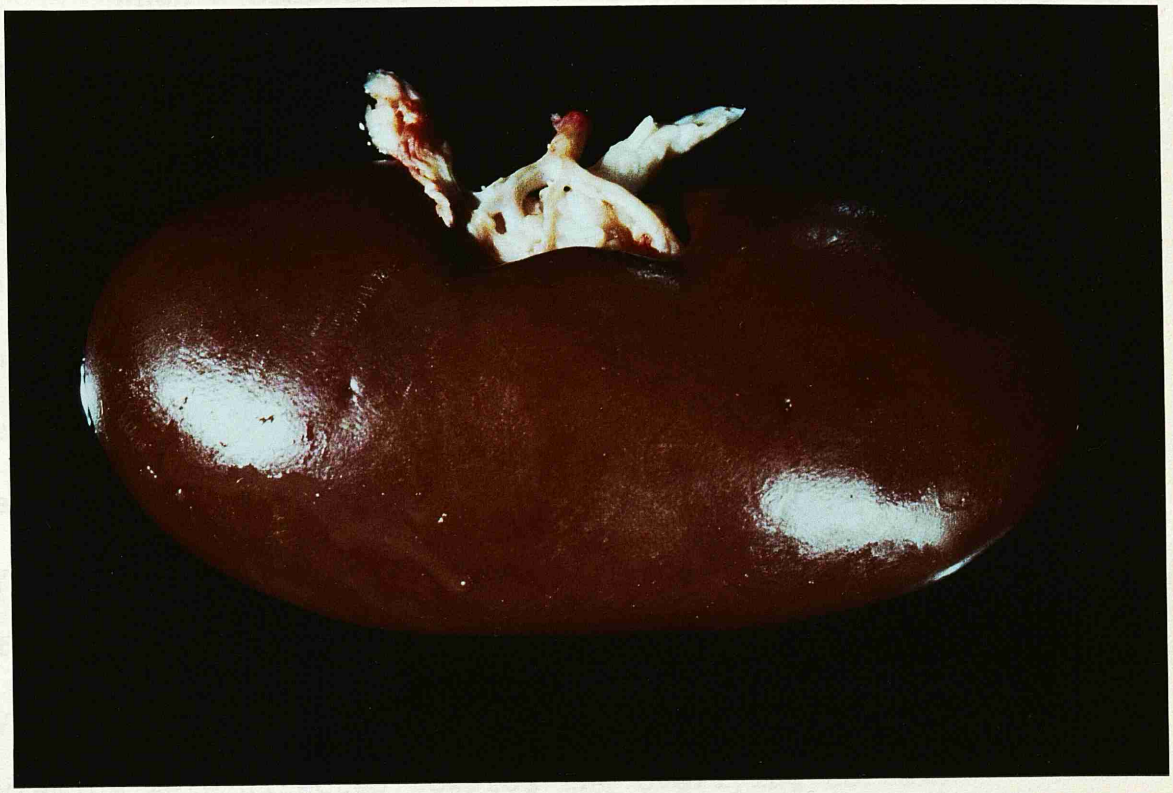

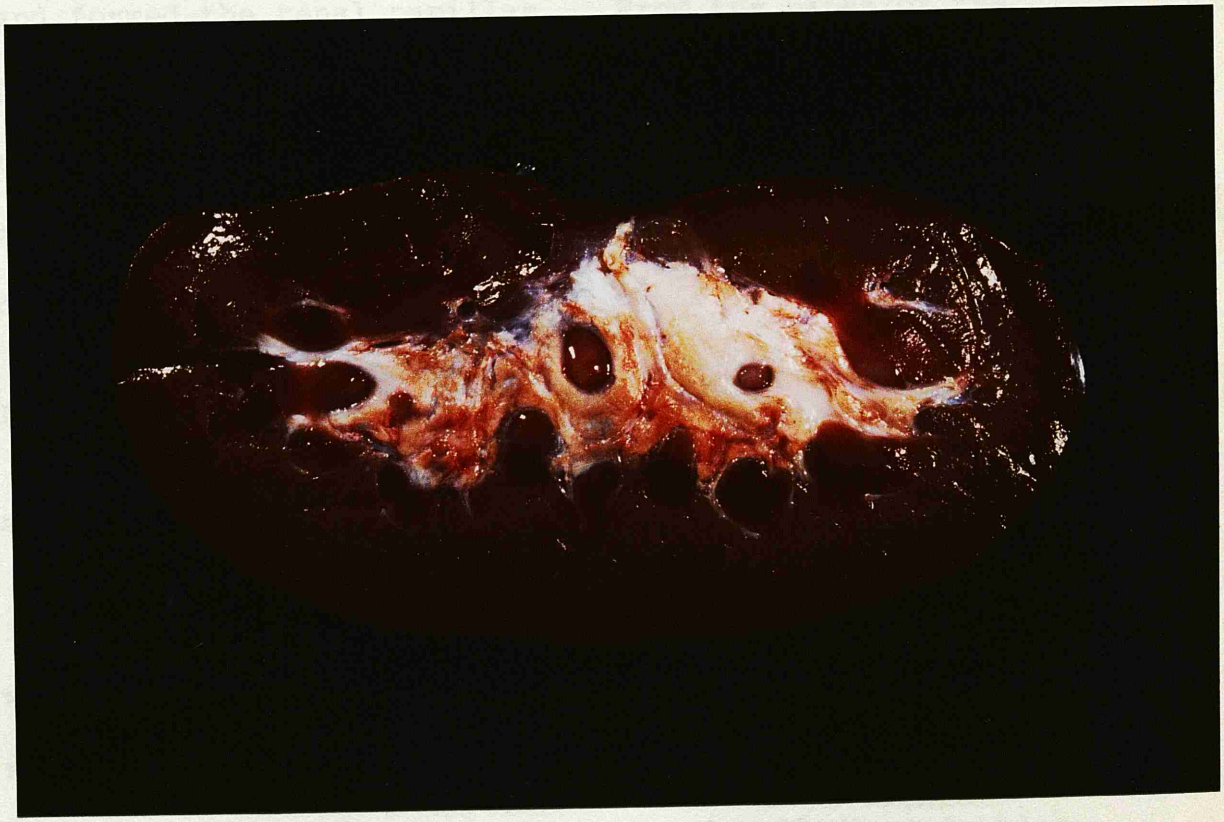

When a hemisection of the pig kidney was examined (Fig. 3.2), the kidney parenchyma can be seen to be arranged into two distinct regions. The outer region, the cortex, was darker, thicker, had a granular appearance and formed a continuous layer beneath the capsule. The inner region, or medulla, was paler, smoother and consisted of from 8-12 cone-shaped structures, the medullary pyramids, which are separated from each other by inward extensions of cortical tissue. The portions of cortex that passed between and separated adjacent pyramids constituted a renal column. The bases of the pyramids were directed towards the overlying cortex, while their apices were oriented towards the renal sinus and formed the renal papillae. From the bases of the pyramids, groups of tubules extended into the overlying cortex giving it a striated appearance. These striations represented a continuation of medullary tissue into the cortex and are referred to as medullary rays.

Light microscopic findings :

A: General :

On lower power observations, the cortex of the kidney was composed of renal corpuscles, various types of tubule and interlobular blood vessels. The medullary rays containing cortical loops of Henle and collecting tubules

Fig. 3.3 Low power view of the renal cortex showing medullary rays (arrows). HE x 65.

Fir. 3.4 A renal corpuscle showing the afferent arteriole (arrow) arising from an interlobular artery. HE x 120.

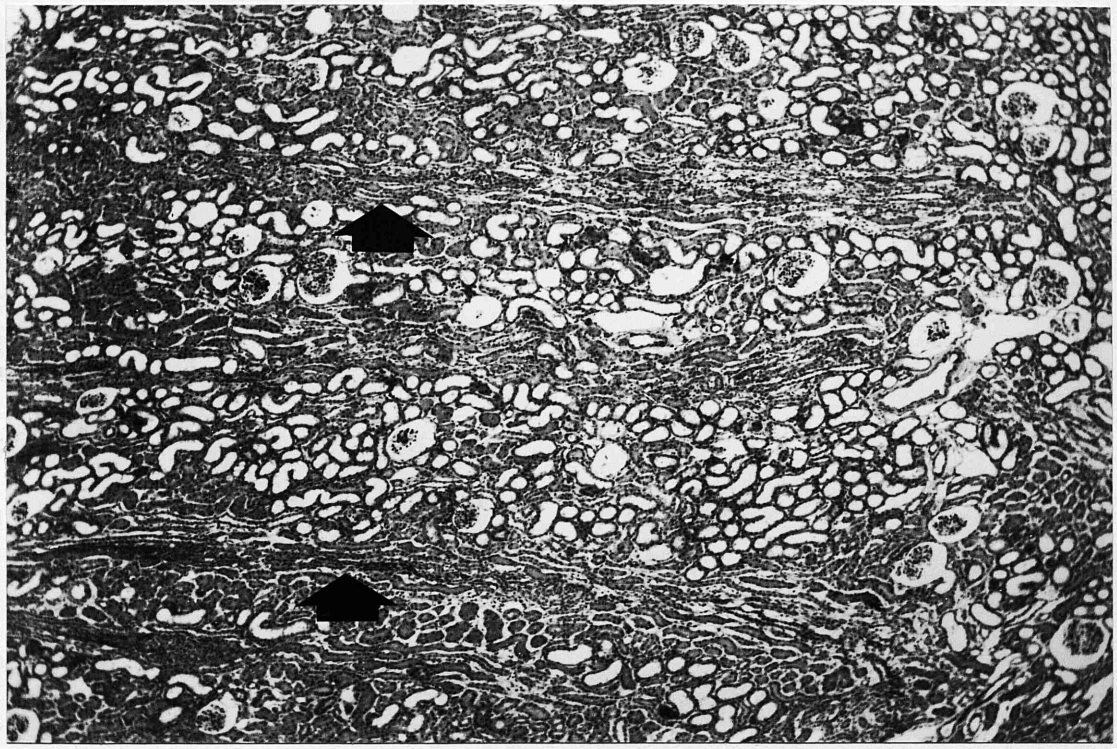

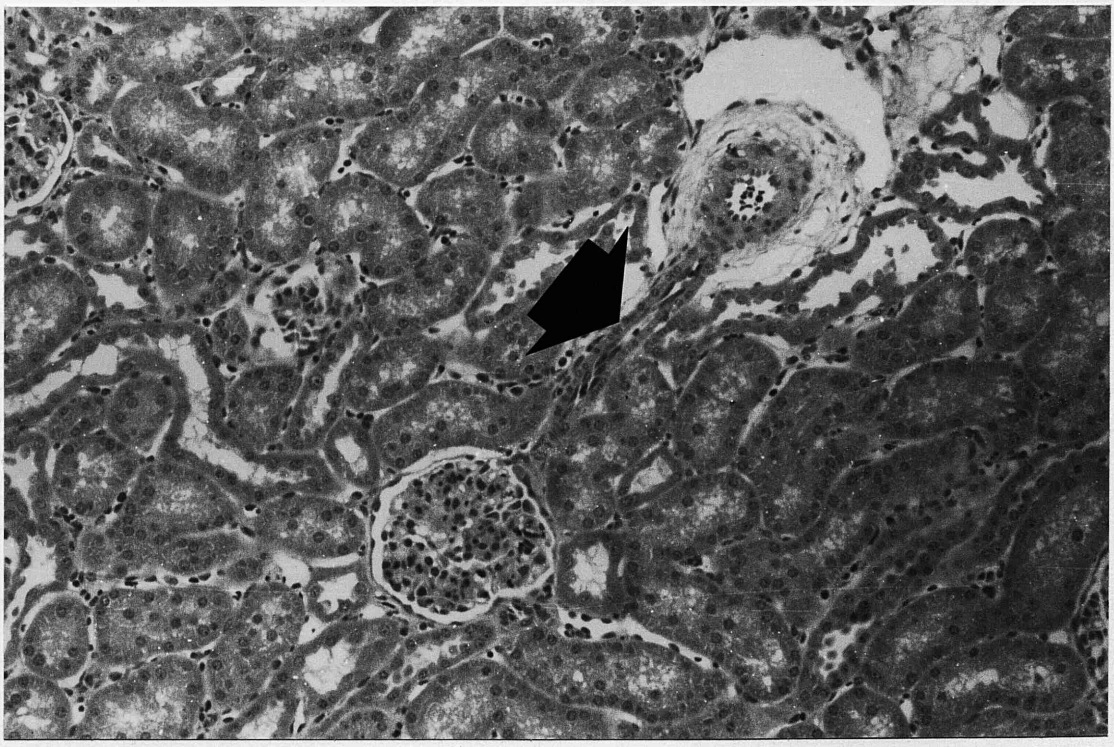

could be seen penetrating the cortex at the cortico-medullary junction and extending throughout the cortex (Fig. 3.3).

At higher magnification, the appearance of the normal renal corpuscle is illustrated in Fig. 3.4. It was composed of a branched capillary tuft, the glomerulus, surrounded by a capsule called Bowman's capsule. The capillary tuft arose from an afferent arteriole which is a branch of the interlobular artery; the capillaries then re-united at the vascular pole to form the efferent arteriole.

The urinary pole, at the opposite side of the corpuscle, was where the lumen of the urinary or Bowman's space was continuous with the lumen of the proximal convoluted tubule and where the squamous parietal epithelium was continuous with the columnar epithelium of the proximal convoluted tubule (Fig. 3.5). The urinary or Bowman's space consisted of a clear zone between Bowman's capsule and the visceral epithelium of the glomerular tuft. A more detailed account of the histology of the pig kidney now follows.

B: The renal glomerulus :

In all cases, the outer cortical glomeruli were

Fig. 3.5 Non-perfused renal corpuscle showing both vascular pole and macula densa (small arrow), and urinary pole (large arrow). Capillary loops are not clearly visible. Bowman's capsule is lined by flattened parietal cells. Note the surrounding proximal tubules (1) and distal tubules (2). HE x 300.

Fig. 3.6 Perfused kidney showing two glomeruli with patent capillary loops. Note the distended urinary space and tubules. HE x 170.

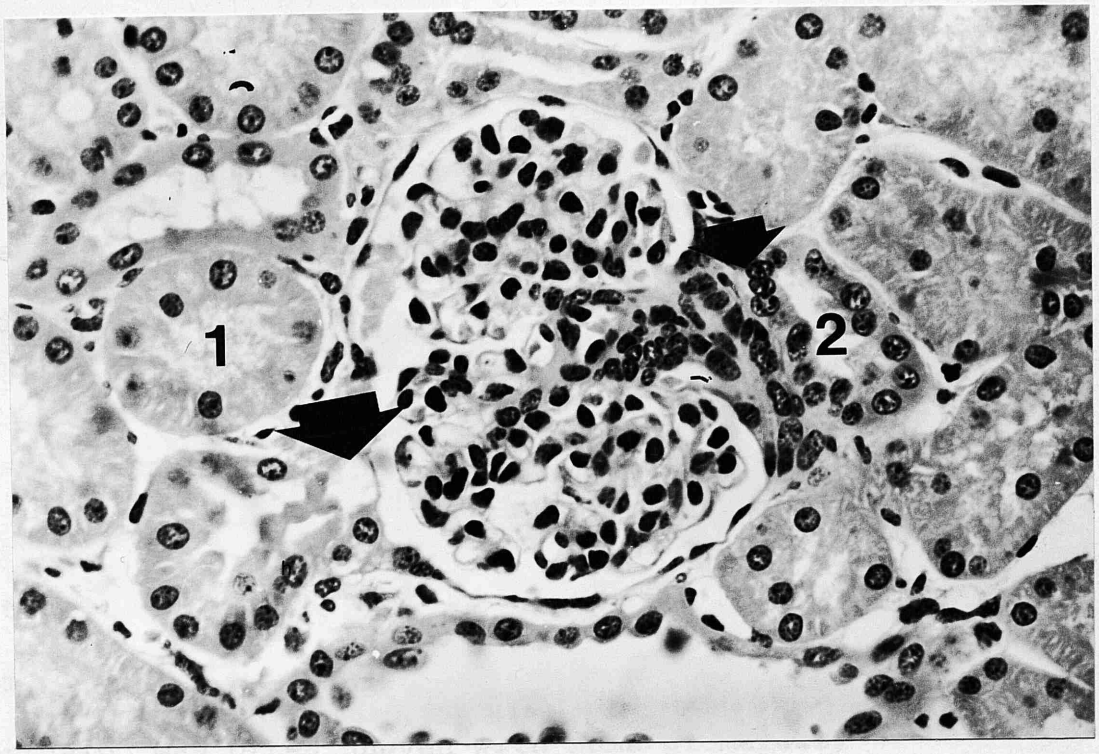
1
2

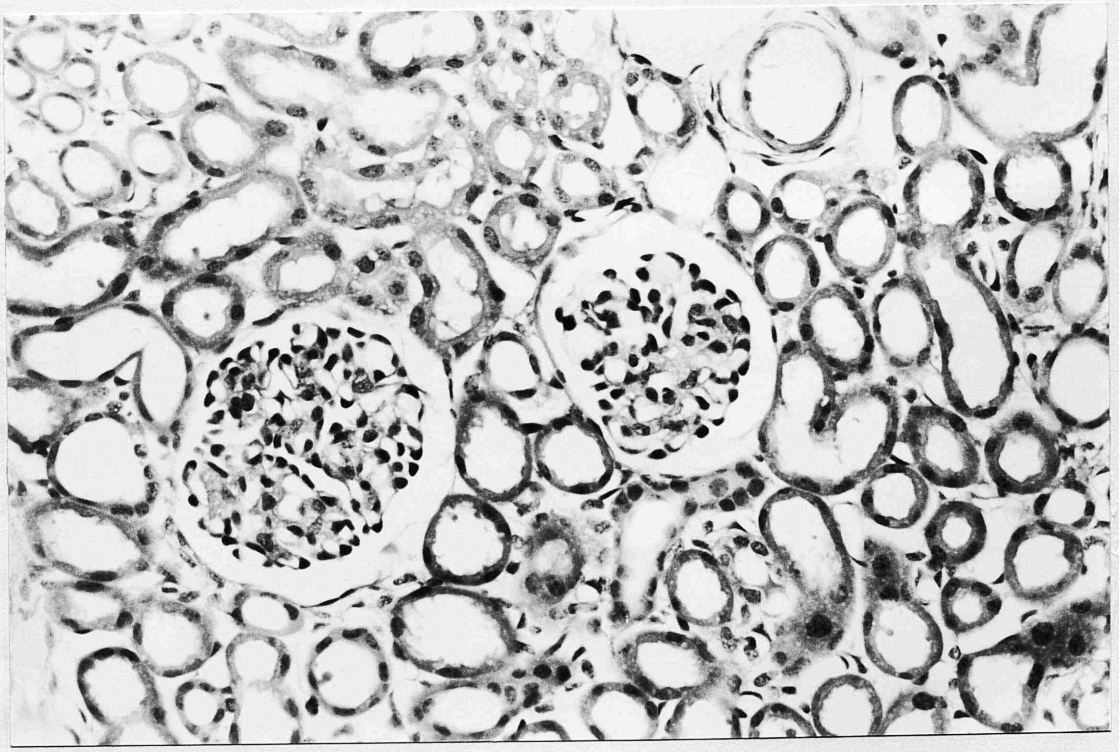

smaller than the juxtamedullary ones and often had closed capillary lumina with resultant difficulty in identifying the various glomerular cell types (Fig. 3.5). In the larger juxtamedullary glomeruli the four main glomerular tissue components were more easily recognized: 1) parietal and visceral epithelial cells, 2) endothelial cells, 3) mesangial cells and matrix and 4) the glomerular basement membrane. In perfused kidneys, the differentiation of constituent glomerular cells was generally easier although the capillary lumina and urinary space were sometimes artificially distended (Fig. 3.6). Furthermore, perfusion was often uneven with some glomeruli, particularly in the outer cortex, not perfused at all.

1) The visceral epithelium :

This epithelium was continuous with the parietal cells of Bowman's capsule at the vascular pole of the renal corpuscle. The visceral epithelial cells of the glomerular tuft, the podocytes, comprised a single layer of cells which were adjacent to the outer aspect of the glomerular basement membrane. Only the nuclei of these cells were visible by light microscopy. The nuclear region of these cells was prominent and protruded into the intracapsular urinary space.

2) The endothelium :

The inner surface of the glomerular capillary was covered with thin endothelium. The most prominent portion of the endothelial cell was the nuclear region, usually found at the axial region of each capillary loop. The nucleus was spherical or ovoid in shape. It was difficult to discern clearly the cytoplasm of the endothelium covering the inner peripheral aspect of the capillary lumen.

3) The mesangium :

The glomerular mesangium was prominent and consisted of mesangial cells and intercellular matrix, the mesangial matrix located in an intercapillary position of the glomerular capillary stalk. The mesangium was separated from the glomerular capillary lumen by endothelial cell cytoplasm and from visceral epithelial cells on its lateral borders by the glomerular basement membrane.

In some glomeruli up to eight contiguous mesangial cells were observed in the mesangial region although up to six mesangial cell nuclei was more usual (Fig. 3.7). More rarely, up to 25 mesangial cells were noted in a few glomeruli.

4) Glomerular basement membrane (GBM) :

The GBM was located between endothelial and visceral epithelial cells in the peripheral portions of the capillary loops and between mesangial cells and visceral epithelial cells in the axial regions. The GBM did not completely surround the entire capillary lumen, but in the axial regions was reflected over the lateral borders of the mesangium.

Juxtaglomerular apparatus :

The four basic elements of the juxtaglomerular apparatus were identified at the vascular pole of the renal corpuscle: 1), in the angle formed between the afferent and efferent arterioles was located the specialized segment of the distal convoluted tubule, the wall of which contained an increased number of nuclei forming the "macula densa" (Fig. 3.5), 2) the terminal portion of the afferent arteriole near the hilum of the glomerular tuft, 3) the extraglomerular mesangial region and 4) the efferent arteriole.

Proximal convoluted tubule :

At the urinary pole there was an abrupt transition between the flattened parietal epithelial cells lining the

Fig. 3.7 Renal corpuscle showing hypercellular mesangium (arrow) with up to 8 contiguous mesangial cells.
HE x 300.

Fig. 3.8 Renal medulla. Note the squamous epithelial cells lining the thin segments of loops of Henle (*) with spherical nuclei bulging into the lumen. Vasa recta containing red blood cells can also be seen (arrows).
HE x 200.

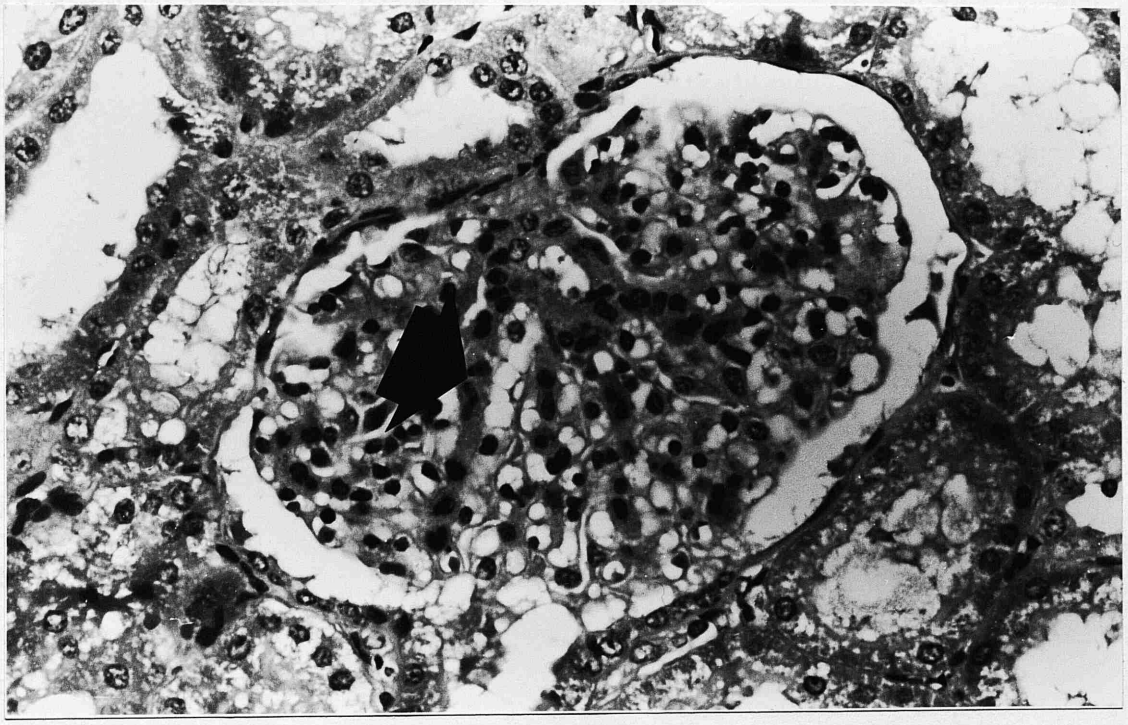

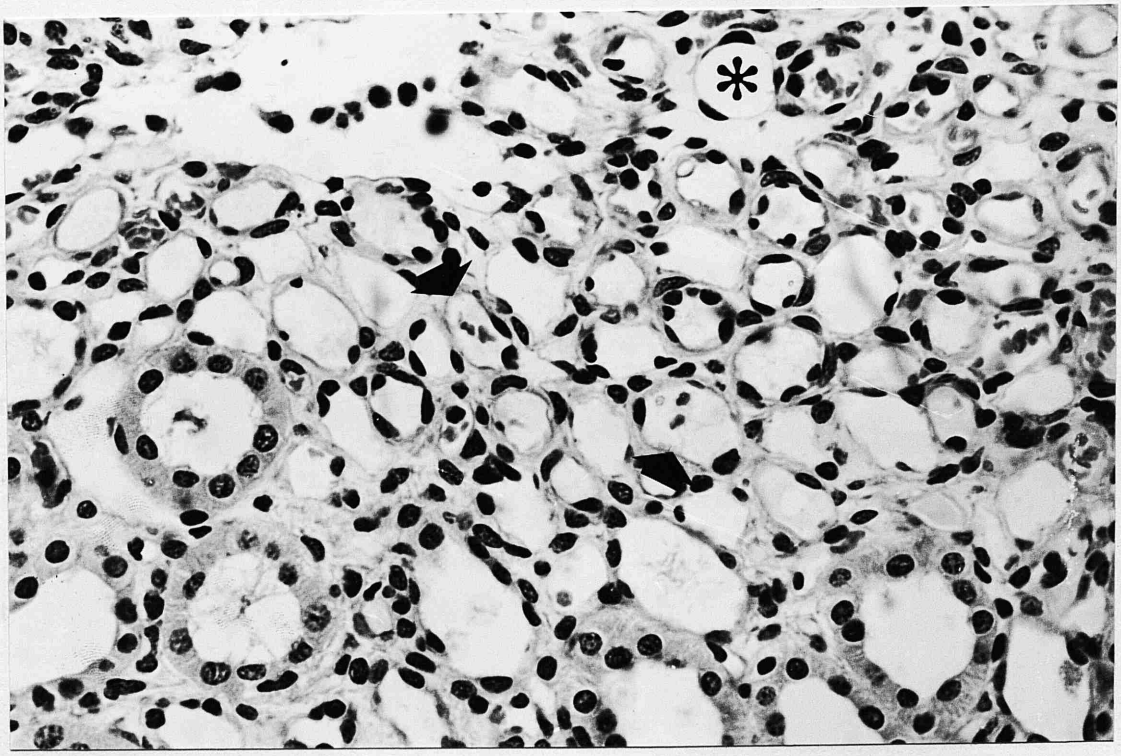

Bowman's capsule and the cells of the initial portion of the proximal tubule (Fig. 3.5). The cells lining the proximal tubule were of the columnar type. The nuclei were usually centrally or basal in location. The general features of the tubule varied with regard to the patency of the lumen. Patent tubules were best seen in kidneys fixed by perfusion (Fig. 3.6). Cellular debris usually occluded the tubular lumina of the immersion fixed kidneys (Fig. 3.5). The brush border along the apices of the cells was rather indistinct.

Loop of Henle :

a) Thin segment :

The thin segment was lined by flattened squamous epithelial cells and arose by an abrupt change from the columnar epithelium of the straight portion of proximal tubule. The cytoplasm of these cells was more or less clear with a spherical nucleus which bulged into the lumen (Fig. 3.8). The lumina were usually patent. The vasa recta had a similar appearance to the thin segment of the loop of Henle but were distinguished from the latter by the presence of red blood cells.

b) Thick segment :

The thick segment began as an abrupt transition

from the flattened squamous epithelium of the thin ascending segment. The cells of the thick ascending loop were low cuboidal and were more eosinophilic than the thin segment (Fig. 3.9).

Distal convoluted tubule :

The cells lining the distal tubule were of the cuboidal epithelial type. In comparison with the proximal tubule, its lumen was larger and the brush border was absent. The cytoplasm was granular and less eosinophilic and the spherical basally-placed nuclei were closer to each other and in general had six to eight nuclei in cross-sections compared to three or four in the proximal tubule (Fig. 3.5).

Collecting tubule :

The collecting tubules were lined by simple cuboidal epithelium with distinct cell boundaries (Fig.3.10). The cytoplasm of the cells was clear, faintly stained and devoid of any characteristic granules. The nuclei were either spherical or oval and basally placed. Each nucleus contained a nucleolus and some deeply stained chromatin granules. The lumen of the collecting tubules became wider and the cells taller towards the papillary duct.

Fig. 3.9 Thick segments of loops of Henle (arrows). Note the low cuboidal cells.
HE x 300.

Fig. 3.10 Renal medulla showing collecting tubules (*) with distinct cell boundaries. Note also the thin segments of the loops of Henle (small arrow) and vasa recta (large arrow).
HE x 200.

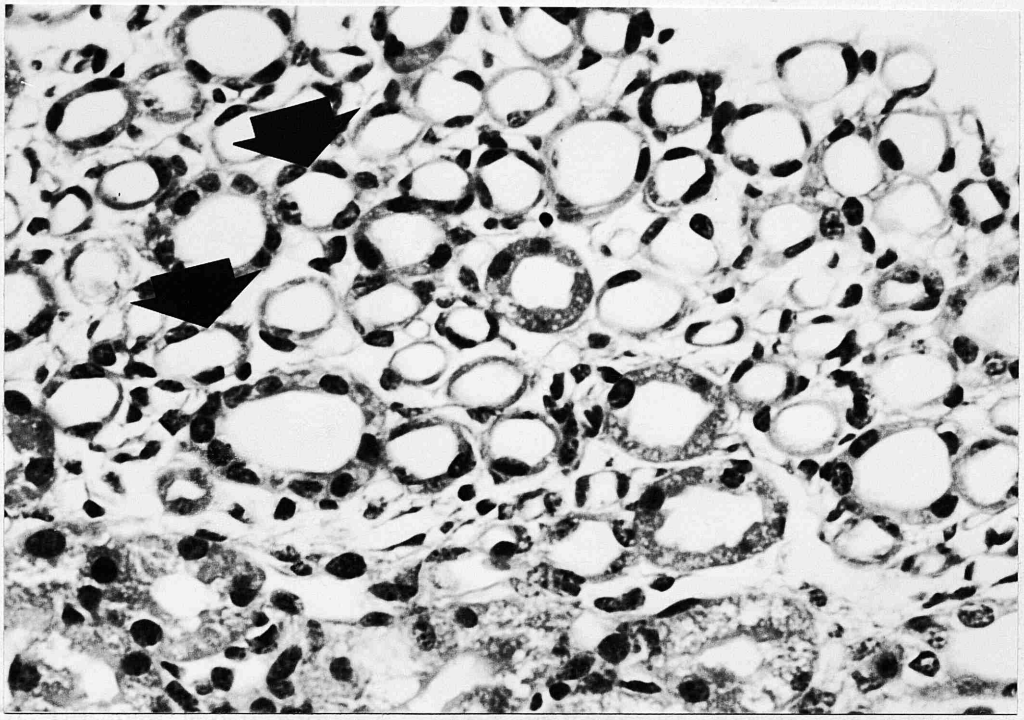

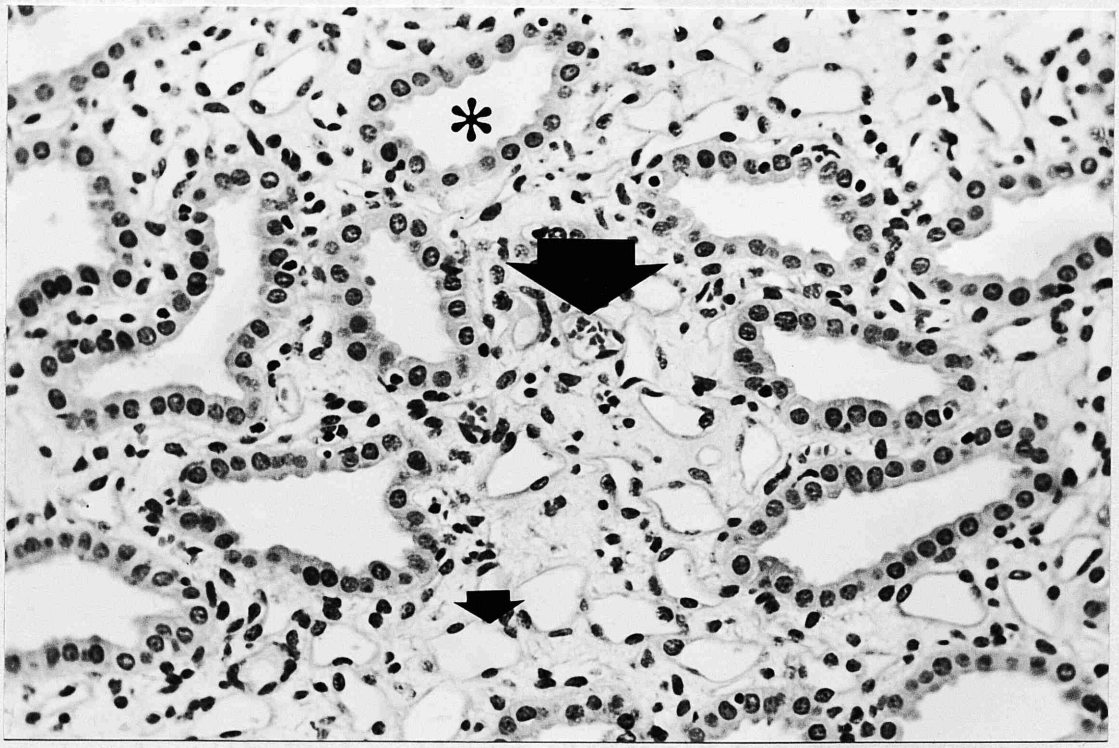

Papillary ducts (of Bellini) :

These possessed the widest lumina as well as the highest columnar epithelium (Fig. 3.11). The papillary ducts opened into the minor calyces through foramina on the surface of the papilla (Fig. 3.12).

The papilla :

The transitional epithelium of the calyx minor was reflected over the papilla. At the angle of reflection, the high transitional epithelium of the calyx minor became much lower. The papillary transitional epithelium thus maintained an almost uniform height over the entire surface of the papilla, except on the sides near the angle of reflection. The renal pelvis and major calyces were lined by high transitional epithelium and contained in their walls abundant smooth muscle cells.

Ultrastructural (TEM) observations :

Renal corpuscle :

The parietal epithelium lining the urinary space formed a continuous flattened layer covering Bowman's capsule and the glomerular tuft. The nucleus of the parietal epithelial cell was elongated and had condensed peripheral chromatin (Fig. 3.13). The cytoplasmic

Fig. 3.11 Papillary ducts (of Bellini). Note the high columnar epithelium lining the ducts.
HE x 200.

Fig. 3.12 Low power view of the tip of a medullary papilla showing the papillary duct orifices.
HE x 65.

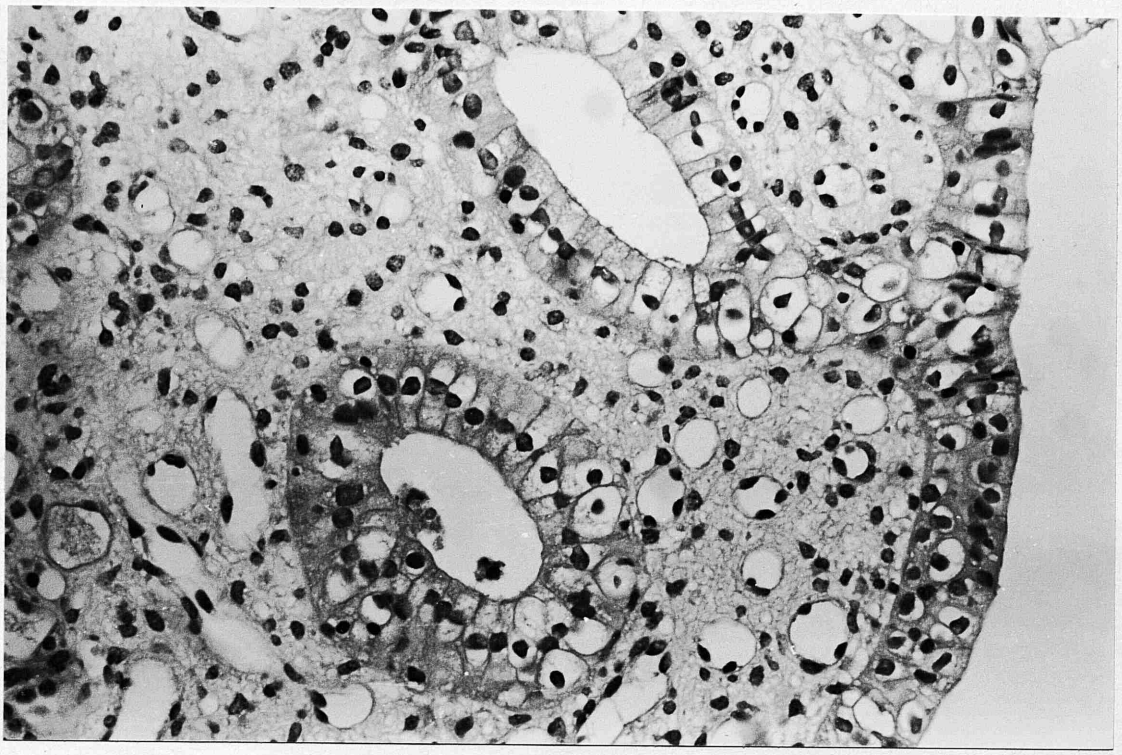

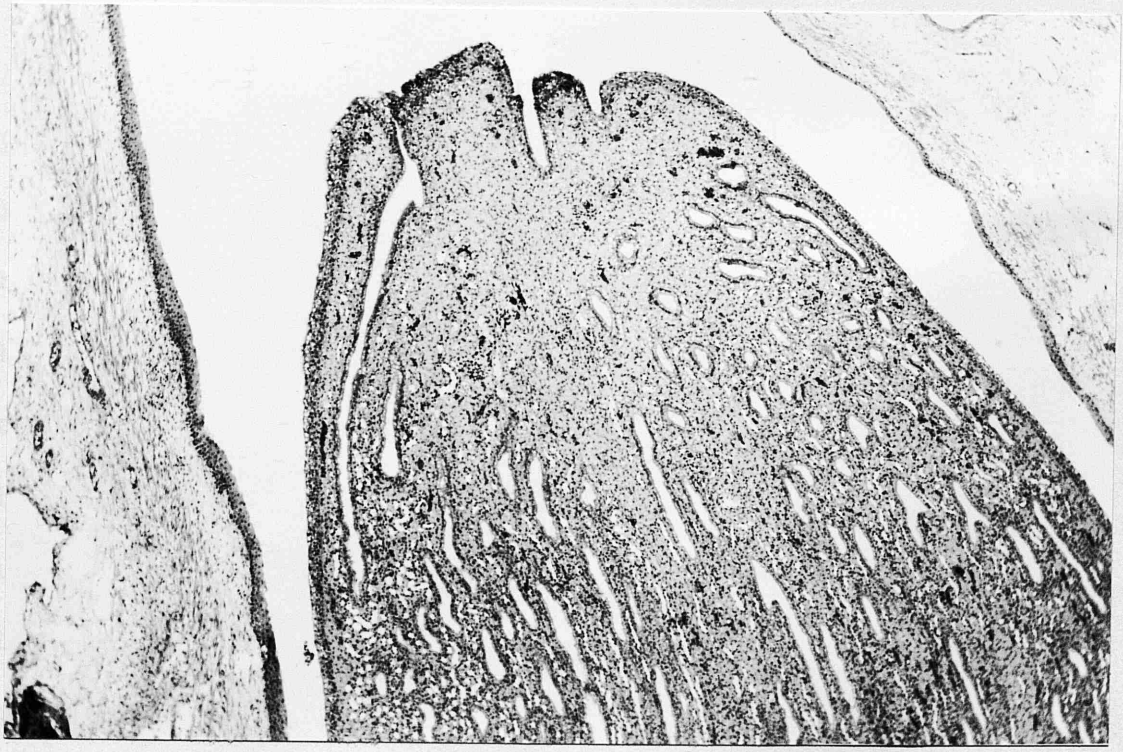

organelles were sparse but a few mitochondria were scattered throughout the cytoplasm and a few strands of rough-surfaced endoplasmic reticulum were occasionally observed. The cell surface sported a few stubby microvillous processes.

At the urinary pole, the flat squamous cells were continuous with the columnar cells of the proximal convoluted tubule (Fig. 3.14).

At the vascular pole of the renal corpuscle the visceral epithelium was continuous with the parietal epithelial cells of Bowman's capsule. No obvious peripolar cells were observed.

The visceral epithelial cells consisted of a main cytoplasmic mass which gave rise to large cytoplasmic extensions from which arose numerous foot processes (Fig.3.15). The main cytoplasmic mass, containing the nucleus, was thick and protruded into the urinary space. The nucleus was usually ovoid in shape and was often slightly indented. The chromatin material was condensed at the margins of the nucleus. A small number of mitochondria was present; they were observed either in transverse section or as longitudinal profiles. The Golgi apparatus was generally inconspicuous; it consisted of flattened cisternae and vesicles grouped near the nucleus. Small amounts of both

Fig. 3.13 Electron micrograph of renal corpuscle showing a flat parietal epithelial cell (arrow). Urinary space (US); visceral epithelial cell (v).
TEM x 5,400.

Fig. 3.14 Electron micrograph showing a flat squamous parietal cell at the urinary pole (small arrow) continuous with a columnar cell of the proximal tubule (large arrow).
TEM x 5,400.

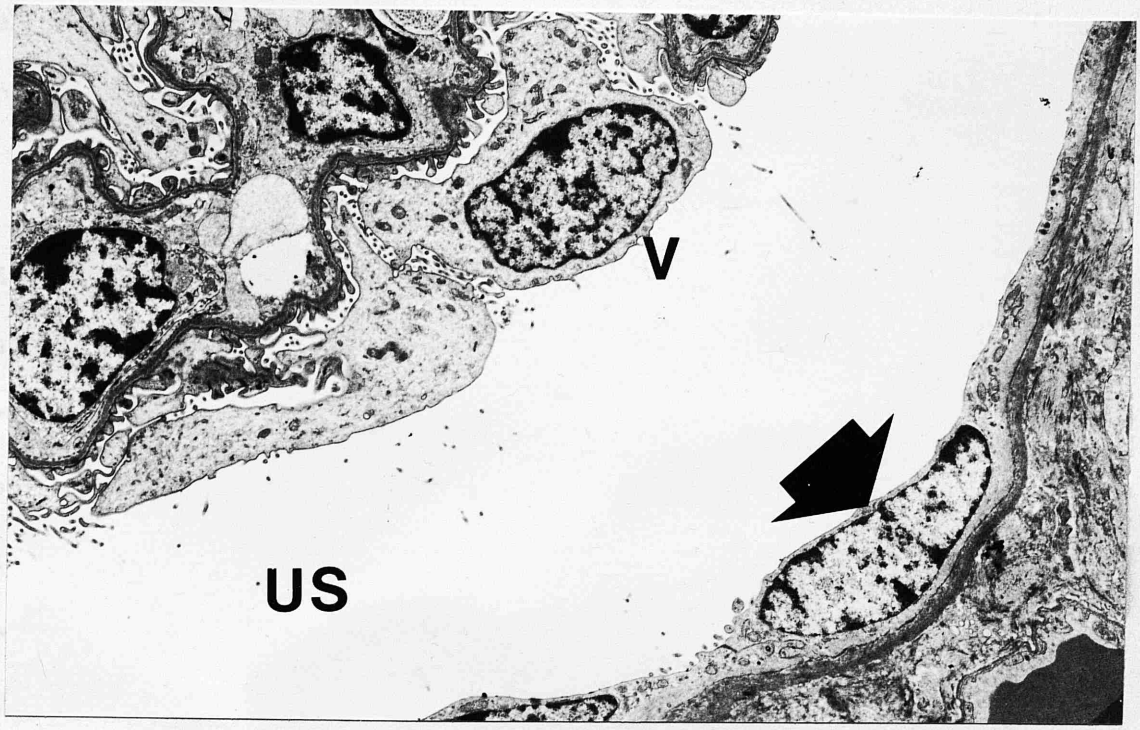
V
US

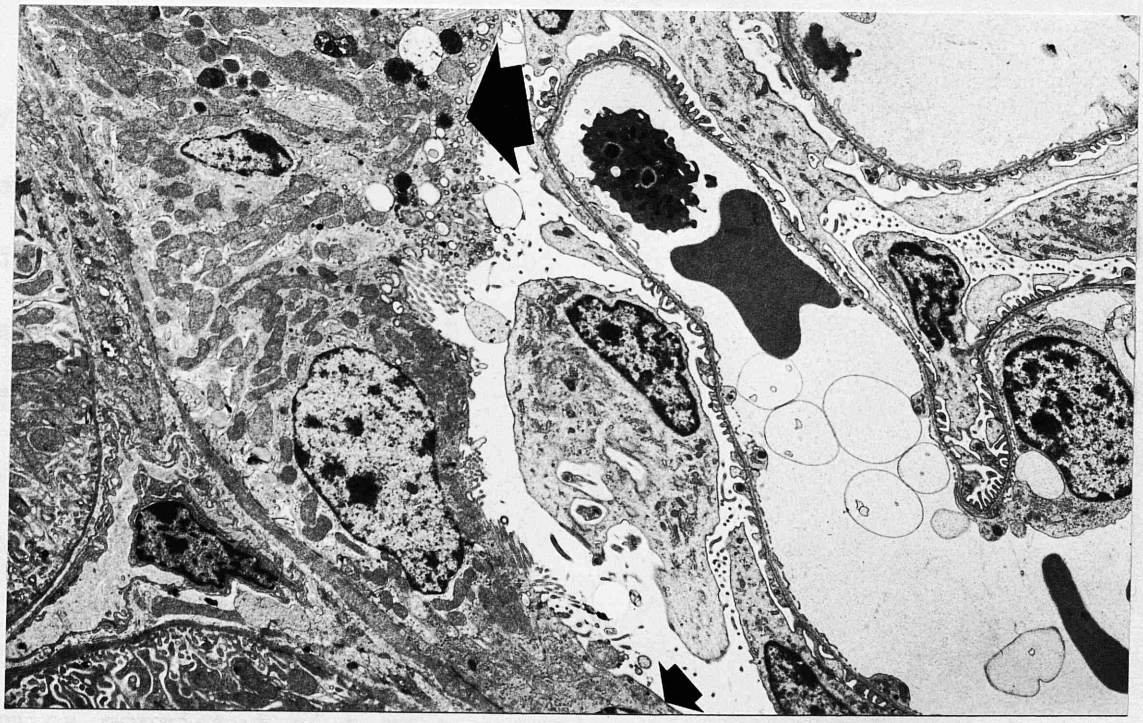

rough-surfaced endoplasmic reticulum and free ribosomes were also noted in the cytoplasm of the visceral epithelial cell (Fig. 3.16).

The cytoplasm extended outwards from the body of the cell to form large trabeculae or primary processes which contained many of the previously mentioned cytoplasmic organelles with the exception of the Golgi apparatus. The former gave rise to secondary processes which in turn branched to form tertiary processes or pedicels that projected from secondary processes towards the GBM where they appeared to be embedded in the lamina rara externa (Fig. 3.17).

The foot processes were separated from each other by fairly evenly-sized gaps, the slit-pores. A delicate membrane could be observed at high magnification between adjacent foot processes; this was the slit-pore membrane. The foot processes differed from the remainder of the cell in that they possessed few cytoplasmic organelles with the exception of a few vesicles and an occasional mitochondrion.

The endothelial cells which lined the capillary lumina consisted of a main cytoplasmic mass which contained the nucleus, usually at the axial region of the loop, and an attenuated portion at the periphery (Figs. 3.18 and 3.19).

Fig. 3.15 Electron micrograph showing a capillary loop (C). Note the visceral epithelial cell (V) and endothelial cell (E). TEM x 8,000.

Fig. 3.16 Electron micrograph showing a visceral epithelial cell (arrow), with ovoid indented nucleus. TEM x 16,000.

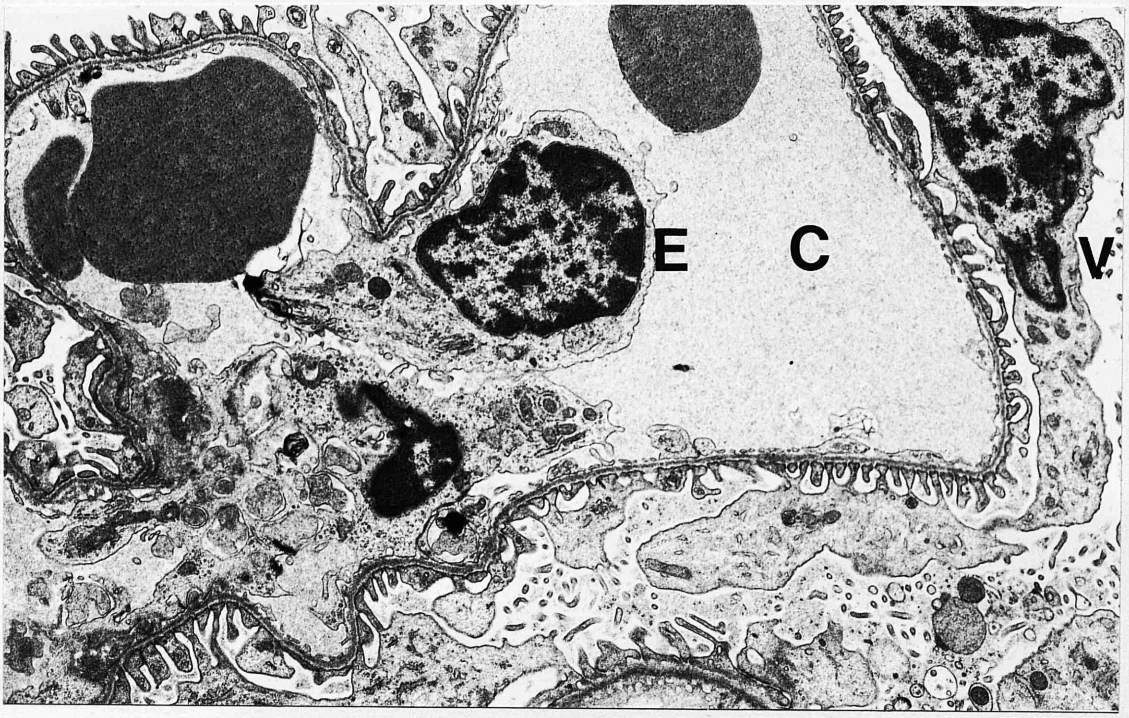
E
C
V

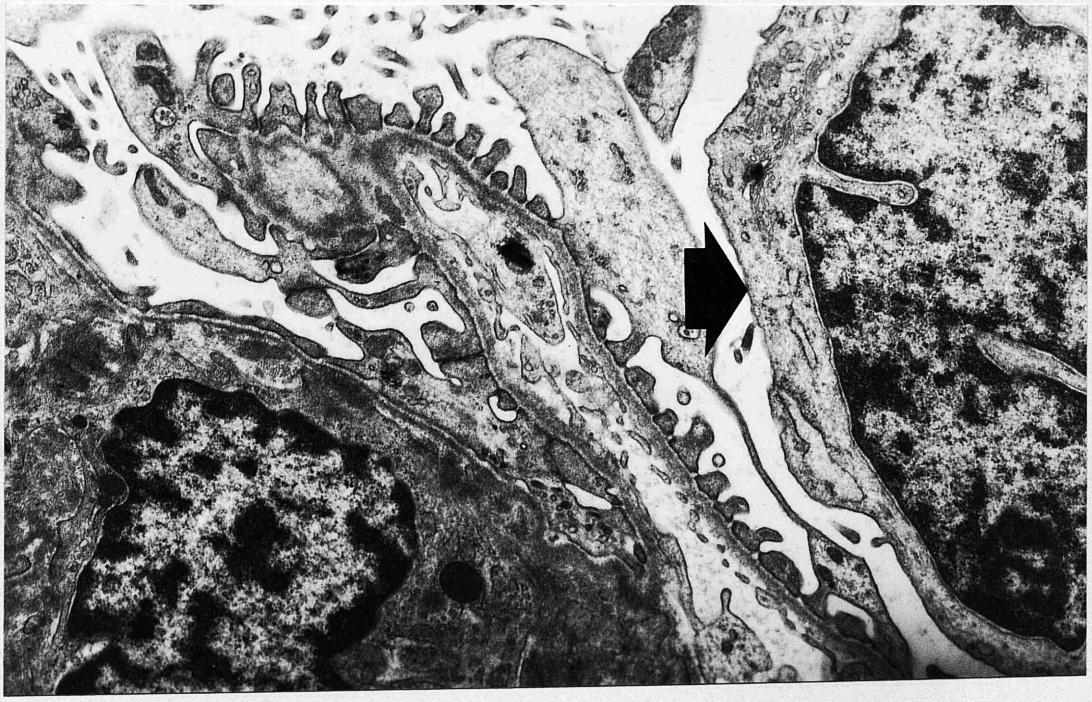

The main cytoplasmic mass contained a round or oval nucleus. The thin attenuated sheet of the cytoplasm extended from the body of the cell and lined the peripheral parts of the capillary lumen and was intimately apposed to the lamina rara interna of the GBM. Numerous perforations or fenestrae were regularly found in the cytoplasm (Fig. 3.17). The cytoplasmic organelles were largely confined to the perinuclear region and there was a marked reduction in the amount of these organelles in the attenuated portion. In general, the mitochondria were smaller and less prominent than those of the visceral epithelial cells although the amount of rough-surfaced endoplasmic reticulum was approximately the same.

The GBM was sandwiched between visceral epithelial and endothelial cells and between visceral epithelial cells and mesangial cells; however, no GBM was found between endothelial and mesangial cells. It was of uniform thickness and was seen to be composed of three layers : 1), a central electron dense layer, the lamina densa, 2) an outer dense layer, the lamina rara externa, which was separated from the urinary space by the slit-membrane and 3) an inner electron lucent layer, the lamina rara interna, which was in contact with the lumen of the capillary at the sites of endothelial fenestrae (Fig. 3.17).

Fig. 3.17 Electron micrograph of the capillary wall showing the trilaminar GBM. The pedicels (P) are separated by narrow spaces, the slit pores, and appear to be embedded in the lamina externa. Note the fenestrations of the endothelium (arrows). Urinary space (US); capillary lumen (C). TEM x 40,000.

Fig. 3.18 Low power electron micrograph showing many capillary loops. Note the endothelial cells at the axial regions of the loops (arrows). TEM x 4,000.

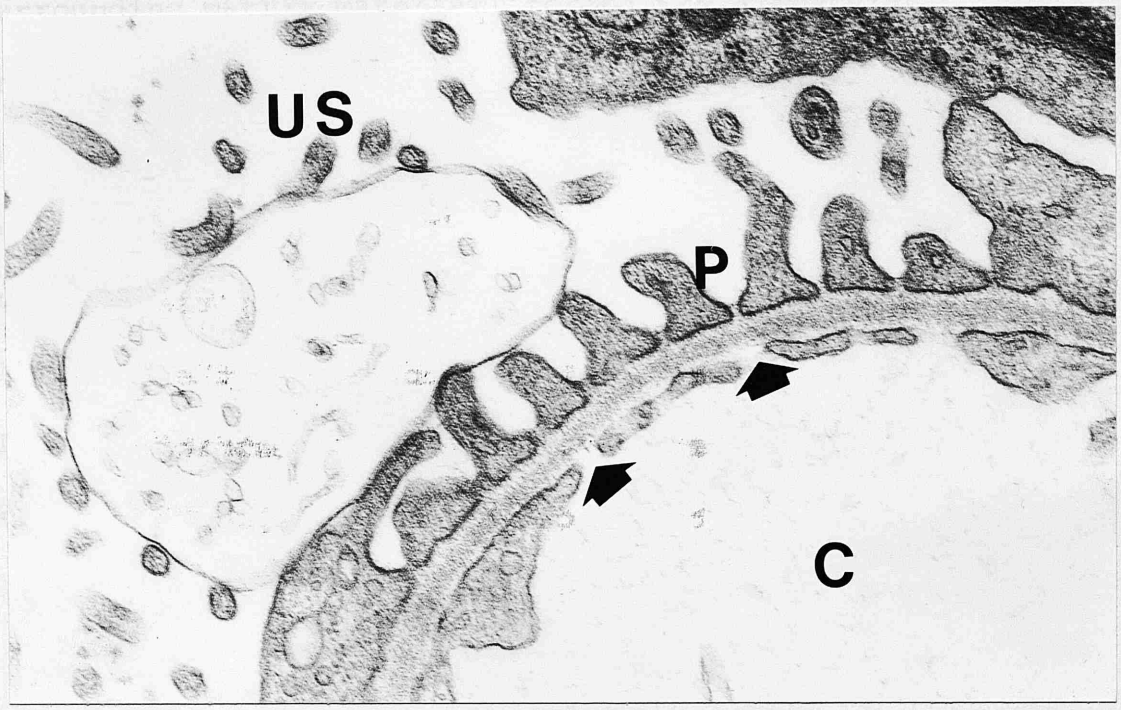
US
P
C

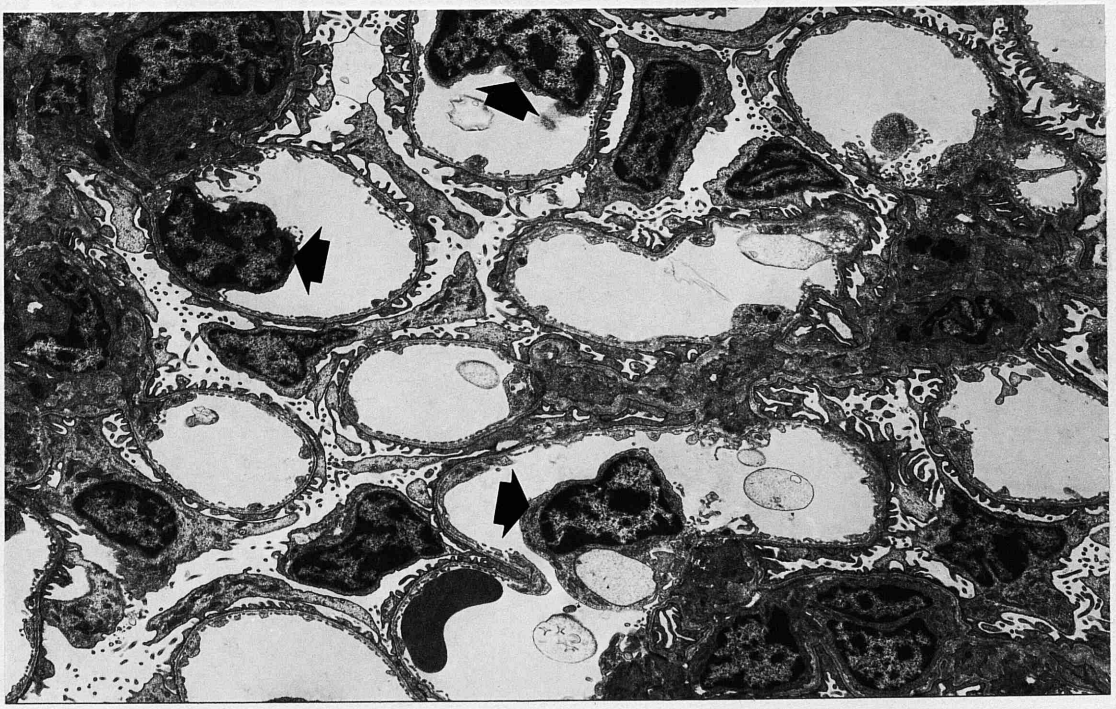

The mesangial cells, together with the surrounding matrix material, formed the glomerular mesangium and was located in an intercapillary position in the glomerular capillary stalk. The mesangial cells were quite irregular in shape with indented nuclei and with numerous elongated cytoplasmic processes extending from the main body of the cell towards the capillary lumen (Fig. 3.20). Occasionally up to six contiguous mesangial cells were found (Fig. 3.21). (c.f. histological findings).

Mitochondria, endoplasmic reticulum, a Golgi apparatus, free ribosomes and vesicles were all noted in the cytoplasm. The mesangium was separated from the capillary lumen by endothelial cells and from adjacent visceral epithelial cells by the GBM. The mesangial cells were surrounded by a variable amount of mesangial matrix, which was an amorphous substance similar in appearance but not identical to the GBM. Fine fibrils and tiny channels were also noted running through it. In 26 of the 38 pigs, electron dense deposits were found in the mesangial matrix (Fig. 3.22).

The juxtaglomerular apparatus :

The modified smooth muscle cells at the terminal portion of the afferent arteriole wall had a centrally

Fig. 3.19 Electron micrograph demonstrating an endothelial cell (E). The cytoplasm extends from the body of the cell to line the capillary lumen, adjacent to the lamina rara interna.
TEM x 20,000.

Fig. 3.20 Electron micrograph showing the position of the mesangium. The mesangial cells (M) are located in the space between the capillary loops. Endothelial cell (E).
TEM x 13,400.

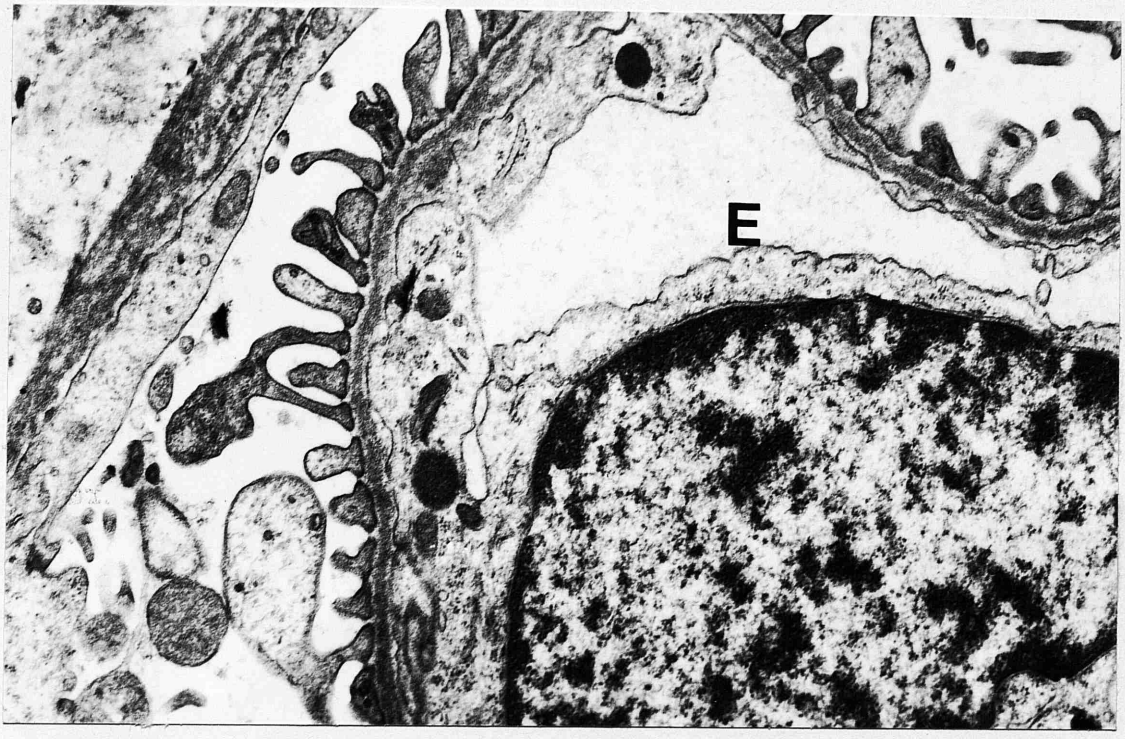
E

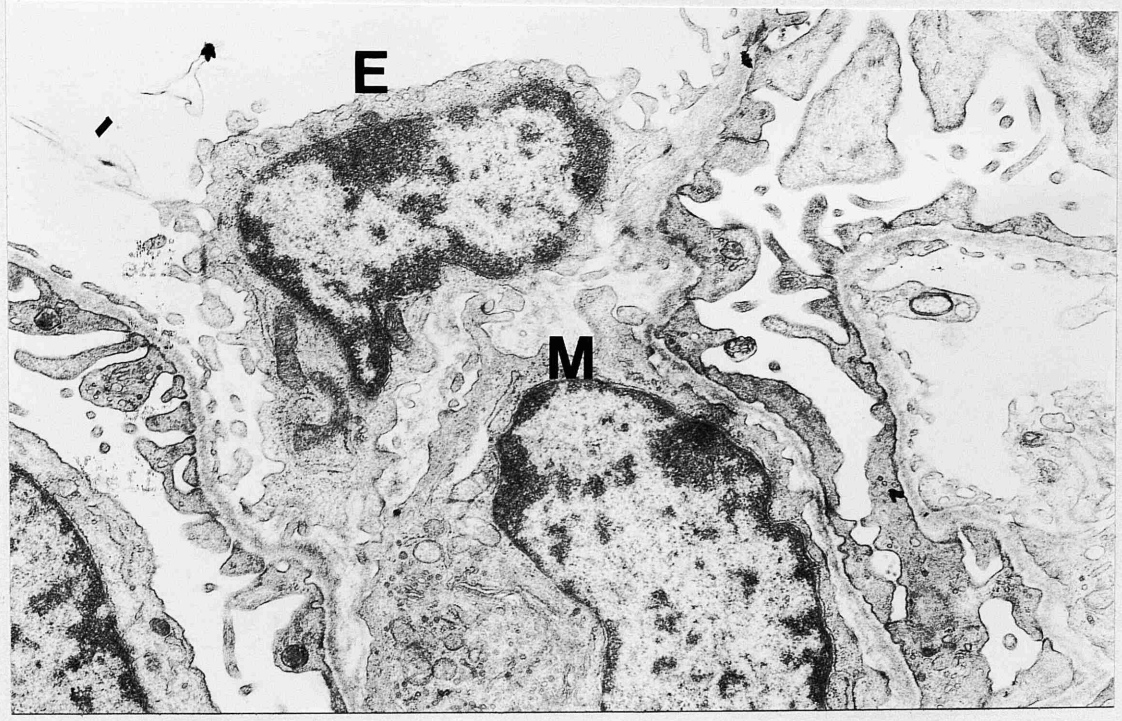
E
M

Fig. 3.21 Electron micrograph showing five contiguous mesangial cells. TEM x 8,000.

Fig. 3.22 Electron micrograph showing electron dense deposits (arrows) in the mesangium (M). TEM x 9,400.

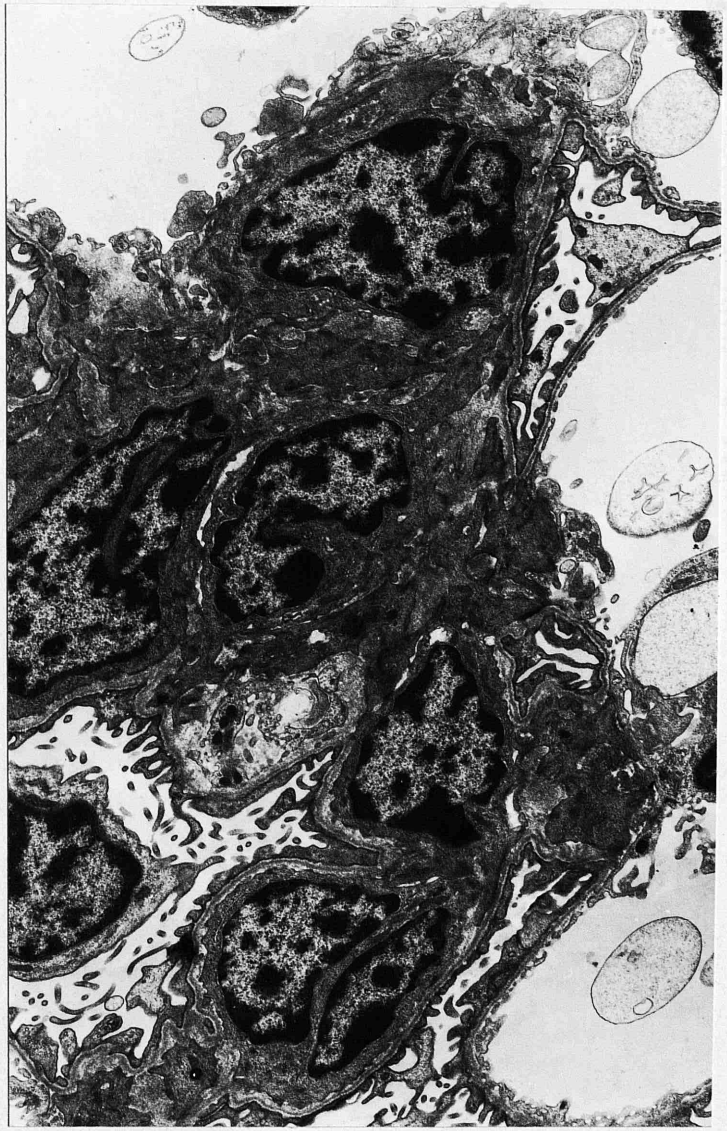

located nucleus and contained varying numbers of electron dense granules (Fig. 3.23).

The macula densa cells of the distal tubule lay in close apposition to the afferent arteriole. These cells, containing dense nuclear chromatin, were narrower and taller than other cells of the distal convoluted tubule, with the nuclei lying closer together. The tubular basement membrane was sometimes, but not always, deficient in this region. The cells had a few randomly-arranged mitochondria and there were fewer basal plasma membrane invaginations than usual in this segment of the tubule (Fig. 3.23).

The extraglomerular mesangial or lacis cells were in intimate contact with the macula densa, the granular cells of the afferent arteriole and intercapillary mesangial cells of the glomerulus. These cells were closely packed, with elongated nuclei and spindle-shaped cytoplasm containing occasional electron dense granules.

Proximal convoluted tubule :

The cells of the proximal tubule were columnar in shape and possessed a well-developed brush border at their apical or luminal surface. The latter consisted of numerous finger-like evaginations of the apical plasma

Fig. 3.23 Electron micrograph demonstrating the juxtaglomerular apparatus. Electron dense granules (small arrows) are located in the cytoplasm of afferent arteriolar cells. Note also the macula densa of the distal tubule (large arrows).

TEM x 5,400.

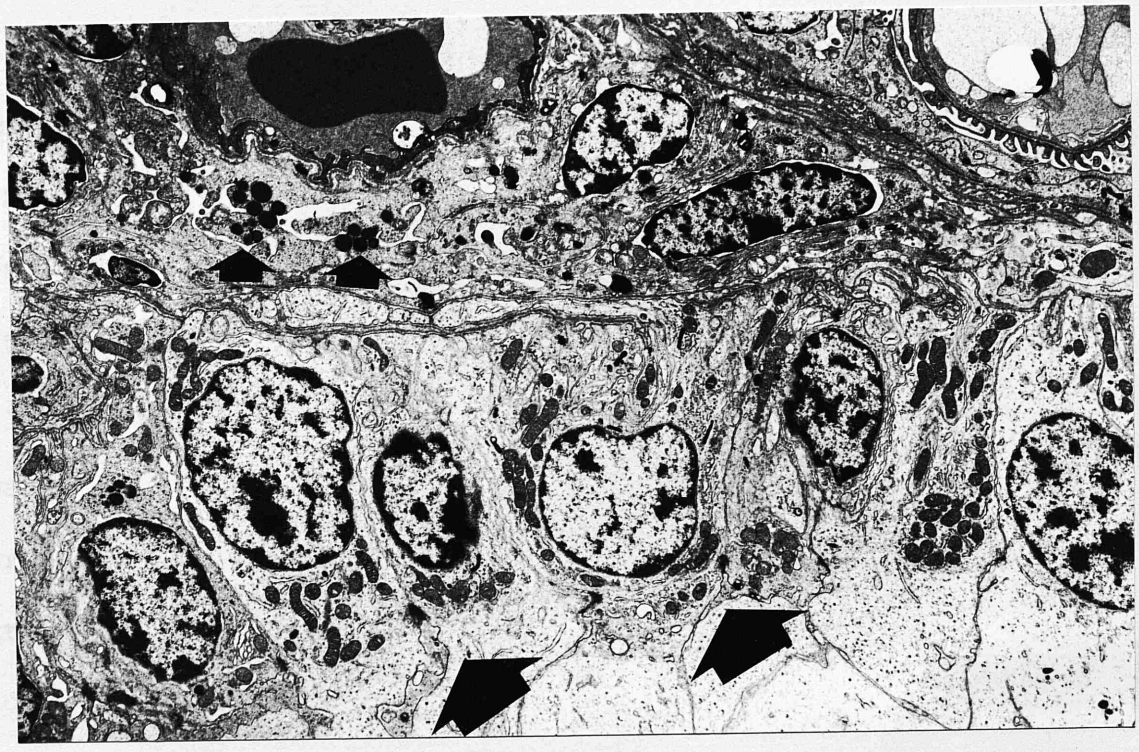

membrane, the microvilli (Fig. 3.24). A moderately electron opaque fuzzy coating was present on the surface of the microvilli. The nuclei were positioned in the mid-region or towards the base of the cell. Numerous elongated mitochondria extended from the base to the apex of the cell and frequently lay in close proximity to the lateral plasma membrane (Fig. 3.25). The individual cells of the proximal tubule were complex in shape. The cell membranes were characterized by the presence of numerous lateral processes which interdigitated with corresponding lateral processes of adjacent cells. As a result a lateral complicated intercellular space was created between adjacent cells. At the upper end of this intercellular space, specialized tight junctions or zonula occludens were present. In addition to the surface microvilli, an extensive system of apical tubules, small coated vesicles and large vacuoles characterized the apical cell cytoplasm. Invaginations between or below the microvilli gave rise to these open and dense apical tubular profiles. In transverse sections, these appeared as vesicles; the outer surface of the small vesicles had a fuzzy appearance. Vacuolar structures situated further basally in the cytoplasm had a larger diameter than the vesicles. They appeared to have a more electron dense outer membrane and a thin "fuzzy" internal lining. Varying amounts of rough

Fig. 3.24 Electron micrograph of a proximal convoluted tubule showing the finger-like microvilli (arrow). TEM x 5,400.

Fig. 3.25 A higher power electron micrograph of a proximal convoluted tubule. Note the large number of mitochondria and apical tubules and vacuoles. TEM x 10,000.

and smooth-surfaced endoplasmic reticulum were observed in the cytoplasm. The rough-surfaced endoplasmic reticulum tended to be more numerous. Free ribosomes were also abundant within the cytoplasm. The Golgi apparatus was found close to the nucleus either in an apical or lateral position. It consisted of flattened cisternae and vesicles. Numerous mitochondria were seen throughout the cytoplasm of the cell. They varied in shape from being either long or slender or crescentic and they contained numerous cristae. The basement membrane was a thin homogeneous structure similar in appearance to the basement membrane of the Bowman's capsule with which it was continuous at the urinary pole (Fig. 3.14).

Loop of Henle :

a) Thin segment :

The lining of epithelium of the descending thin loop of Henle contained two cell types. The first, Type I, was a low cuboidal cell with no lateral interdigitations with adjacent cells (Fig. 3.26). The nucleus was oval, centrally located in the cytoplasm with a dense condensation of chromatin around the nuclear margin. Few microvilli were observed on the luminal cell surface. Various ovoid or spherical mitochondria were observed sparsely distributed in the cytoplasm; relatively sparse

smooth and rough-surfaced endoplasmic reticulum, lysosomes, microtubules and small vesicles were also found.

The second type of epithelial cell, Type II, was flatter and contained an elongated nucleus that was positioned along the axis of the tubule (Fig. 3.27). Owing to their large size with respect to cell height, they bulged into the lumen. The chromatin had a fairly homogeneous distribution although slight clumping and peripheral margination could be seen in some nuclei. The apical cell membrane formed a few short irregular microvilli. The basal cell membrane occasionally showed short infoldings.

The basement membrane of the thin limb was thin and generally consisted of a homogeneous electron dense material. In some areas it appeared to consist of separate dense layers between which there was an electron lucent area.

b) Thick segment :

The cells throughout the thick ascending limb of Henle were generally irregular in shape and more cuboidal than those of the thin segment (Fig. 3.27). Numerous elongated mitochondria were oriented perpendicularly to the basement membrane and enclosed by invaginations of the

Fig. 3.26 Electron micrograph showing a thin segment (TS) of a loop of Henle. Note the low cuboidal cells with oval-centrally located nuclei. Note also the adjacent vasa recta containing red blood cells.
TEM x 5,400.

Fig. 3.27 Electron micrograph of a thin segment of a loop of Henle (TS) showing the flat type II cells. Note also part of a thick ascending limb of Henle (arrow) which has more cuboidal epithelium than the thin segment. A collecting tubule (C) can also be seen.
TEM x 5,400.

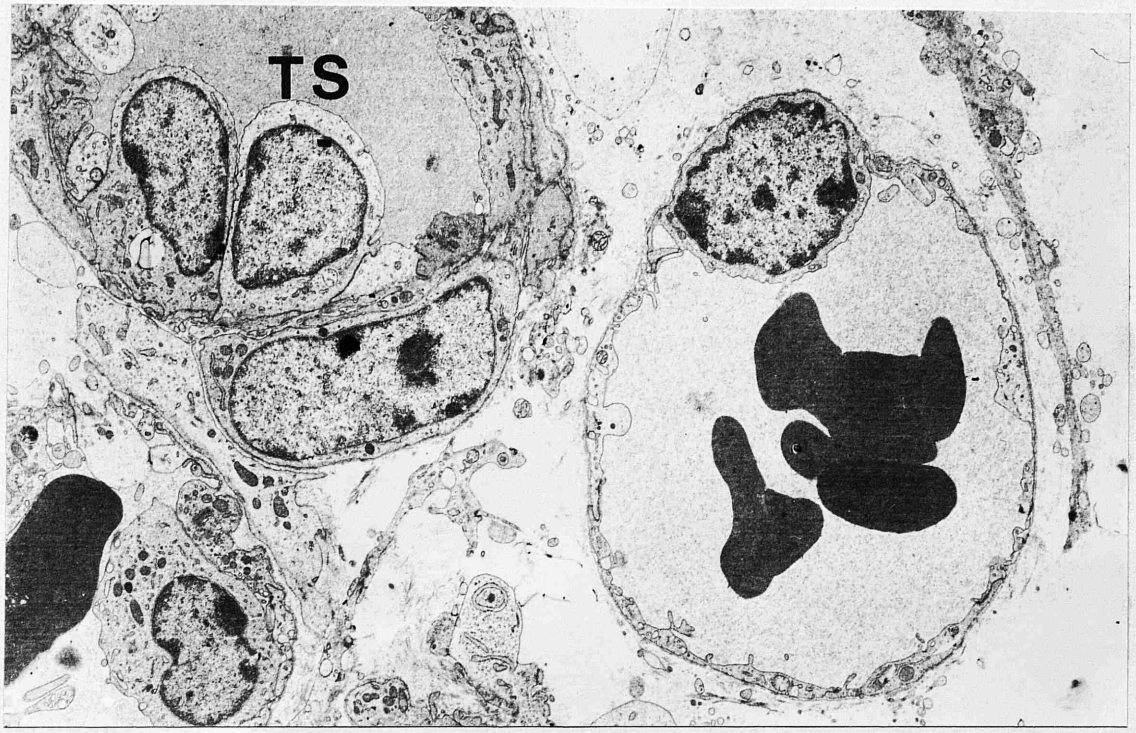
TS

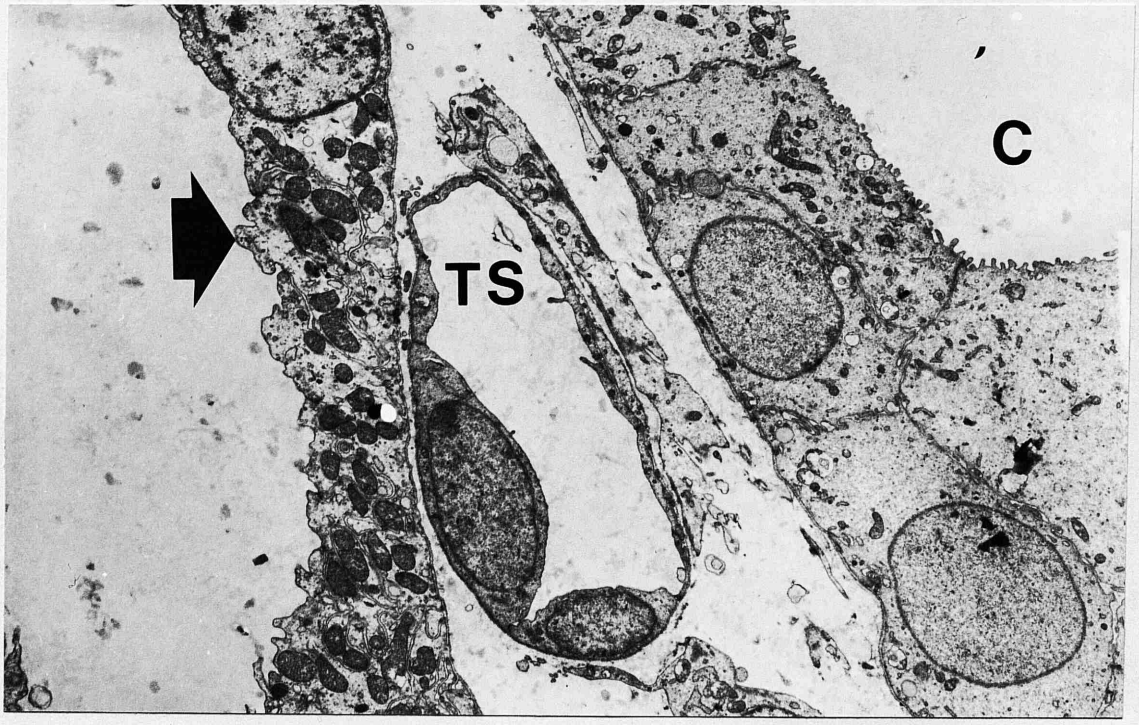
C
TS

basal plasmalemma. Other subcellular organelles in this segment include a well-developed Golgi apparatus and abundant quantities of smooth and rough endoplasmic reticulum.

Distal convoluted tubule :

The cells lining this portion of the nephron were cuboidal in appearance. The nuclei occupied a mid to basal position in the cell. They were spherical to oval in shape and nuclear chromatin was evenly distributed apart from occasional clumps (Fig. 3.28). Individual cells often had a convex luminal surface covered with short, blunt microvilli. However, these cells lacked the well-developed brush border and the extensive system of apical tubules and vacuoles of the proximal convoluted epithelial cell.

The most characteristic feature of the cells of the distal tubule were the elaborate lateral and basal processes, the basal interdigitations being more numerous (Fig. 3.29). Prominent junctional complexes were present at the apical region of the cell. The mitochondria were prominent, elongated, extending from the basal to the apical cell surface and were closely aligned with the lateral cell membrane. Smooth and rough-surfaced endoplasmic reticulum were rare but free ribosomes and a well-developed Golgi apparatus were located in the apical portion of the cell. The specialised cells of the macula

Fig. 3.28 Electron micrograph of a distal convoluted tubule. Note the sparse short microvilli and numerous mitochondria.
TEM x 4,000.

Fig. 3.29 Electron micrograph of a distal tubule. The prominent basal interdigitations and junctional complexes are difficult to see at this magnification.
TEM x 5,400.

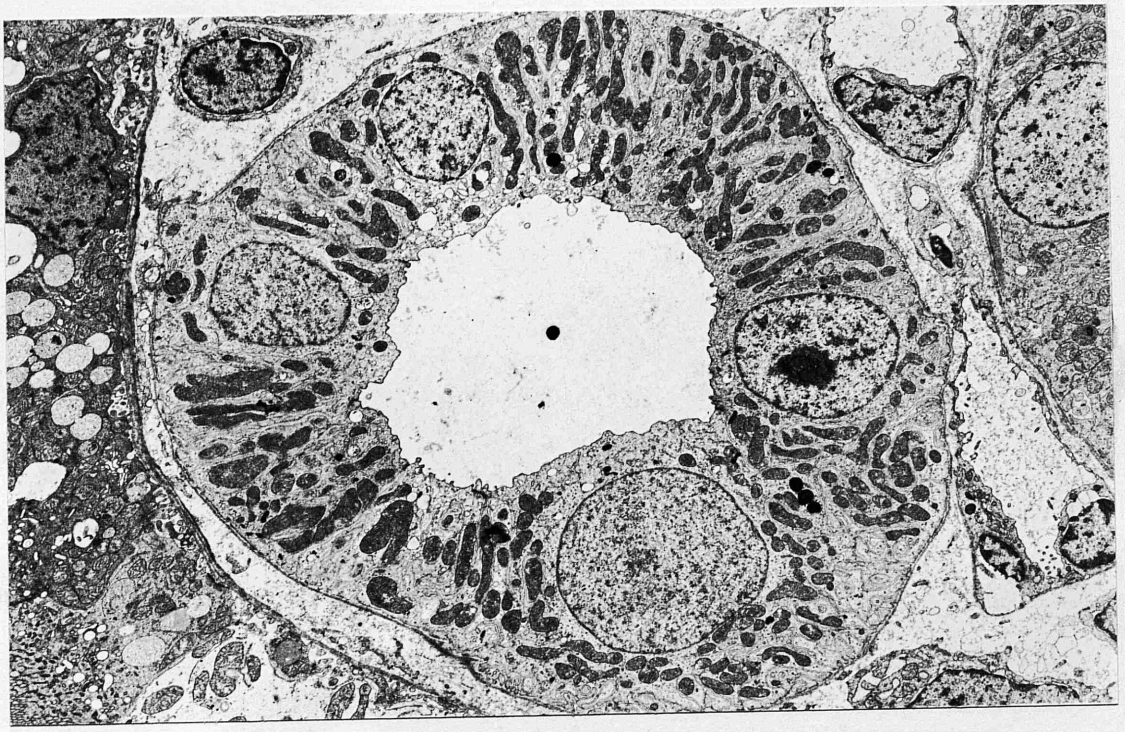

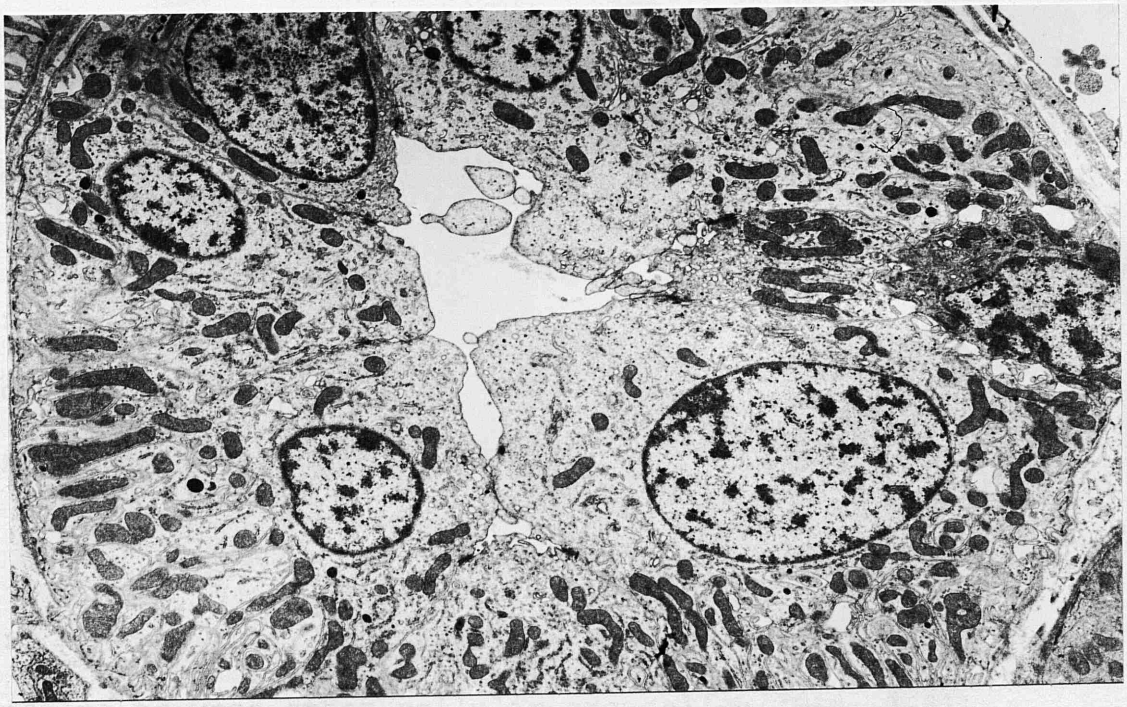

densa have already been described.

Collecting tubule :

Two cell types were recognized in the collecting tubule, light cells and dark cells. Throughout the entire collecting duct the major cell type was the light cell (Fig. 3.30). These cells possessed clear cytoplasm containing small numbers of randomly orientated mitochondria. All cell organelles within the light cells appeared to be decreased in concentration in comparison with other parts of the nephron. Sparse rough-endoplasmic reticulum, occasional cytosomes and various sizes of vacuoles were observed. The nuclei were large and spherical and contained evenly dispersed chromatin. The lateral cell borders were interrupted by small inter-digitating processes with adjacent cells. At the base of the cells, short invaginations of the plasmalemma were also observed. On the luminal cell surface, short blunt microvilli were present. Tight junctions were noted between adjacent light cells.

The dark cells often exhibited a convex luminal surface covered with microvilli. Mitochondria were numerous as were other cellular organelles (Fig. 3.31). The basal membrane showed more invaginations than the light cells. The nuclei were spherical or oval, located in the

Fig. 3.30 Electron micrograph showing light cells of a collecting tubule. A few short blunt microvilli are present on the luminal cell surface. Note the sparse amount of organelles.
TEM x 8,000.

Fig. 3.31 Electron micrograph of a dark cell (arrow) of a collecting tubule. Note the convex luminal surface covered with microvilli and the numerous mitochondria.
TEM x 8,000.

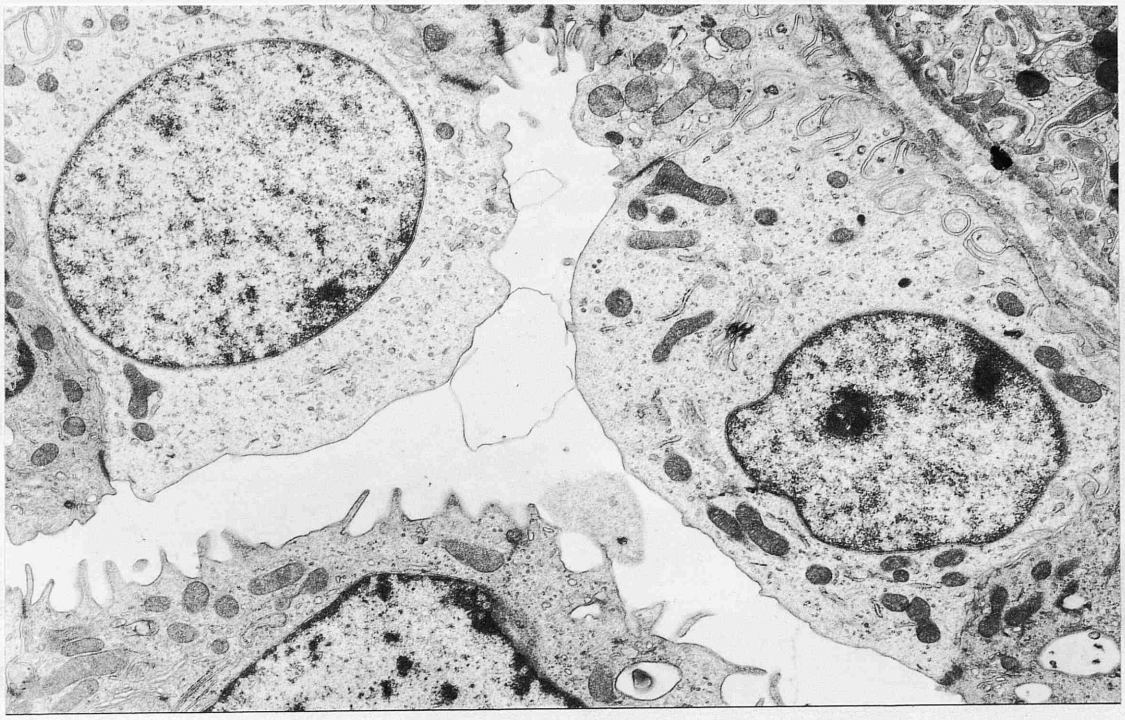

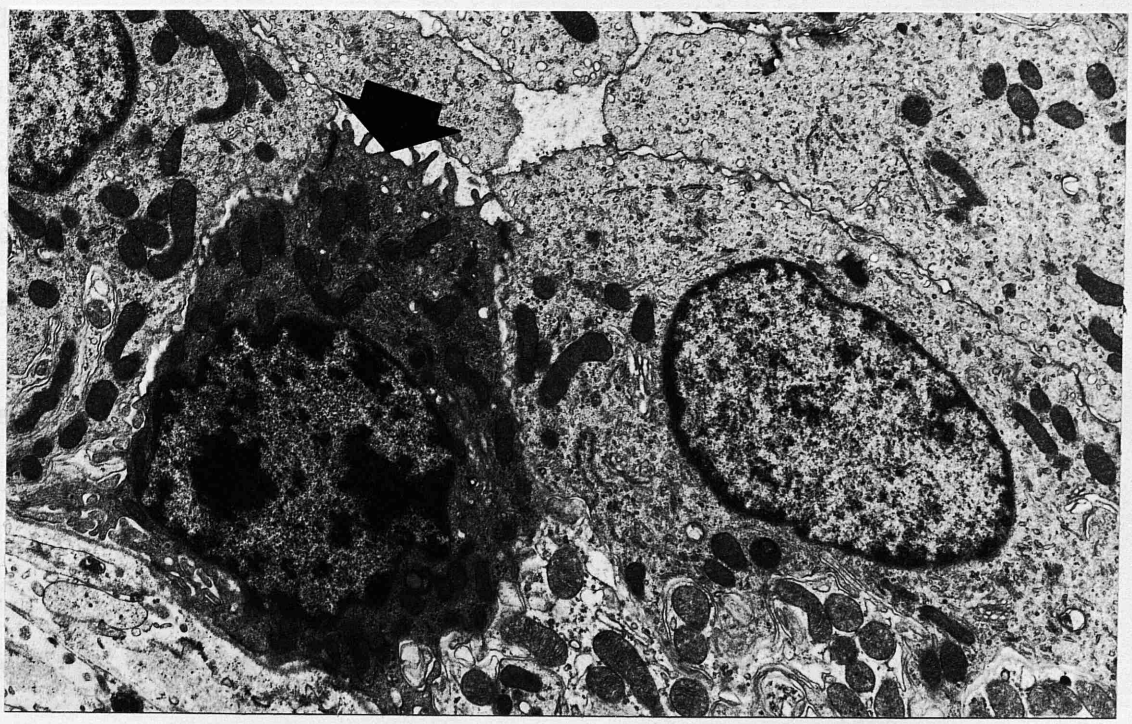

basal portion of the cell and the chromatin was more condensed.

Papillary duct :

In the papillary ducts, the cells were more columnar and resembled the light cells of the collecting ducts; no dark cells were found.

Ultrastructural (SEM) observations :

Under low magnification, the cut surface of the renal cortex was made up of many renal corpuscles and closely-packed proximal and distal convoluted tubules and blood vessels (Fig. 3.32). In many renal corpuscles, Bowman's capsule was cut open in such a way that the glomerulus was exposed sitting in a bowl-like capsule; other capsules were empty, the glomeruli having been lost during processing. Each glomerulus consisted of a highly coiled and branched capillary tuft nestling within Bowman's capsule (Fig. 3.33).

Parietal epithelium :

Bowman's capsule was thin, spherical in shape and lined by simple squamous epithelium. The nucleated region of each cell often protruded slightly into the urinary or capsular space. One, and occasionally two, long slender cilia arose from near the nucleated centre

Fig. 3.32 Scanning electron micrograph illustrating the cut surface of the renal cortex revealing whole and sectioned renal corpuscles and closely packed convoluted tubules. Note the two empty capsules where the glomeruli were lost during processing.
SEM x 90.

Fig. 3.33 Scanning electron micrograph illustrating an intact glomerulus enclosed within its (Bowman's) capsule. Note the urinary pole (U) opening into the proximal convoluted tubule.
SEM x 1,200.

Fig. 3.34 Scanning electron micrograph of parietal epithelial cells showing slender cilia (large arrows) arising from the centre of some of the cells. Note also the numerous microvilli of the proximal tubule (small arrow) as it leaves the urinary pole.
SEM x 5,000.

Fig. 3.35 Scanning electron micrograph of an intact glomerulus. Note that each capillary is invested with visceral epithelial cells.
SEM x 1,280.

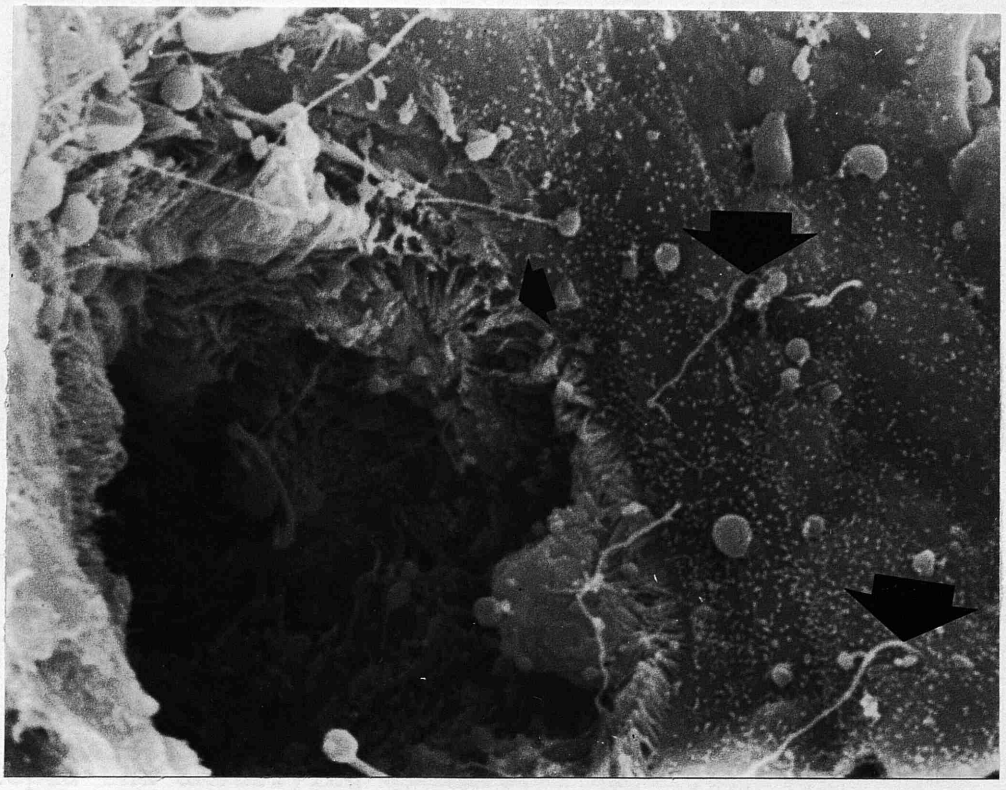

of each parietal cell (Fig. 3.34); these often appeared bent and twisted. The remainder of the parietal surface was covered with a sparse population of finger-like or bleb-like microvilli which were particularly abundant along the cell borders.

Visceral epithelium :

The most prominent feature of each glomerulus was the visceral epithelium or podocytes. These cells consisted of a large nucleated cell body from which arm-like cytoplasmic processes of varying length emerged and enveloped the underlying glomerular capillary loops (Fig. 3.35). The diameter of the major processes varied significantly along their length. The main or primary processes were flattened and ran, mainly in a circular direction, embracing the glomerular capillary wall (Fig. 3.36). From the lateral border of the primary processes issued thinner branches, the secondary and tertiary processes. Arising at right angles from these processes and sometimes from the cell body itself, were smaller, finger-like pedicles or foot processes. Foot processes also varied significantly in width and length; sometimes they were branched and they always interdigitated with foot processes arising from the same or adjacent podocytes and sometimes had bulbous swellings (Fig. 3.37). The cell body and the

Fig. 3.36 Scanning electron micrograph of glomerular podocytes. Note the complicated arrangement of the cytoplasmic processes.
SEM x 5,000.

Fig. 3.37 Scanning electron micrograph illustrating a podocyte cell body (P) with primary (1) and secondary (2) processes. Note the irregular arrangement of the pedicels (arrow) and the surface bleb-like microprojections.
SEM x 20,000.

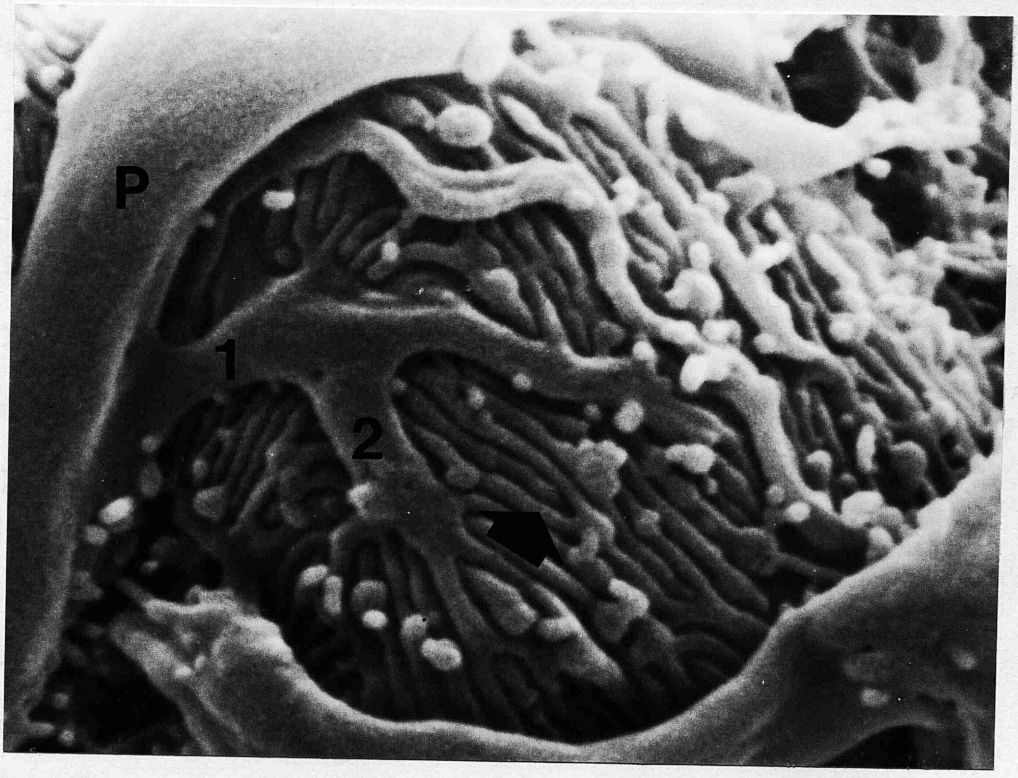
P
1
2

processes were generally uneven in surface configuration and often showed a population of finger-like or bleb-like microprojections arising from their surfaces.

In some sectioned glomeruli, the luminal surface of the capillaries was exposed. At high magnification, the endothelial fenestrae were represented by round or hexagonal pores. From the thickened nuclear portion of the endothelium extended narrow cytoplasmic ridges which were devoid of pores (Fig. 3.38).

Proximal tubule :

Most proximal tubules appeared either collapsed or full of what appeared to be debris so that the luminal surface morphology could not be clearly distinguished. Usually, however, enough segments remained patent and free of debris to allow suitable SEM observations (Figs. 3.39 and 3.40). The brush border, characterizing proximal tubules, was first detected on the luminal surface of Bowman's capsule adjacent to the urinary pole orifice (Fig. 3.34).

Long and slender cilia or tendrils were also observed in some cells and these were usually bent and twisted. These tendrils appeared to arise from cells on one side of the lumen and end with their tips expanded

Fig. 3.38 Scanning electron micrograph demonstrating the appearance of the endothelial surface of a glomerular capillary. Numerous endothelial pores or fenestrae are evident.
SEM x 20,000.

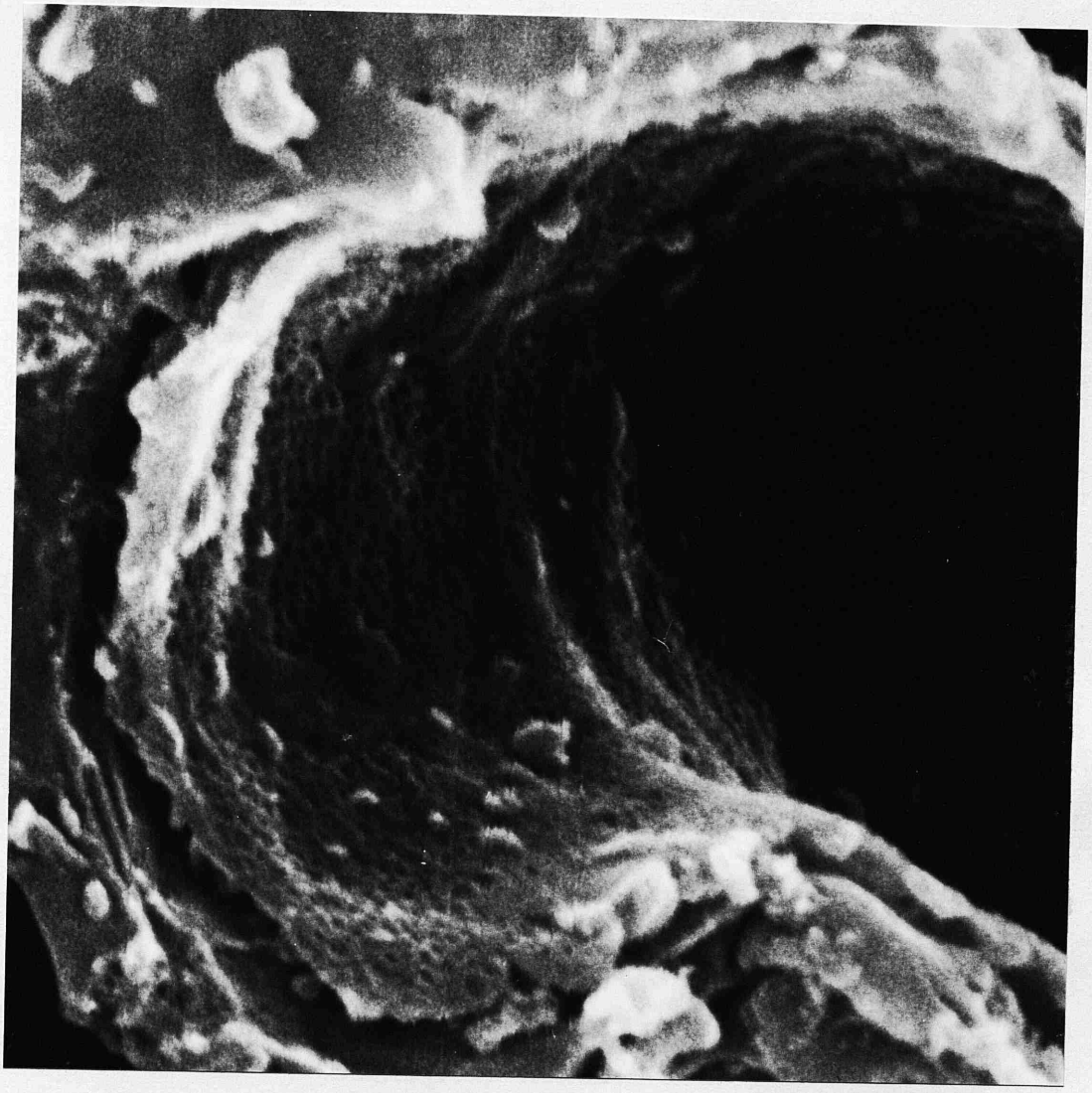

Fir. 3.39 Scanning electron micrograph of a transverse section of a proximal tubule. Note the numerous microvilli (arrow) covering the luminal surface.
SEM x 10,000.

Fig. 3.40 Scanning electron micrograph of the luminal surface of a proximal tubule showing the dense microvillous brush border.
SEM x 10,000.

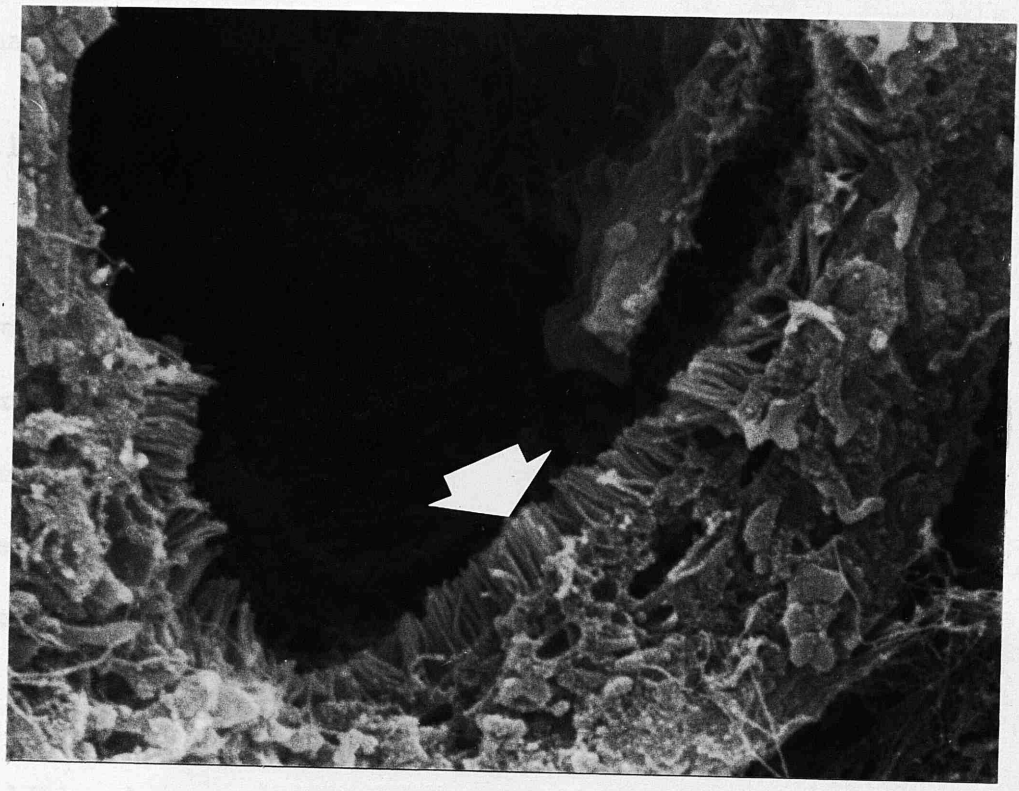

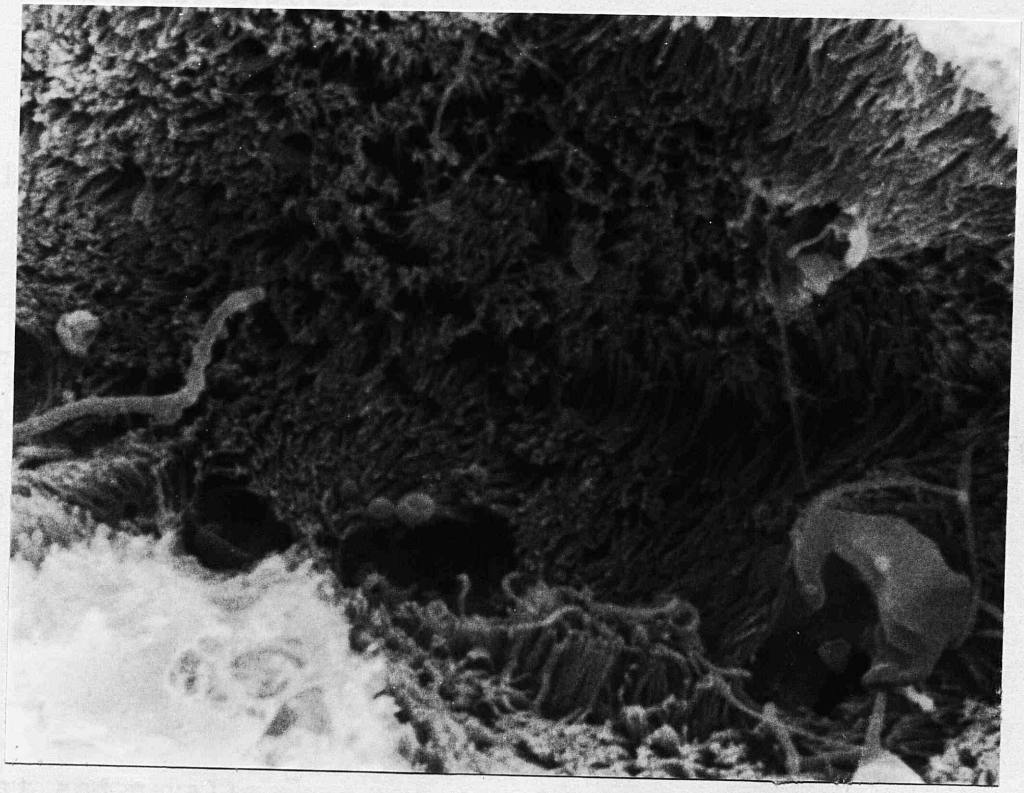

into variously sized globular masses on the opposite luminal side.

Thin limb of the loop of Henle :

The most distinguishing characteristic of these tubules was their very thin wall (Fig. 3.41). The cells appeared to bulge into the luminal surface in the region of the nucleus. The luminal surface of each thin loop cell exhibited a single, long, central cilium and a very sparse population of short, nub-like microprojections (Fig. 3.42).

Thick limb of the loop of Henle :

This was similar to the thin limb although on cross section the cells were more prominent (Fig. 3.43).

Distal convoluted tubule :

The identification of the distal tubule proved to be particularly difficult. Generally, it was composed of relatively thick cells which protruded into the lumen more so than the thick segment. The luminal surface of these cells exhibited either a few, or considerable numbers, of microprojections and most cells had a single central cilium (Fig. 3.44). These cilia were either long or short and usually were twisted and had bent tips.

Fig. 3.41 Scanning electron micrograph of transverse section of thin segments of the loop of Henle.
SEM x 2,500.

Fig. 3.42 A higher power scanning electron micrograph of a thin segment of the loop of Henle. A single cilium (arrows) projects from occasional cells. The presence of red blood cells is an artefact.
SEM x 5,000.

Fig. 3.43 Scanning electron micrograph of a transverse section of the thick ascending limb of Henle. Note the cuboidal epithelium.
SEM x 2,500.

Fig. 3.44 Scanning electron micrograph of the luminal surface of distal tubule. Short microprojections cover the luminal surface. A single cilium (arrow) arises from some of the cells.
SEM x 5,000.

Collecting tubule :

These tubules were easily identified in the medullary rays in the cortex and also in the medulla of the kidney by their large size and by their characteristic surface morphology. The shape and arrangement of surface epithelial cells gave a cobblestone appearance to the collecting tubular lumina (Fig. 3.45). The cells had a rounded or dome-shaped outline which protruded into the lumen (Fig. 3.46). Two distinct cell types were clearly distinguishable in the collecting tubules. One cell type (Type I) was characterized by its relatively smooth surface, paucity of surface microprojections and by the presence of one, and occasionally, two cilia (Fig. 3.47); the latter were usually bent or twisted. The microvillous projections on these ciliated cells appeared as minute bleb-like structures. The second cell type (Type II) did not possess a cilium, was usually covered with a moderate number of large microprojections and microplicae and often protruded into the lumina. The microprojections appeared either as short finger-like microvilli or as winding ridge-like microplicae. Microvilli, which were taller than those of the former cell type, were often at the borders of the cell and they served to distinguish the cell junctions.

Fig. 3.45 Scanning electron micrograph of collecting tubules demonstrating the cobblestone appearance of the tubular lumina.
SEM x 1,200.

Fig. 3.46 A higher power scanning electron micrograph of a collecting tubule demonstrating the cells with a round or dome-shaped outline protruding into the lumen.
SEM x 1,850.

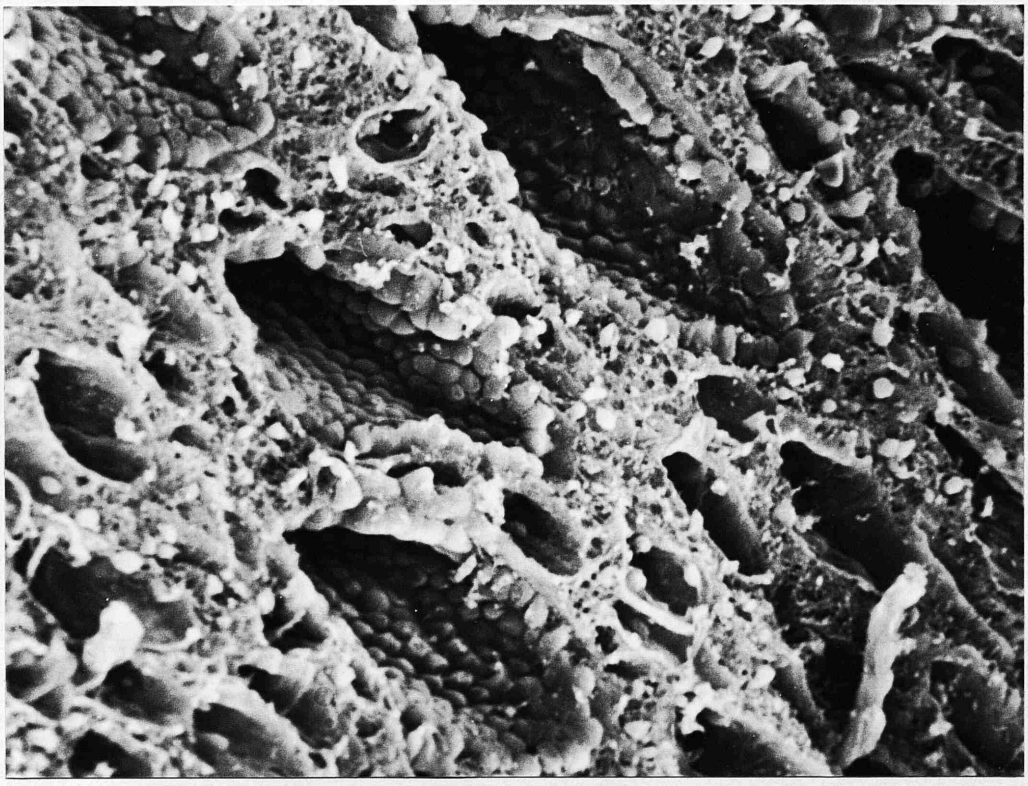

Fig. 3.47 Scanning electron micrograph of the luminal surface of a collecting tubule showing mainly type I smooth-surfaced epithelial cells. A cilium (large arrow) can be seen arising from the centre of one cell. Note also the type II cell with its surface microprojections (small arrow). SEM x 5,000.

Fig. 3.48 Scanning electron micrograph of a papillary duct. Note the cobblestone appearance of the luminal surface. Short cilia are occasionally noted (arrow). SEM x 5,000.

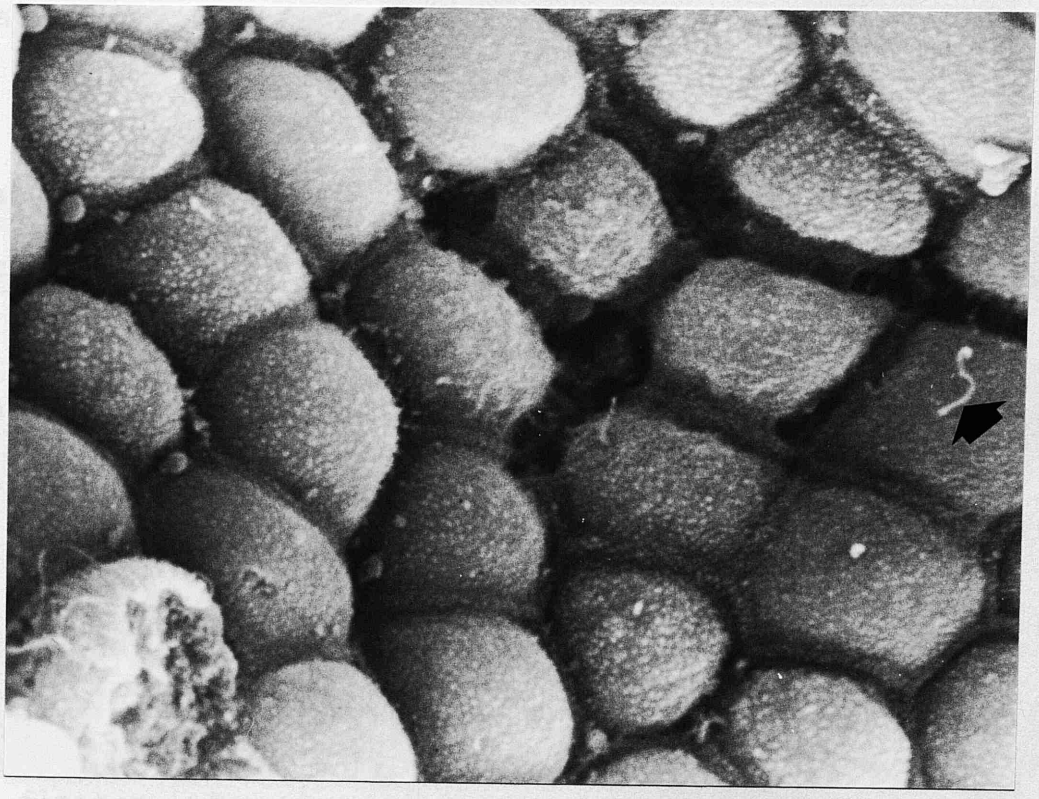

The Type I ciliated cells were more numerous than the non-ciliated Type II cells and usually the latter occurred singly rather than in groups.

Unlike the other parts of uriniferous tubules, the cell boundaries of collecting tubule cells were usually quite distinct. As the collecting tubules descended into the inner medulla, their lamina became larger and unciliated cells were found less frequently until the papillary duct was formed. The columnar papillary duct cell was characterized by stubby rounded surface microprojections and only occasionally had they a very short cilium (Fig. 3.48).

Renal papilla :

At low magnification, the renal papilla appeared as a cone with a blunt end (Fig. 3.49), on the top of which 12-20 small orifices were observed (Fig. 3.50). The openings generally were slit-like or oval in shape. On higher magnification, secondary pores were observed opening into the main orifices.

The epithelial cells at the opening of the papillary ducts had a cobblestone appearance while the cells in the areas between the openings of the ducts were much flatter, of various size and had a distinctive

Fig. 3.49 Scanning electron micrograph of a cone-shaped papilla. Note the numerous openings of the papillary ducts onto the surface.
SEM x 80.

Fig. 3.50 Scanning electron micrograph of the tip of a papilla. Note the slit-like openings.
SEM x 640.

pentagonal or hexagonal outline; this gave a honeycombed appearance to the papillary surface (Fig. 3.51). Some of the cells covering the external surface of the papilla were slightly higher than others and were characterized by deep grooves or ridges. These cells either occurred singly or in groups. Adjacent flatter cells lacked surface specialisations although randomly scattered microprojections were observed. These cells were sometimes slightly convex or showed a central depression (Fig. 3.52). Another cell type found on the wall of the papilla was characterized by numerous microprojections in the form of microplicae (Fig. 3.53).

Renal calyx :

The epithelium of the calyx was composed of irregularly shaped cells with grooves on their surface; however, "cobblestone" like cells with microprojections were also observed (Fig. 3.54).

Arterial casts of the kidney :

In corrosion tensol casts of the kidney, the vascular architecture (Fig 3.55) was clearly demonstrated. The renal artery before or after entering the hilus, usually divided into two main branches. Each branch divided into four to seven interlobar arteries (Fig. 3.56).

Fig. 3.51 Scanning electron micrograph of a papilla illustrating the honeycombed appearance of the surface. These epithelial cells are generally pentagonal or hexagonal in outline.
SEM x 2,500.

Fig. 3.52 Scanning electron micrograph of the surface of a papilla. Note the honeycombed appearance of the cells which are of various heights; some are slightly convex while others show a central depression. Note the prominent cell borders.
SEM x 5,000.

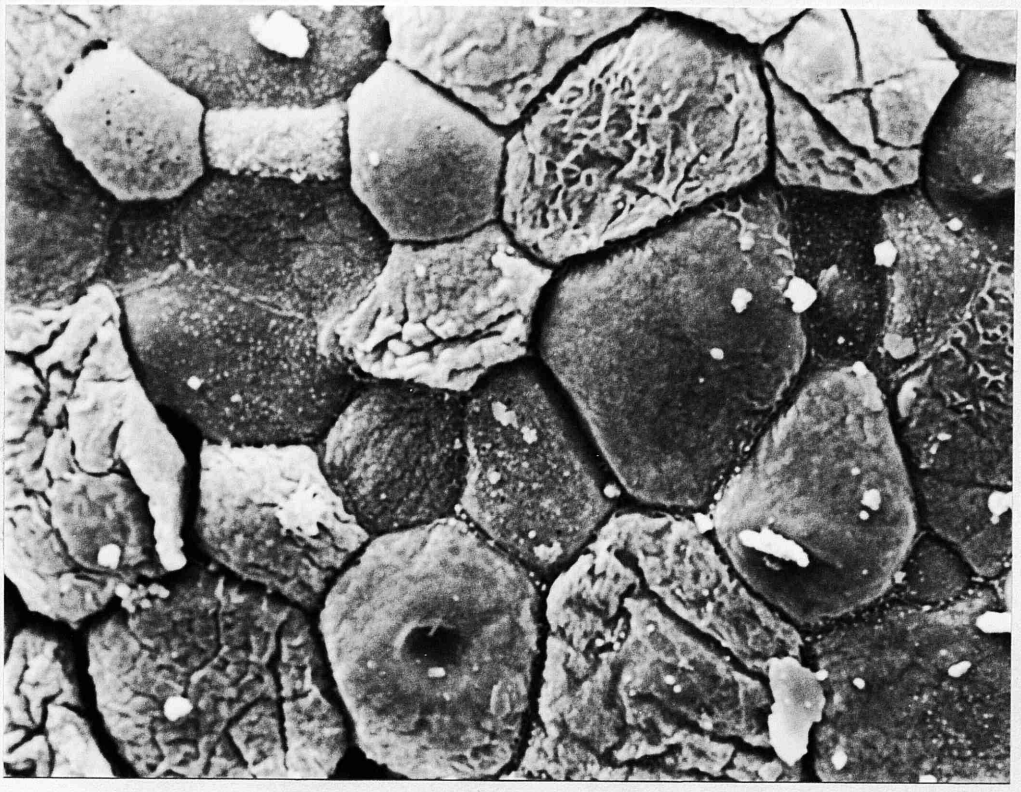

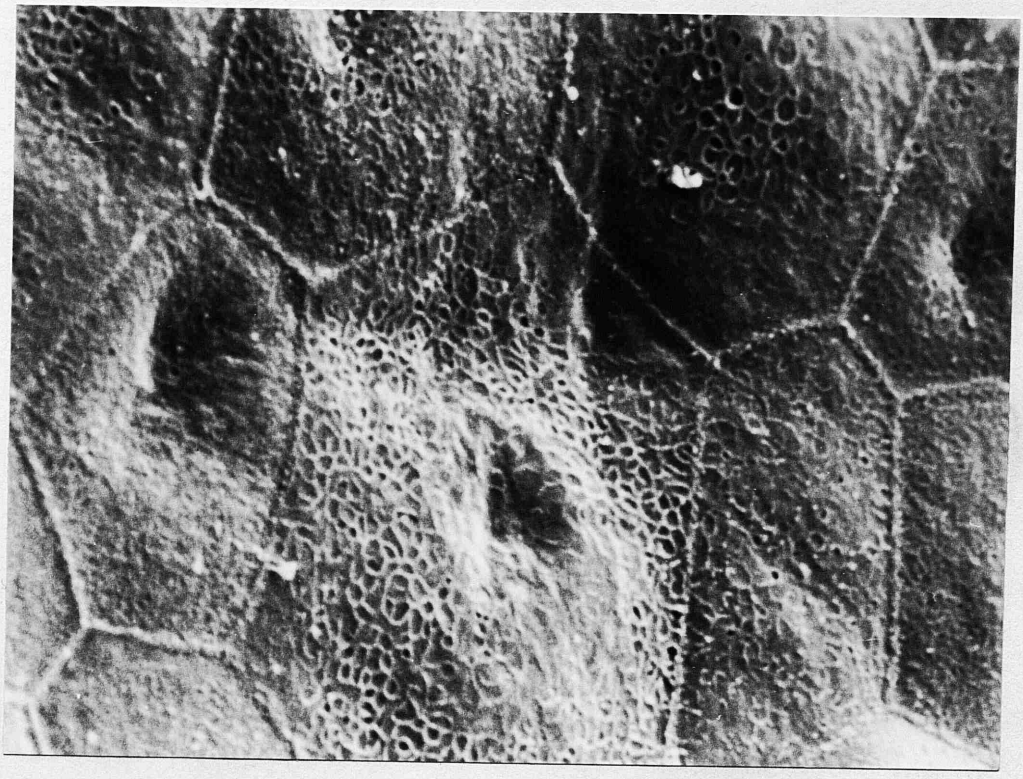

Fig. 3.53 Scanning electron micrograph of the wall of the papilla. These cell types are characterized by numerous microprojections in the form of microplicae.
SEM x 5,000.

Fig. 3.54 Scanning electron micrograph of the calyx illustrating the irregular cobblestone surface.
SEM x 640.

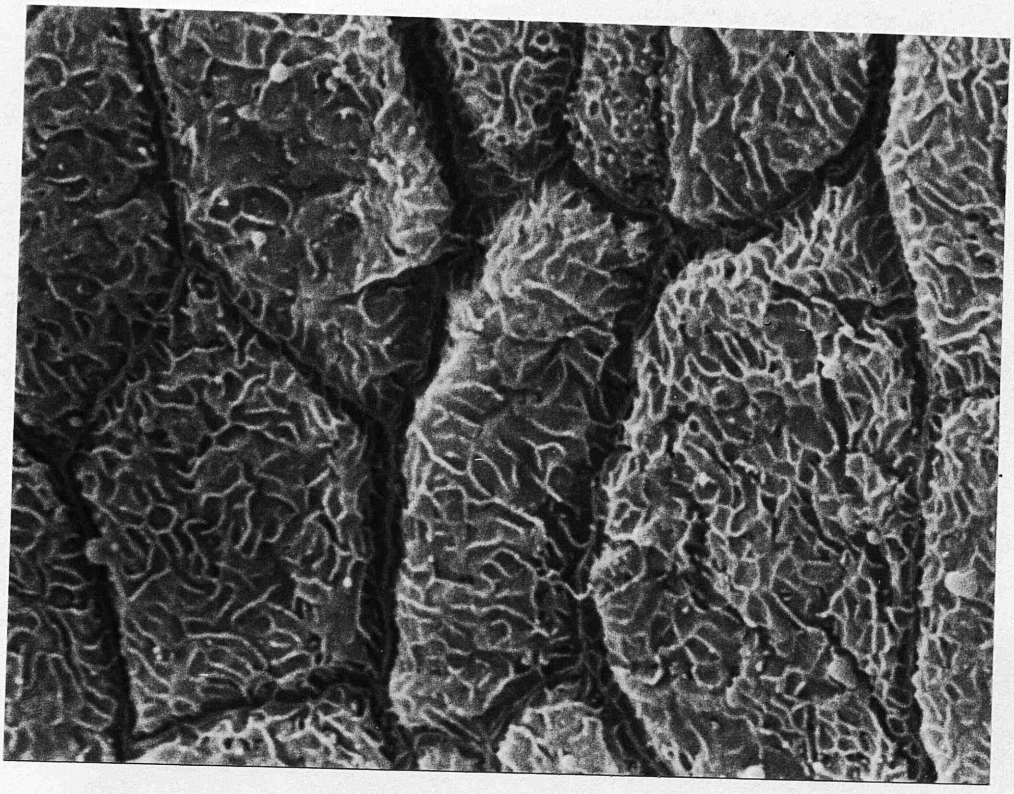

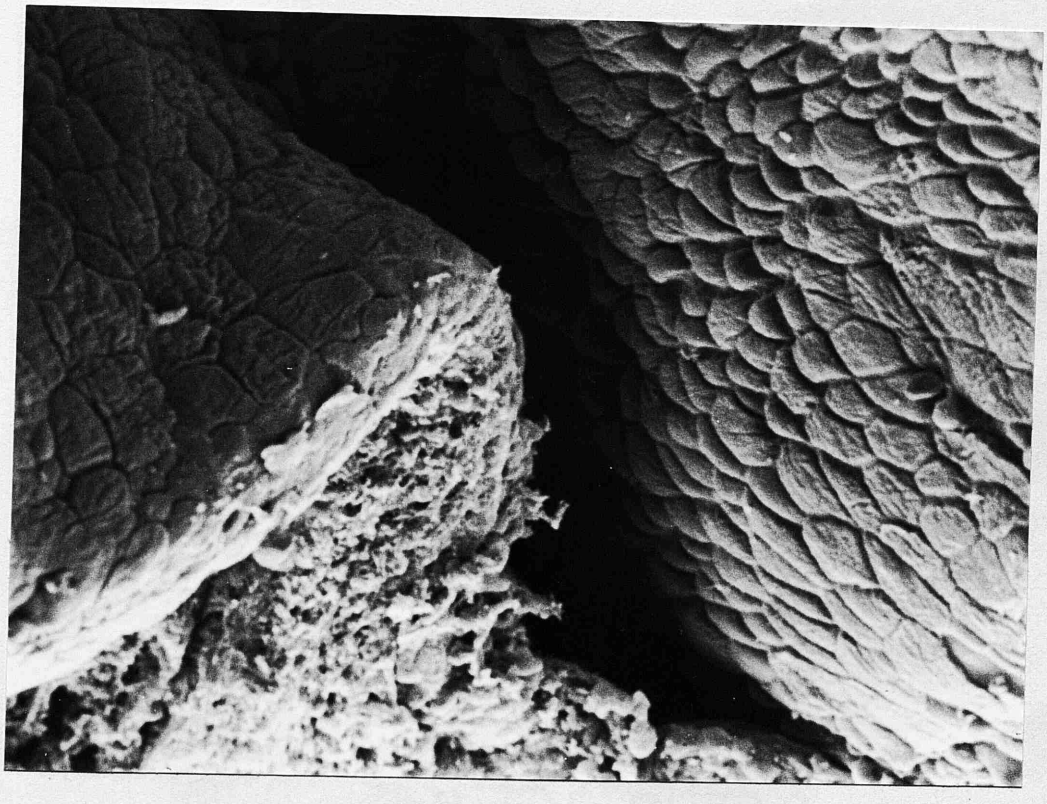

Fig. 3.55 Vascular cast of a swine kidney.

Fig. 3.56 Longitudinal section of a vascular cast illustrating the renal artery which divides into a number of interlobar arteries (arrows). The yellow-white structures are the calyces which were also filled with cast material.

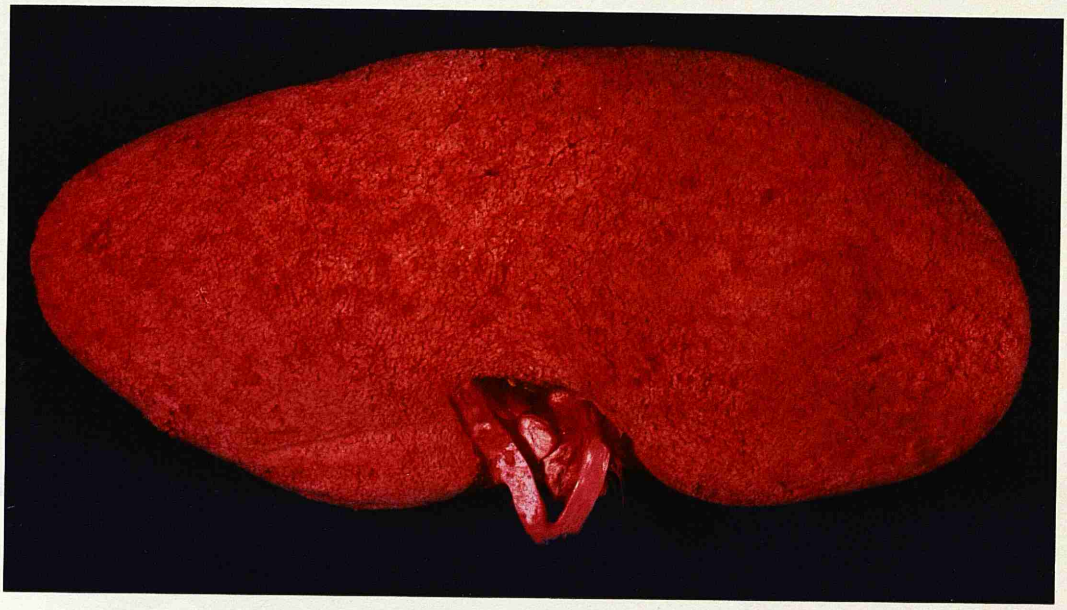

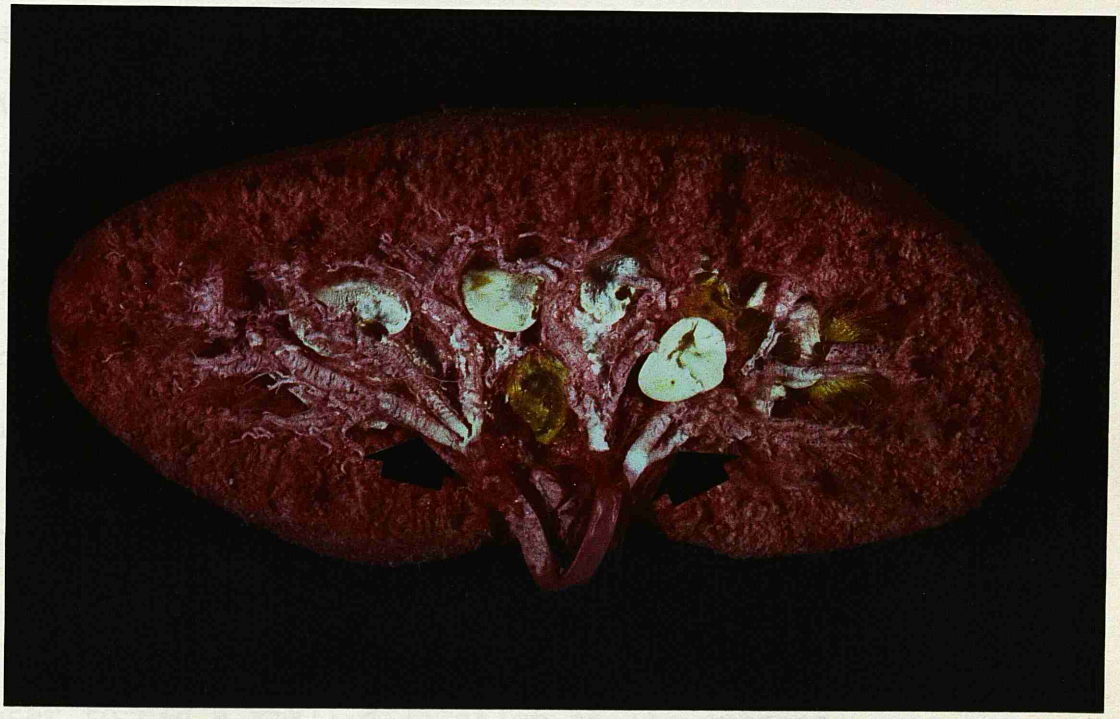

The interlobar arteries ran between adjacent medullary pyramids. These were traced by dissection with the aid of magnifying lens.

With SEM, the interlobular arteries were traced running vertically through the cortex and giving rise to afferent arterioles (Fig. 3.57). The afferent arterioles usually then divided into three-four major branches (Fig. 3.58). These inturn formed numerous uniform anastomoses forming a tuft of capillaries, the renal glomerulus (Fig. 3.59). The efferent arteriole, emerging from the glomerulus, was always thinner than the afferent arteriole. The peritubular capillary network, derived from the efferent arteriole leaving glomeruli, was noted to have a complicated anastomosing arrangement (Fig. 3.60).

The vasa recta, derived from the efferent arterioles of deep cortical and juxtamedullary glomeruli, were clearly shown as thin parallel-orientated vessels coursing through the medulla (Fig. 3.61).

Corrosion casts of the ureter :

The ureteral casts clearly exhibited that the ureter formed a small dilatation at its entrance into the kidney representing the renal pelvis. From the latter,

Fig. 3.57 Scanning electron micrograph of a vascular cast demonstrating the glomeruli arising from the afferent arterioles (arrows).
SEM x 160.

Fig. 3.58 Scanning electron micrograph of a vascular cast showing the afferent arteriole (A) dividing into three to four major branches.
SEM x 320.

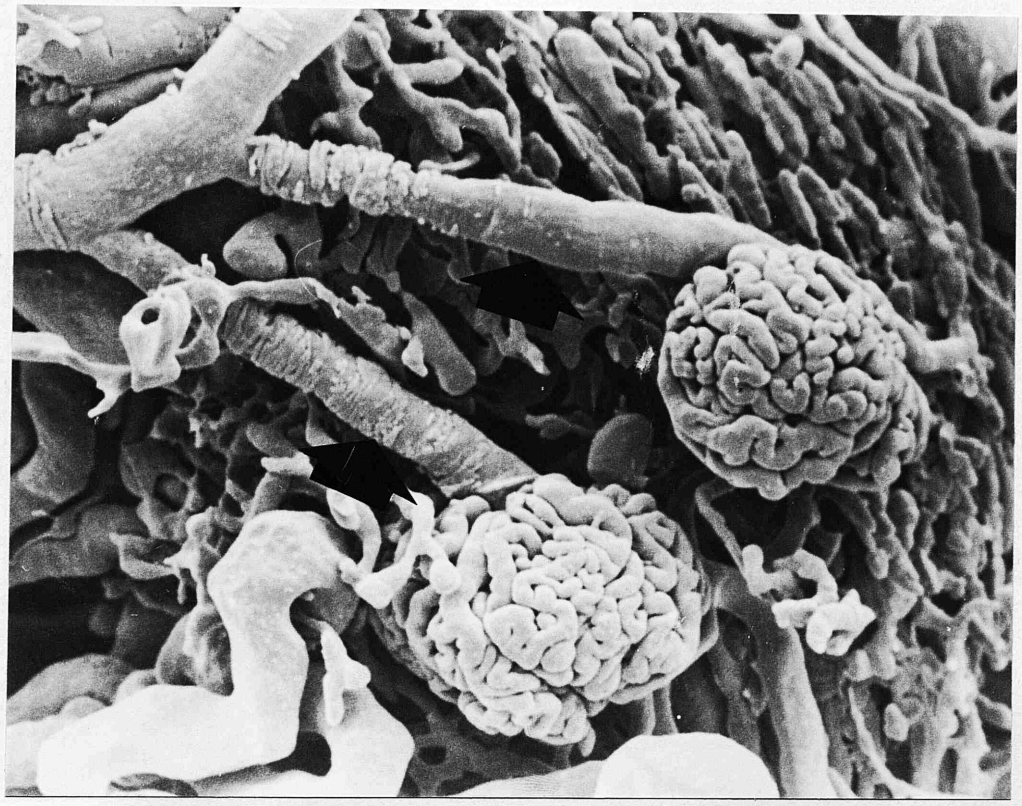


A

Fig. 3.59 Scanning electron micrograph of a single glomerulus. It consists of a rounded tuft of anastomosing capillaries.
SEM x 320.

Fig. 3.60 Scanning electron micrograph of vascular cast demonstrating the peritubular capillary network (arrow) derived from the efferent arteriole.
SEM x 160.

two major calyces extending to each pole of the kidney were formed, these in turn gave rise to many cup-shaped minor calyces, each associated with a medullary papilla (Fig. 3.62). Feathery structures observed at the end of some of the calyces represented casts of the papillary ducts.

b) Part II : Glomerular morphogenesis in neonatal pig kidneys.

Light microscopic observations :

The histological features of nephrogenesis in newborn piglets at one day is depicted in Fig. 3.63.

The nephrogenic zone was wide, occupying about 25% of the cortical width, and consisted of loose metanephric mesenchyme containing various stages of developing nephrons including caps of metanephric cells overlying the ampullae, oval-shaped metanephric vesicles and S-shaped structures. Immediately beneath the nephrogenic zone there was a zone of poorly developed glomeruli characterized by dark cuboidal visceral epithelial cells and poorly patent capillaries (Fig. 3.64). The visceral epithelial cells of corpuscles deeper in the cortex were more squamous and stained less intensely. In these corpuscles, many of the capillaries were patent

Fig. 3.61 Scanning electron micrograph of a vascular cast of the medulla demonstrating the straight vasa recta.
SEM x 160.

Fig. 3.62 Ureteral cast. The junction of the ureter (U) and major calyces (C) shows a dilation suggestive of a renal pelvis. Minor calyces (*). Note the papillary duct and collecting tubules draining into one calyx (arrow).

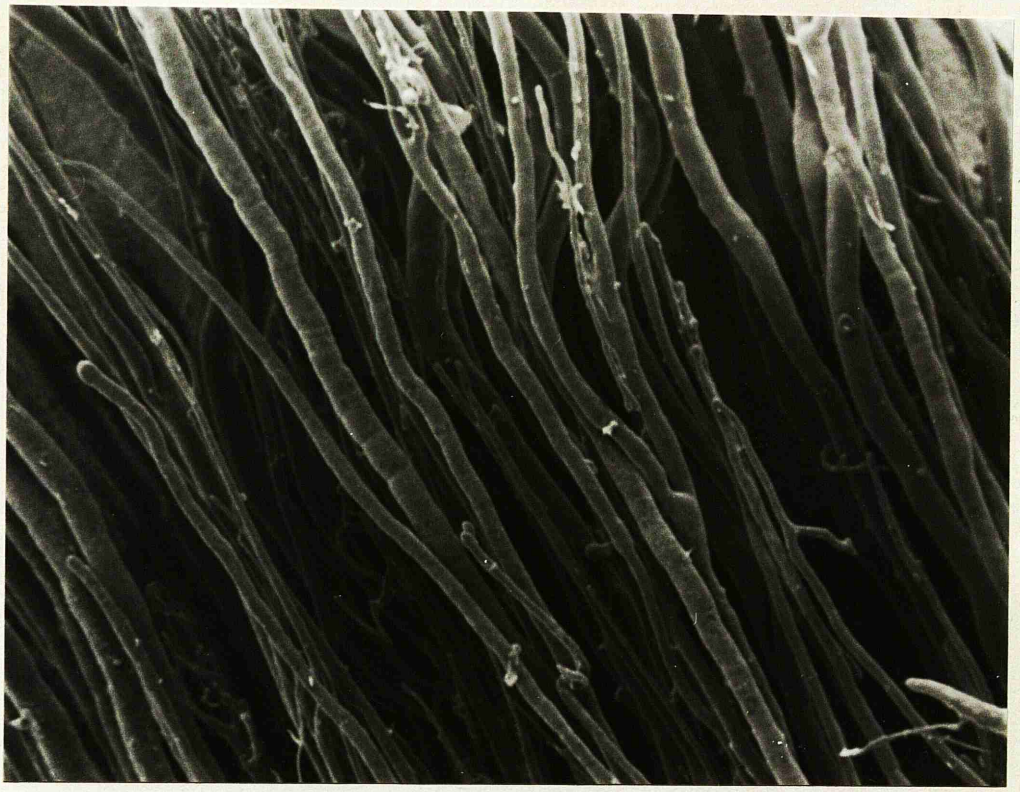

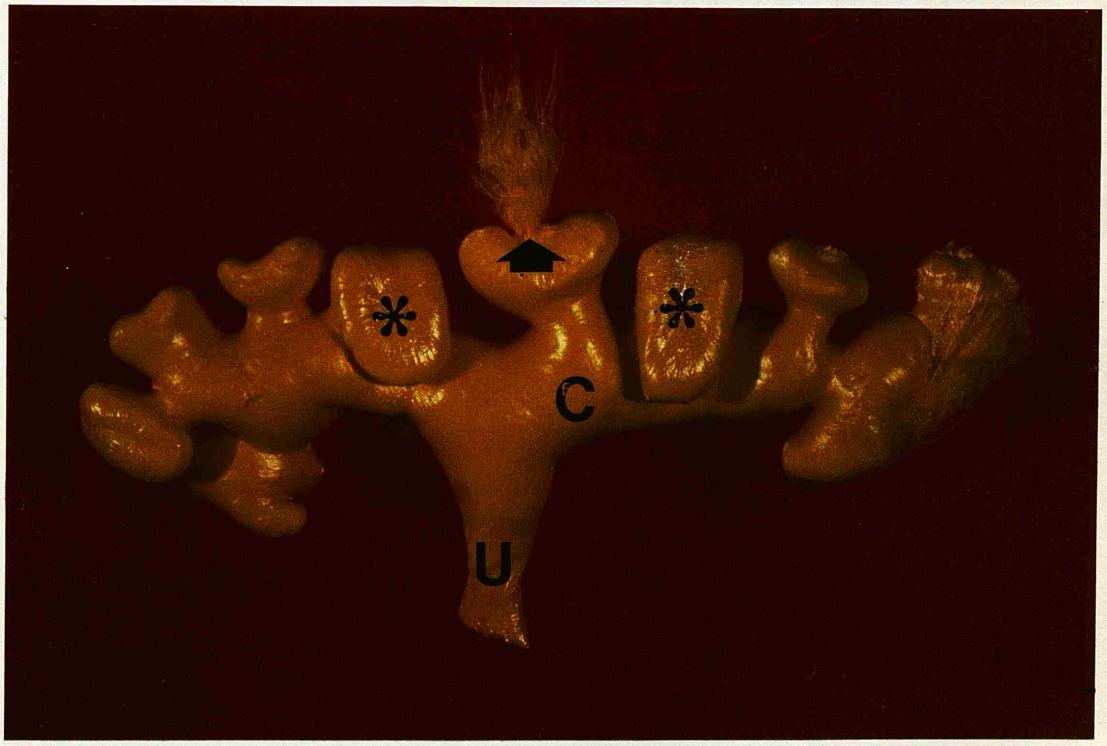
*
*
C
U

Fig. 3.63 Section of outer cortex at day one of age showing a broad nephrogenic zone consisting of metanephric mesenchyme. Note the oval-shaped metanephric vesicles (small arrow) and S-shaped structures (large arrow). Note also two straight branches of the ureteric bud (*).
HE x 120.

Fig. 3.64 Section of deep cortex at day one of age showing poorly developed glomeruli with few patent capillaries. Note the prominent cuboidal visceral epithelial cells situated around the perimeter of each glomerulus.
HE x 120.

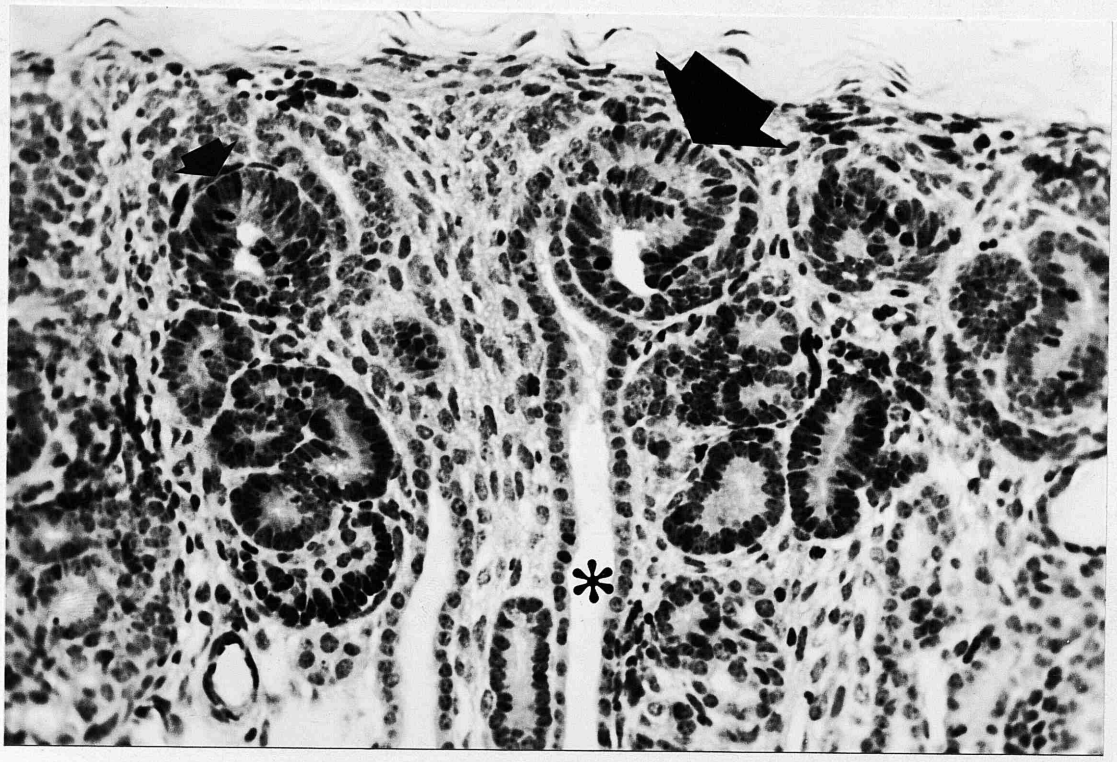

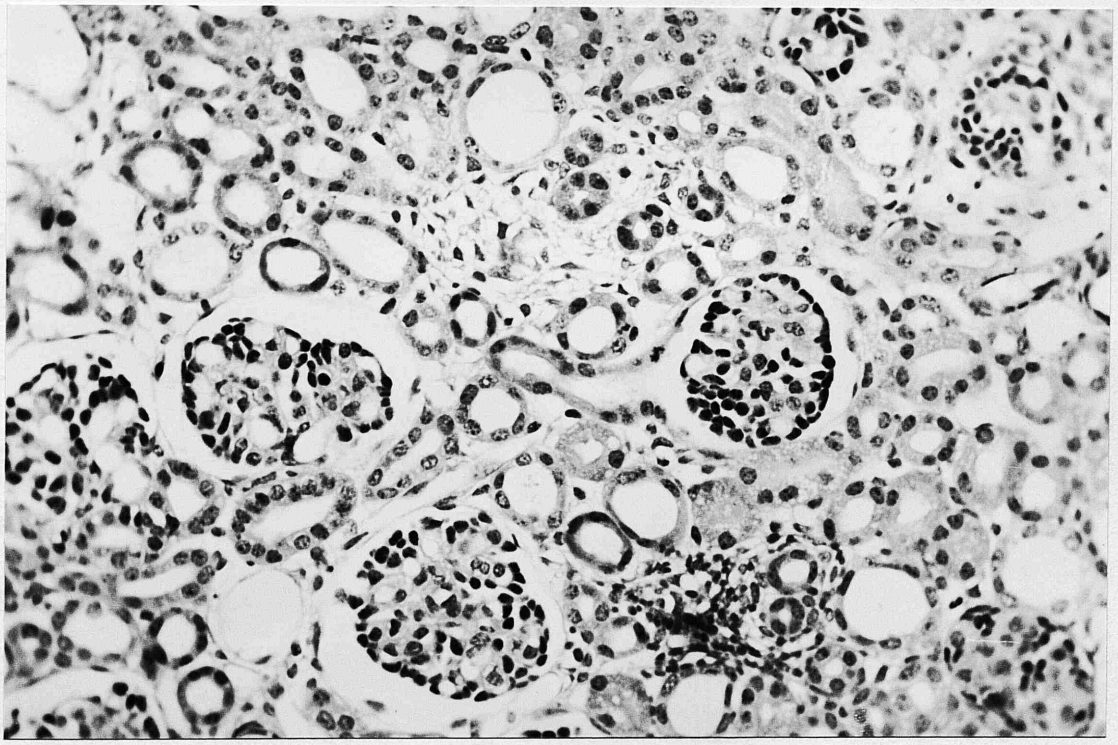

(Fig. 3.65). At this time, the number of functioning glomeruli (i.e. glomeruli with patent capillaries) comprise approximately 10% of the total.

At one week, the nephrogenic zone was still present but narrower and confined to the outer cortical region (Fig. 3.66).

Approximately 25% of the total number of glomeruli were judged to be functional in as much as they had patent capillary loops.

By two weeks, the nephrogenic zone was still present, although confined to a narrow subcapsular band (Fig. 3.67). The number of functioning glomeruli had increased.

By four weeks, the nephrogenic zone had all but disappeared (Fig. 3.68) and the percentage of functioning glomeruli had increased to approximately 50% of the total. Many immature glomeruli with few patent loops and prominent visceral epithelium, however, could still be seen scattered throughout the outer and mid cortical regions.

By six weeks mature functioning glomeruli predominated but, even at this stage, approximately 10% of glomeruli still showed prominent cuboidal visceral

Fig. 3.65 Section of the deep cortex at day one of age showing more patent capillaries in these inner cortical glomeruli. Note the visceral epithelial cells are now more squamous in form.
HE x 200.

Fig. 3.66 Section of outer cortex at one week of age showing a much narrower nephrogenic zone.
HE x 65.

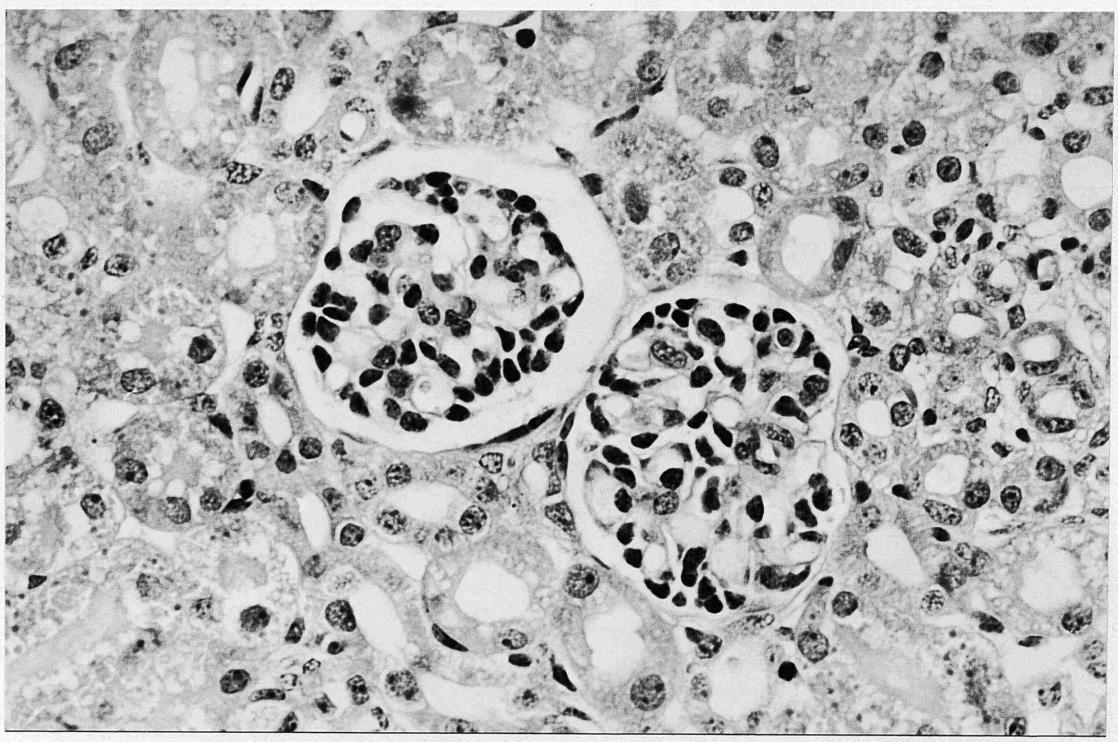

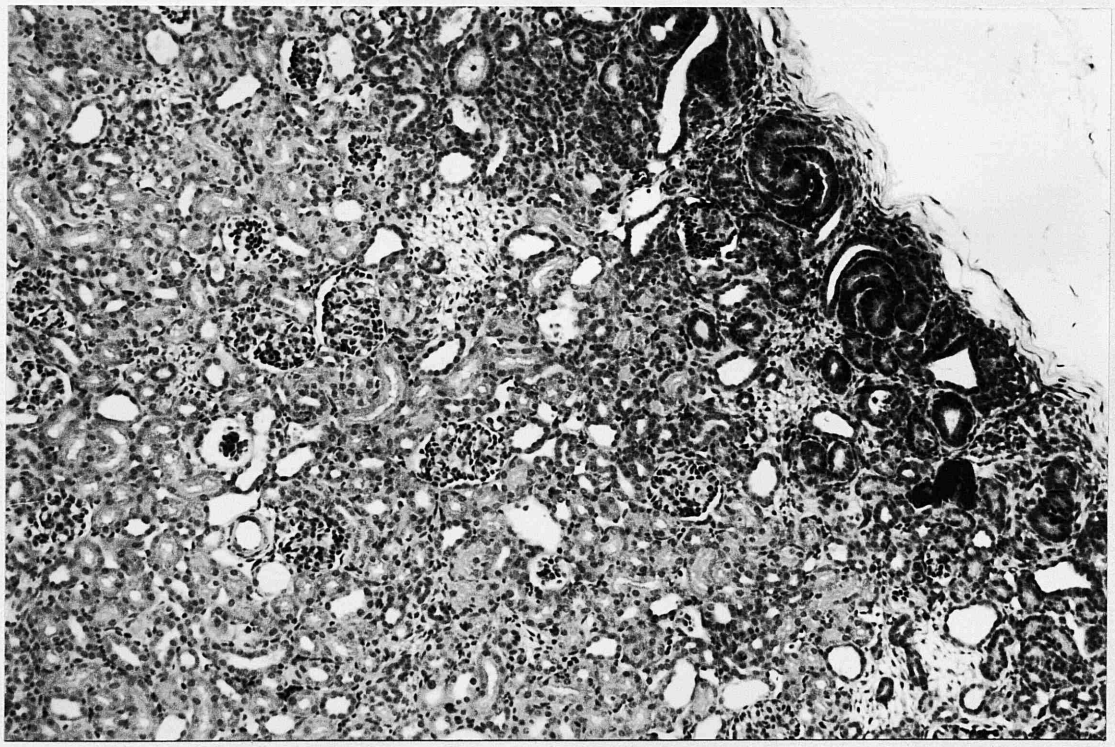

Fig. 3.67 Section of renal cortex at two weeks of age. The narrow nephrogenic zone is confined to the immediate subcapsular area.
HE x 65.

Fig. 3.68 Section of renal cortex at four weeks of age. The nephrogenic zone has vanished but immature glomeruli with few patent loops can still be found scattered throughout the outer and mid cortical regions.
HE x 120.

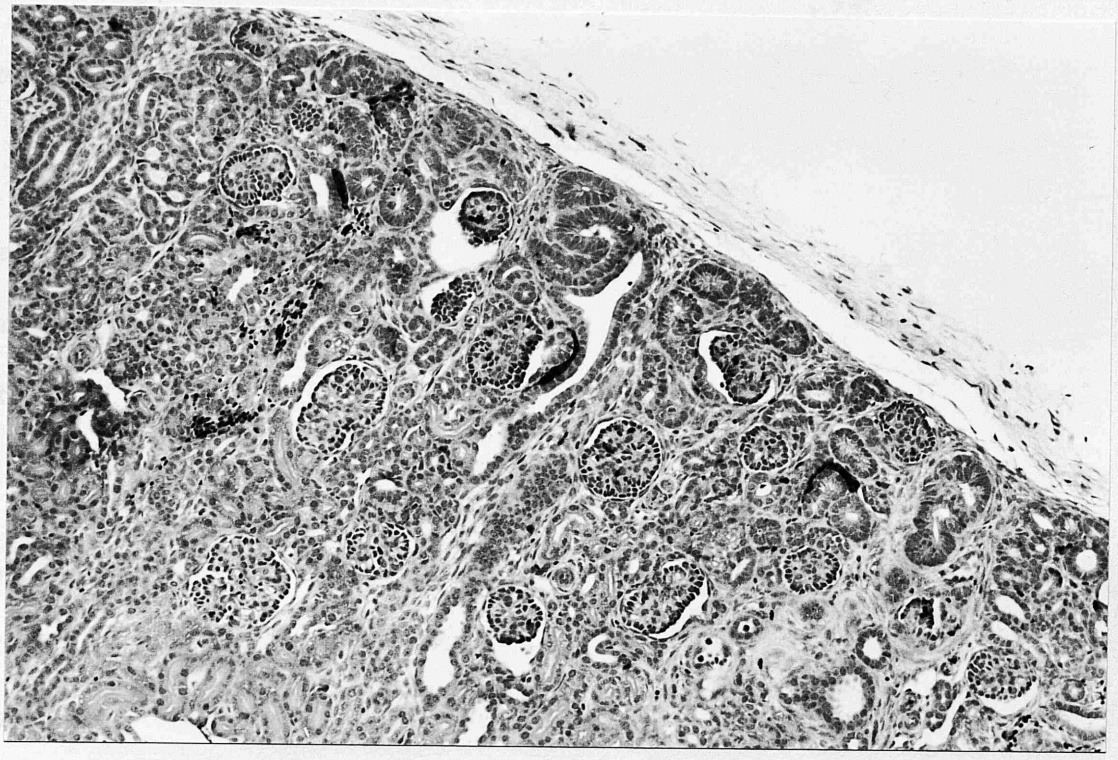

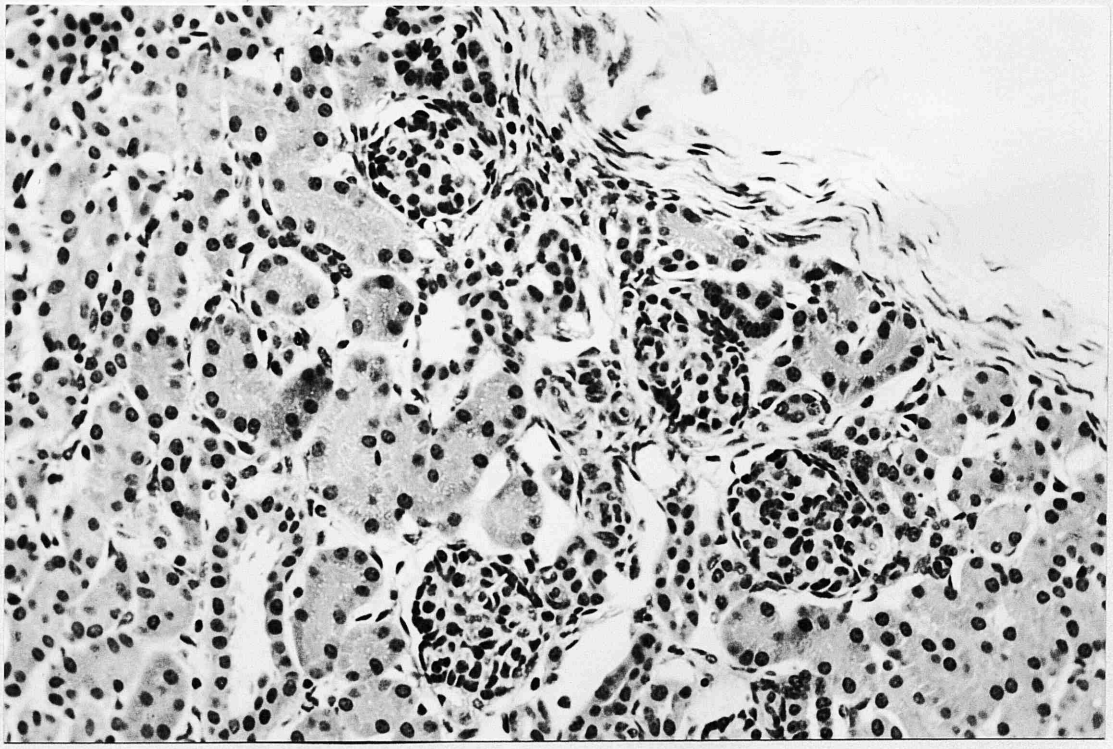

epithelium and with few patent loops.

TEM observations :

In this part of the work, emphasis was placed in examining identifiable immature glomeruli in the outer cortical region and comparing their structure with the mature functional glomeruli in the deep cortex.

The immature glomerulus was spherical and with a distinct Bowman's space and a few or no capillary loops. Endothelial and mesangial cells were difficult to distinguish. The prominent visceral epithelial cells with apically disposed nuclei were separated by narrow intercellular clefts at the basal third of which junctional complexes were present (Fig. 3.69).

The elongated cytoplasmic part of the endothelial cells extending around the inner aspect of the capillary loops contained numerous small pores or fenestrae each closed by a thin diaphragm (Fig. 3.70). However, in more mature glomeruli in the deep cortex, more patent capillary loops were observed (Fig. 3.71) and at this stage the visceral epithelial cells, while still prominent, were separated by wide spaces and had developed the characteristic foot processes.

In the most developed glomeruli in the deep

Fig. 3.69 Electron micrograph of an immature glomerulus showing cuboidal visceral epithelial cells (arrow) separated by narrow intercellular clefts. Note the absence of patent capillaries.
TEM x 4,000.

Fig. 3.70 Electron micrograph of a more mature deep cortical glomerulus showing the elongated cytoplasmic part of the capillary endothelium around the inner aspect of the GBM. Note that the fenestrae are bridged by a thin diaphragm (arrow).
TEM x 40,000.

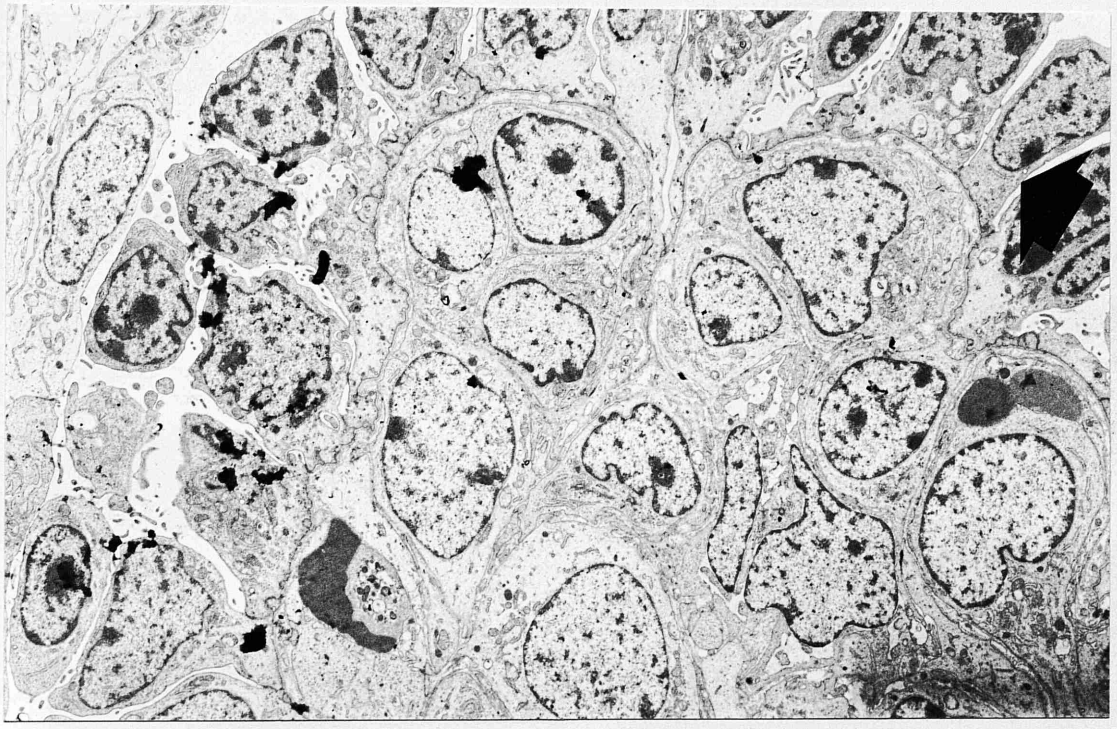

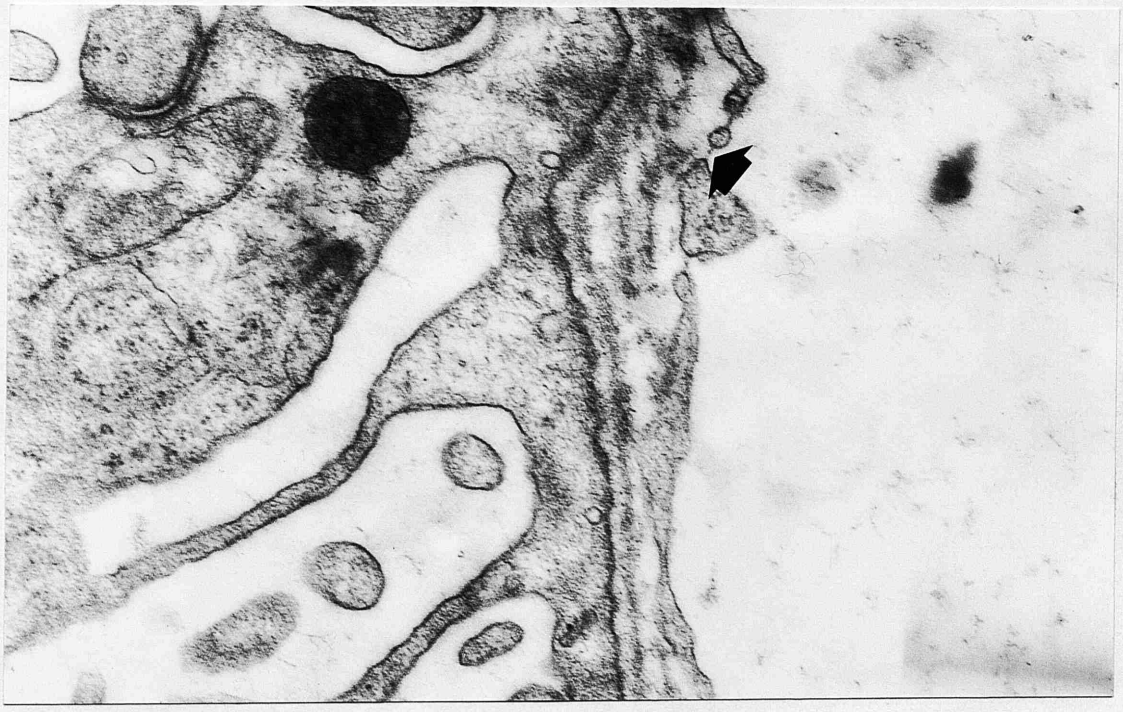

Fig. 3.71 Electron micrograph showing more patent capillary loops in a more mature glomerulus in the deep cortex.
TEM x 5,400.

Fig. 3.72 Electron micrograph from the deep cortical region showing multiple patent capillary loops.
TEM x 2,800.

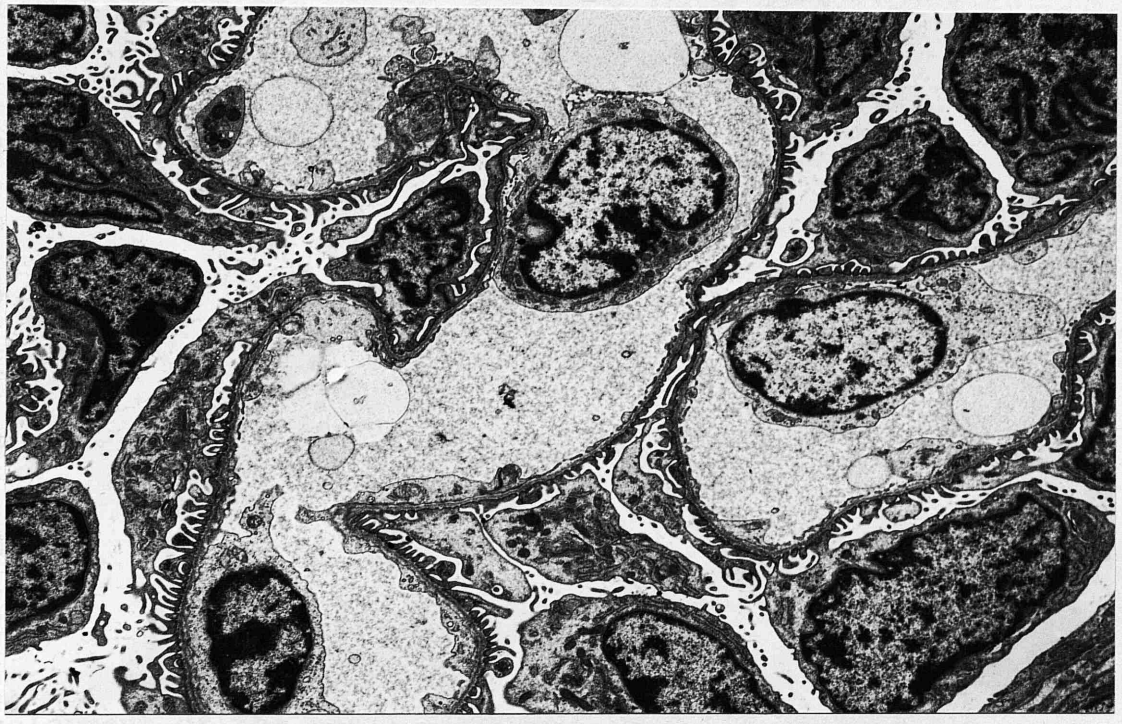

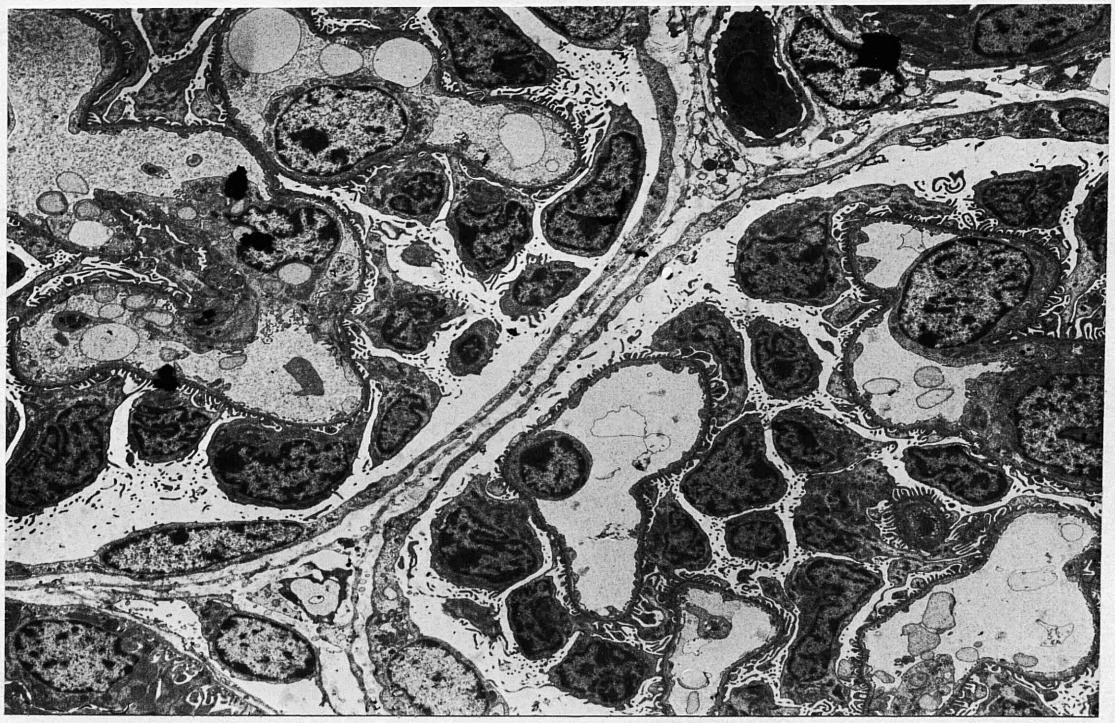

cortical region of the piglets examined from one day to six weeks, multiple patent capillary loops were always to be found (Fig. 3.72). The visceral epithelial cells had achieved their mature flattened configuration with numerous primary processes and foot processes (Fig. 3.73). The endothelium contained numerous fenestrations but unlike the less mature glomeruli in the outer cortex, the diaphragms covering the fenestrae had disappeared.

SEM observations :

The earliest recognisable structures in the development of the renal corpuscle were the metanephric vesicles (Fig. 3.74) and S-shaped structures (Fig. 3.75), corresponding to those found on light microscopy.

In the least differentiated glomeruli, capillary loops were not discernible (Fig. 3.76) and the visceral epithelial cells were cuboidal to columnar in shape and closely apposed to each other. The plasma membrane of these cells was studded with small projections, and no foot processes were evident (Fig. 3.77).

In later stages of glomerular development, the visceral epithelial cells started to give off cytoplasmic processes which interdigitated between two adjacent cells (Fig. 3.78). Subsequently, the cell bodies separated from

Fig. 3.73 Electron micrograph of a mature glomerulus showing well developed visceral epithelial cells with numerous primary processes and foot processes. At this stage (4 weeks), the fenestrae do not have diaphragms. TEM x 16,000.

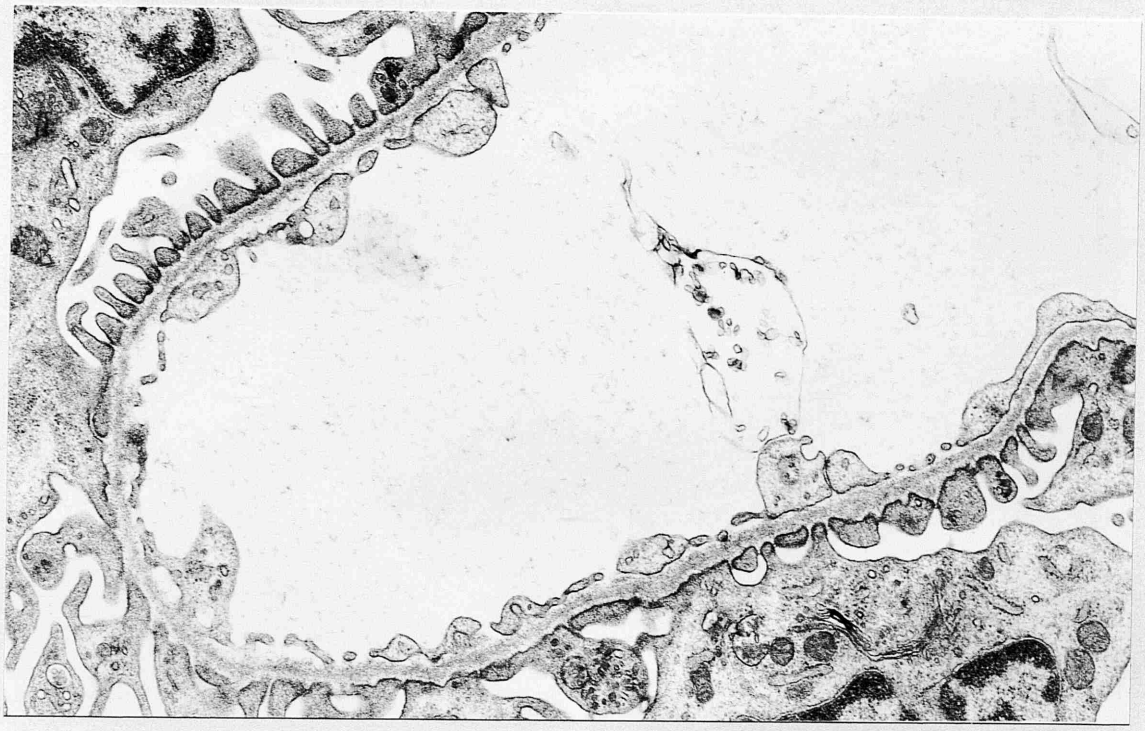

Fig. 3.74 Scanning electron micrograph showing the earliest recognisable structures in the development of the renal corpuscle, the metanephric vesicles (arrows).
SEM x 320.

Fig. 3.75 Scanning electron micrograph of an S-shaped structure (arrow).
SEM x 640.

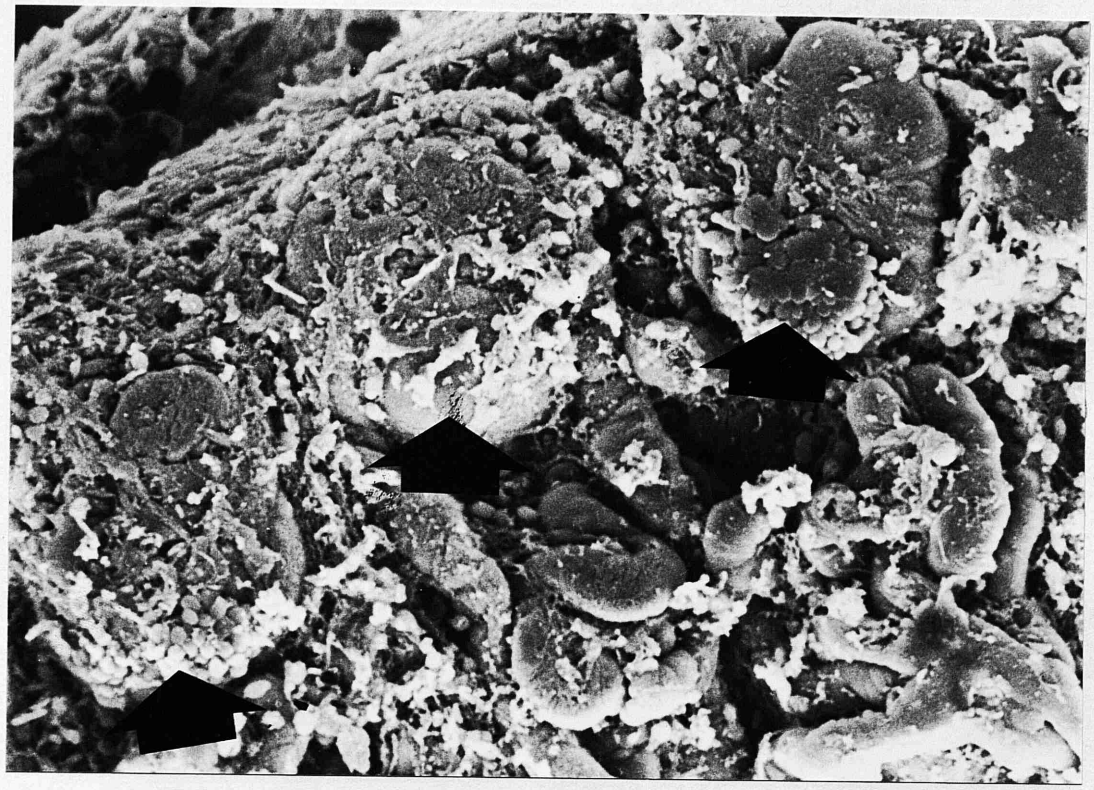

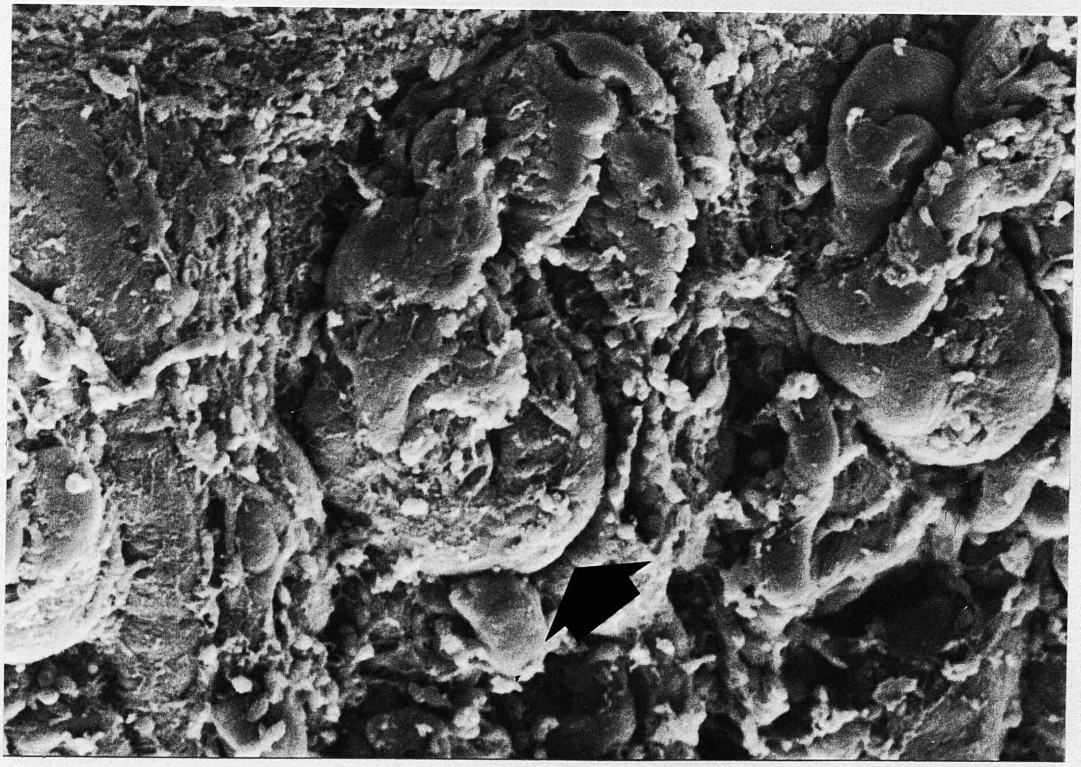

Fig. 3.76 Scanning electron micrograph showing a poorly developed glomerulus within its capsule. Note that the capillary loops are not discernible.
SEM x 2,500.

Fig. 3.77 Scanning electron micrograph of a developing glomerulus showing cuboidal visceral epithelial cells. Small projections are present on the plasma membrane, but there are no foot processes.
SEM x 10,000.

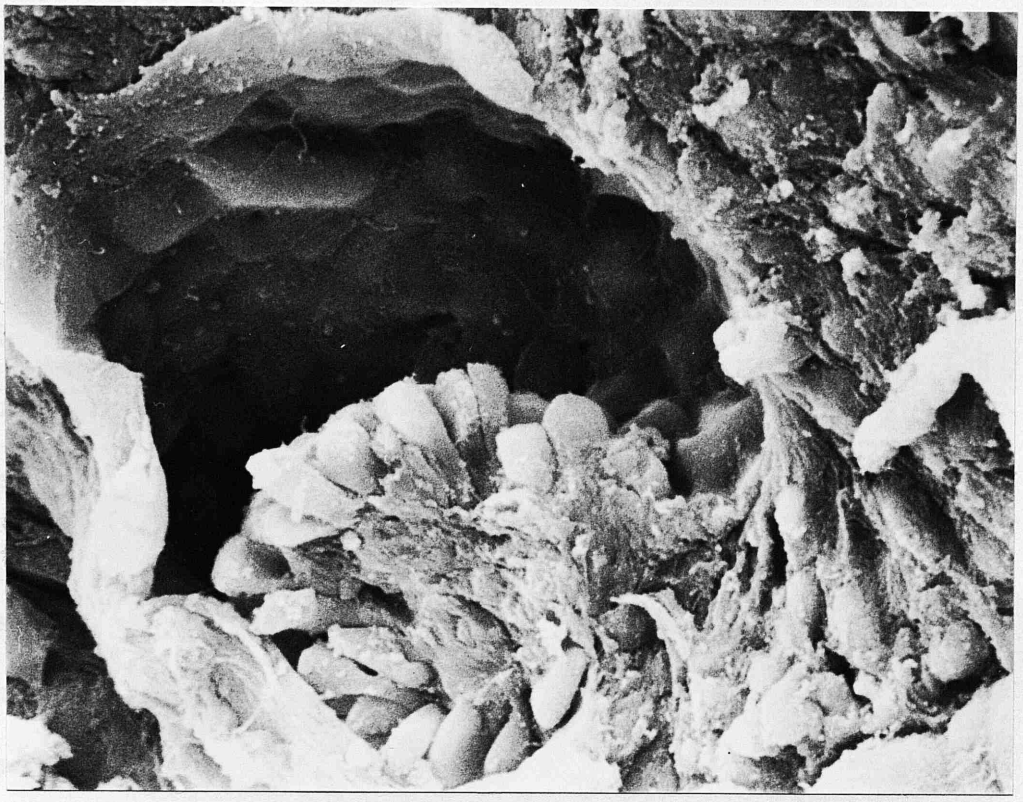

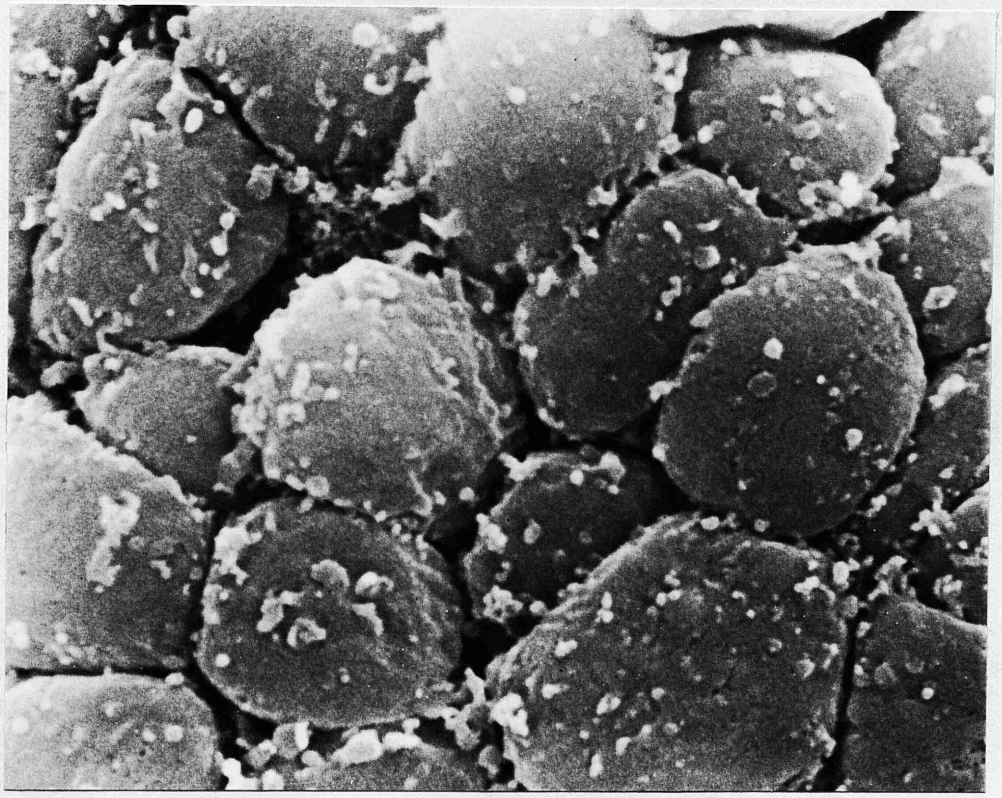

each other and the interdigitating foot processes also became more discernible (Fig. 3.79).

Mature glomeruli were recognized by their large size and by the presence of lobules created by tortuous capillary loops as well as fully developed squamous visceral epithelial cells (podocytes). The cytoplasmic processes of the latter cells overlaid the capillary loops (Fig. 3.80). Wide and flat primary cytoplasmic processes arose from the cell body of each podocyte and branched to form secondary and sometimes tertiary processes. Smaller, fingerlike processes usually arose from the secondary processes and interdigitated with pedicles from other visceral epithelial cells.

Discussion :

The gross anatomical features of the pig kidney reported in this study were consistent with those of other reports (Sisson, 1975; Nickel et al, 1979; Frandson, 1981). The externally smooth but multipapillated appearance of the pig kidney indicated partial fusion of their lobes, similar to that reported in human kidneys (Tisher, 1981). It is well established that the externally lobed appearance of the mammalian kidney is an embryonic characteristic (Arey, 1954; Du Bois, 1969). In the present study, only a few kidneys, all from young pigs, showed partial surface lobation.

Fig. 3.78 Scanning electron micrograph of a developing glomerulus showing early differentiation of foot processes.
SEM x 10,000.

Fig. 3.79 Scanning electron micrograph of a more mature glomerulus showing more advanced development of the interdigitating foot processes.
SEM x 10,000.

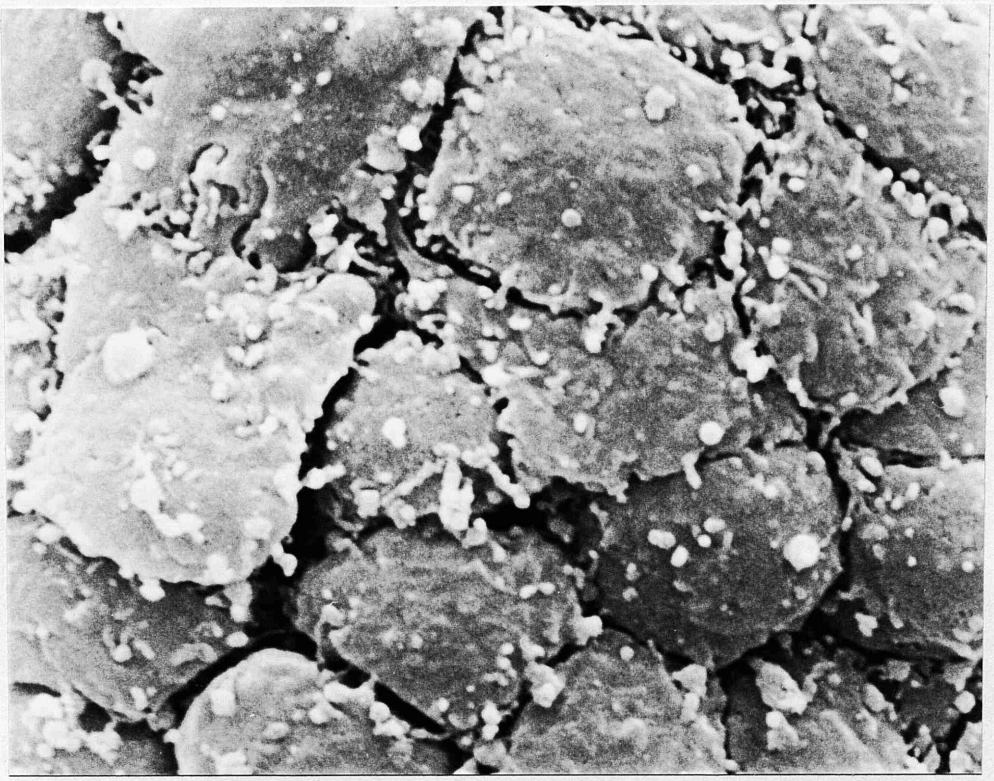

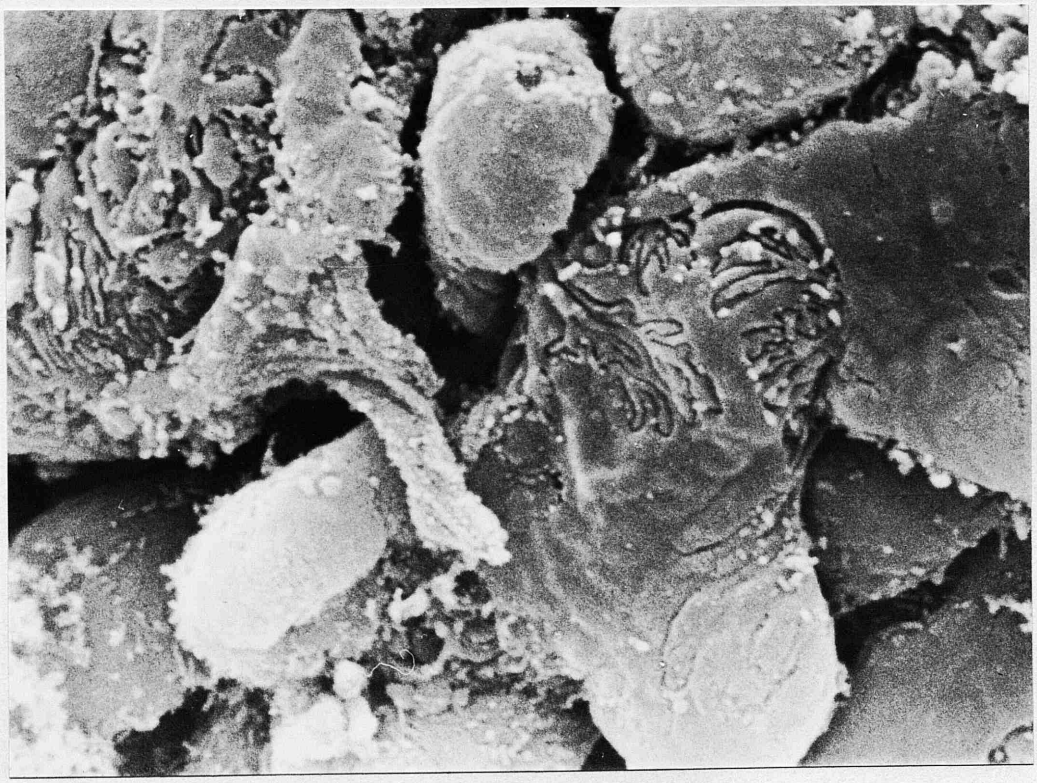

Fig. 3.80 Scanning electron micrograph of a mature glomerulus. Visceral epithelial cells are now clearly well-developed.
SEM x 2,500.

Graham (1953) reported that both human and pig kidneys have a small flattened pelvis from which two major calyces arise, each dividing into several smaller minor calyces which receive individual renal papillae. This was confirmed in the present study.

The internal morphology of the mammalian kidney has been thoroughly studied in a number of mammalian species including the rat (Trump and Bulger, 1968; Thoenes and Langer, 1969; Latta, 1973; Maunsbach, 1973; Osvaldo-Decima, 1973), man (Tisher et al, 1966; Myers et al, 1966; Bulger et al, 1967; Trump and Bulger, 1968; Tisher et al, 1968; Jorgensen and Bentzon, 1968), rabbit (Wellings and Wellings, 1975, 1976) and non-human primates (Tisher et al, 1969; Andrews, 1975). Despite the similarity between the mammalian kidneys, these studies highlighted the fact that there are profound morphological differences among the species studied and, despite the frequent use of pigs as experimental animals, no comprehensive morphological study of their kidneys has been reported.

The only histological study performed on the pig kidney appears to have concentrated on comparative aspects with other mammals (Yadava and Calhoun, 1958). These workers reported that, in the pig, the juxtamedullary

corpuscles are larger than the cortical ones. The present study confirmed the above findings and added the observation that the outer cortical glomeruli had closed capillary lumina with resultant difficulty in identifying the constituent glomerular cell types.

The comparison made in the present study between perfusion and immersion fixation showed that, although both methods produced good fixation for both conventional light microscopy and electron microscopy, perfusion fixation appeared to be superior to immersion fixation with respect to patency of the glomerular capillaries which allowed better differentiation of glomerular cells on light microscopy. The disadvantages of perfusion fixation were that the capillary lumina and urinary space were sometimes artificially widened and, while some glomeruli were evenly perfused, others, particularly in the outer cortex, were not perfused properly and their capillary lumina remained closed.

Although Osborne and Vernier (1973) cites Trump and Bulger (1968) as regarding the renal corpuscle of all mammals to be similar in morphology, the pig kidney has never been examined in detail by light microscopy and no TEM or SEM study has been carried out.

The literature concerning Bowman's capsule and

parietal epithelium is very sparse. It appears that, in the majority of mammals, the parietal epithelial lining of the capsule is a single layer of squamous cells. This was the appearance recorded in the present study. However, Mayer and Ottelenghi (1947) showed that the parietal epithelium of the renal corpuscle of dogs and cats varied between three types a) squamous cells lining the capsule with a sudden transition to the cuboidal cells of the proximal convoluted tubule at the urinary pole, b) predominantly squamous cells at the vascular pole with gradual increase in cell height near to the urinary pole and c) capsule completely surrounded by cuboidal epithelium. In the present study, the pig parietal epithelium appeared to conform with the first type.

The SEM appearance of the parietal epithelium covering Bowman's capsule has only rarely been described. Andrews and Porter (1974) and Webber and Lee (1974) were the first to report the presence of one or two long cilia arising from near the nucleated centre of each parietal cell in rats; Spinelli (1974), on the other hand, found cilia in the centre of only occasional cells. In the present study, it was noted that one and occasionally two long cilia arise from near the nucleated centre of each parietal cell.

When studied by SEM, the cell body of the visceral epithelial cell often show a large number of surface microvilli and microprojections (Buss and Kronert, 1969; Fujita et al, 1970; Arakawa, 1970; Arakawa and Tokunaga, 1972). In the present study, the surface of the podocytes and processes were generally uneven and often showed a population of finger-like or bleb-like microprojections arising from their surface. The functional significance of these structures remains unknown. There appears also to be some disagreement among the early workers concerning the pattern of interdigitation of the foot processes of visceral epithelial cells. Buss and Kronert (1969) described neighbouring foot processes as arising either from different podocytes or from the same cell. This view is compatible with that of Trump and Benditt (1962) who, using the TEM, described adjacent foot processes as being derived from the same cell; however, Fujita et al (1970) using SEM reported their observations on the renal podocytes of the rat and rabbit clearly indicated that neighbouring processes always came from different cells. In the present work, the foot processes varied significantly in width and length, sometimes they were branched and they always interdigitated with foot processes arising from the same or adjacent podocytes. In this respect, the present study concurs

with that of Buss and Kronert (1969).

According to Simon and Chatelanat (1969), the absolute and relative thickness of the three layers of the GBM vary according to the species. The lamina densa of the rabbit GBM accounts for approximately one third of the width. In the present study, the lamina densa of the pig GBM appears to be similar to that of the rat and mouse, accounting for almost the entire width of the membrane.

In the present study, the mesangial region was noted to be particularly prominent with up to eight contiguous mesangial cells being commonly found. More rarely, up to 25 mesangial cells were noted in a few glomeruli. Quiesser and Drommer (1982) found that, in the rat, the mesangium was generally only one cell thick while Guttman and Anderson (1968) noted the mesangium of mice to be more cellular and occupied a proportionately larger area of the glomeruli.

Crowell et al (1974), studying the dog glomerulus, considered that at least three mesangial cells should adjoin one another before the term mesangial hyperplasia could be associated with glomerular disease. Owing to the greater proportion of mesangial cells in the pig kidney, it is possible to presume that they, therefore, have a greater functioning capacity than in other species. If

this is so, it could be postulated that there is more efficient removal and disposal of filtration residues which become trapped in glomerular capillaries.

It is of special interest to note that TEM studies of the mesangium showed a high incidence 26/38 (68.4%) of electron dense deposits suggestive of immune complex formation. In some forms of immune complex glomerulonephritis in man and animals, mesangial hypercellularity is accompanied by electron dense deposits in the mesangial matrix (Murray and Wright, 1974; Woodroffe et al, 1982). In the light of this, it was considered worthwhile to carry out a more detailed TEM and immunofluorescence study with a view to assessing the overall incidence of immune complex formation in the glomerular mesangium of clinically normal pigs. This part of the work is described in Chapter 4.

The arrangement of the glomerular capillaries using corrosion casts has been studied in many species by light microscopy (Vimtrup, 1928; Hall, 1954; Boyer, 1956). However, these conventional methods are insufficient for the effective elucidation of the three dimensional ramifications and arrangement of the capillaries because of the limited resolution and shallow focus of the light microscope.

Studies of vascular casts of glomerular capillaries, peritubular network and the branches of interlobular arteries with SEM take advantage of the exceptional depth of field of scanning electron micrographs thus illuminating the special orientation of the glomerular capillaries (Murakami et al, 1971; Murakami, 1972, Spinelli, 1976; Anderson and Anderson, 1976). In one such study in the rat, Murakami (1972) reported that the glomerulus is lobulated, each lobule being composed of capillaries freely and numerously anastomosing into a genuine network. Each lobule, however, represented an independent functional and anatomical unit for conveying blood from the afferent to the efferent arteriole.

The observations on the pig glomerular casts in the present study were similar to that of other mammalian species. However, renal corpuscles with two efferent arterioles as reported by Murakami et al (1971) were never found in pig kidney and also the present study confirmed the opinion of Spinelli et al (1972) in that no inter-arteriolar shunts are present in pig renal corpuscles.

The light microscopical and TEM appearance of the tubular part of the mammalian nephron is now well understood (Pease, 1955; Bulger, 1965; Rouiller, 1969). With the advent of the SEM, it has been possible to add a new

dimension to the characterization of the surface structure of the tubules. Of all the constituent tubular parts of the nephron the proximal tubule has provoked the most interest, partly due to its possession of a well-developed microvillous brush border. Many workers have described the proximal tubule as composed of two segments, an initial convoluted segment "pars convoluta" and a more distal segment "pars recta"; only minor structural differences are apparently present between the two (Rouiller, 1969). Maunsbach (1964, 1966) and Tisher (1981) have, however, recognized up to three or four distinct morphological segments in the proximal tubule of the rat and rhesus monkey. In the present study, no significant structural segmentation of the proximal tubule was recorded. The numerous organelles and inclusions contained in the proximal tubule cytoplasm are related to the processes of absorption and secretion by the cells (Ericsson and Trump, 1969). The description of the luminal surface of the pig proximal tubule reported in the present study concurs with the majority of other studies (Andrews and Porter, 1974; Bulger et al, 1974; Siegel et al, 1974; Evan et al, 1978).

Light microscopical TEM and SEM observations on the structure of the thin loop of Henle made by Osvaldo and Latta (1966), Bulger et al (1967), Andrews and Porter (1974),

Siegel et al (1974), Bulger et al (1974), Andrews (1975) and Hucker and Frenzel (1975) were also similar to those reported in the present study.

Although Allen and Tisher (1976) reported two different patterns of surface structure of the thick limb of Henle in rats, only one type of cell was prominent in the pig kidney.

The observations made concerning the morphology of the distal tubule concur with previous studies. Although only the rat, mouse and human tissues have been studied by Rhodin (1958) and Trump and Bulger (1968), no significant differences in the appearance of the cells between species appears to be present.

Morphologists have known for over a hundred years that the mammalian collecting duct is composed of two cell populations, Schachowa (1879) (cited by Le Furgey and Tisher, 1979), being first to recognize this fact. The functional significance of differing luminal surface configuration and intercellular anatomy in the two cell types remains speculative. However, it does seem reasonable to suggest that the dark cells are metabolically more active than the light cells. The light and TEM observations of the pig collecting tubule are similar to previous studies (Myers et al, 1966; Ericsson and Trump, 1969;

Le Furgey and Tisher, 1979). The Type I cell recognized in this study with SEM would appear to correspond to the light cell while the cell Type II corresponds to the dark or intercalated cell (Andrews and Porter, 1974; Le Furgey and Tisher, 1979).

The possible functional significance of the variations in surface structure of light and dark cells was also considered by Le Furgey and Tisher (1979). Microvilli have often been assumed to increase cell surface area and enhance cell absorptive capacity, while microplicae have been implicated in pinocytosis and secretory processes. Despite this and other information regarding membrane surface structures the function of both microvilli and microplicae in cells of the collecting duct remains uncertain.

The appearance of the pig papilla was similar to that of the rat except that there were more openings on the surface due to its larger size (Carrol et al, 1974).

In the pig, as in many other species with a short gestation period, the kidneys are still in a foetal state at birth. In the peripheral cortex the nephrogenic zone persists with aggregates of mesenchymal cells, renal vesicles and S-shaped bodies in close apposition to the distal extremities of the collecting ducts which are

thought to transmit inductive signals for nephrogenesis (Gruenwald, 1952; Grobstein, 1957). Deeper in the cortex the nephrons are in more advanced stages of differentiation, but only the most juxtamedullary regions appear relatively well developed in all species studied. This situation, however, lasts for only a very short time. Although some earlier often-cited works reported the formation of new nephrons in the rat for several days or even weeks after birth (Kittelson, 1917; Arataki, 1926), recent published reports (Larsson, 1975; Kazimierczak, 1978) indicate that nephrogenesis terminates in the rat within a few days after birth and that the adult number of nephrons is already established at this time.

The light microscopic observations in the present study showed a prominent nephrogenic zone present at day one in the outer cortex. At this time only approximately 10% of the total number of glomeruli seemed to be functional as judged by patency of their capillary loops. By four weeks, however, the subcapsular nephrogenic zone had disappeared and was replaced by immature, non-functioning glomeruli which formed 50% of the total glomeruli. From six weeks onwards mature functioning glomeruli predominated.

The present TEM study concentrated mainly on the examination of identifiable immature glomeruli in the

outer cortical region and comparing their structure with the mature functional glomeruli in the juxtamedullary region. The immature glomerulus was spherical with a distinct Bowman's space and few or no patent capillary loops.

Endothelial and mesangial cells were difficult to identify. The prominent visceral epithelial cells were separated by narrow intercellular clefts, at the basal third of which junctional complexes were present. Rhodin (1962) has described the endothelial fenestrae in the mouse glomerulus being closed by diaphragms in contrast to that reported for the fenestrae in the glomerulus of the rat and of man (Farquhar, 1975). Endothelial diaphragms have also been recognized in the glomerulus of the newborn piglets (Kazimierczak, 1971; Bergelin and Karlsson, 1975). The present study showed the appearance of endothelial diaphragms in the immature glomerulus but these disappeared during further differentiation of the endothelium. No diaphragms were found in the fenestrae of mature functioning glomeruli.

Most of the progress made in recent years in the study of morphology of the developing rat renal glomerulus has been due to the introduction of SEM (Spinelli, 1976; Kazimierczak, 1980). SEM findings in the present work on

the post-natal development of pig glomerulus showed that the initial stage of nephron development was the metanephric vesicle, followed by S-shaped structures corresponding to those found on light microscopy. The immature glomeruli were represented by circular groups of closely apposed cuboidal or columnar visceral epithelial cells. In later stages of glomerular development, the visceral epithelial cells became progressively flatter and started to sprout cytoplasmic processes which interdigitated between two adjacent cells.

In summary, the present study has provided the first detailed description of the light, transmission and scanning electron microscopic aspects of the pig kidney; as such it has established a firm basis for future studies concerned with evaluating the morphological changes which accompany various kidney disorders.

C H A P T E R 4

A STUDY OF IMMUNE COMPLEX DEPOSITS, PREDOMINANTLY IgA, IN THE RENAL GLOMERULI OF CLINICALLY NORMAL PIGS

Introduction :

In Chapter 3, during a histological and ultrastructural study of 38 normal pig kidneys, many were found to have electron dense deposits in the glomerular mesangium. This finding together with the observation that, in the pig glomerulus, it was not unusual to find up to eight contiguous mesangial cells with resultant prominence of the mesangial matrix, suggested a mesangiopathic form of glomerulonephritis (GN).

It was considered worthwhile, therefore, to carry out a more detailed investigation of the pig glomerulus. As fresh kidney material from all 38 pigs was stored at $-20^{o}C$, it was decided to carry out an immunofluorescence study of these and a further group of 92 kidneys in order to confirm the existence of a mesangiopathic form of GN in pigs and to assess the incidence in a total of 130 pigs.

Brief review of the literature :

Due to its apparent predisposition to damage by immunological mechanisms, the kidney has probably attracted more attention from investigators in the field of immunopathology than any other organ. A search for the role of immune mechanisms in the pathogenesis of kidney

disease dates back as early as the foundation of immunology itself in the last decades of the 19th and the early part of the 20th centuries.

During the last 40 years, the increasing utilization of immunohistochemical and electron microscopic techniques in the study of spontaneous glomerular disease of man and animals as well as in experimentally-induced glomerulonephritis (GN), has led to the realization that spontaneous GN in man and animals is immunological in origin.

Seventy years of laboratory experimentation have served to describe two main but quite distinct pathogenetic mechanisms whereby the host's antibody response may cause GN. Extension of these studies to man has demonstrated that the same two pathogenetic mechanisms are also operative in spontaneously occurring human and animal GN and apparently can account for virtually all cases of this disease; central to each mechanism is the deposition of antibody within the renal glomeruli.

The first of these mechanisms is based on the production by the host of antibodies capable of reacting with its own glomerular basement membrane (GBM) antigen(s). This type of glomerular disorder known as anti-GBM nephritis or nephrotoxic nephritis (Lerner et al, 1967;

McClusky, 1971).

The second mechanism which accounts for most forms of human and animal GN depends on the production by the host of antibodies capable of reacting with non-glomerular endogenous or exogenous antigen(s) in the bloodstream with the resultant formation of circulating soluble antigen-antibody complexes which are subsequently trapped in the glomerular capillary wall and/or mesangium (Germuth, 1953; Dixon et al, 1961, Germuth et al, 1972).

With respect to this second type of (immune complex-mediated) GN, recent advances in our knowledge of basic glomerular structure and physiology have altered traditional concepts of its pathogenesis. Whereas immune deposits in the glomeruli were once thought to arise primarily by deposition of circulating soluble immune complexes (Cochrane and Koffler, 1973), it is now known to be equally possible that they form in situ (Border et al, 1982). There is now good evidence that a non-glomerular antigen may interact with the glomerulus, retain its antigenicity and remain bound until it reacts with specific antibody. Thus Golbus and Wilson (1979) reported in situ immune complex formation in the sub-endothelial space of the rat glomerulus using the

glycoprotein-binding properties of the lectin concanavalin which was utilized to "plant" an antigen in the glomeruli.

Several other investigators have also convincingly demonstrated *in situ* immune complex formation in the mesangium, subepithelial or subendothelial space of experimental laboratory animals (Couser *et al*, 1978; Van Damme *et al*, 1978; Ford and Kosatka, 1979; Fleuren *et al*, 1980).

Despite the elucidation of this alternative mechanism by which glomerular immune deposits may form, the precise factors that influence the precise anatomical sites at which they localize remain poorly understood. In this regard, the recent discovery that the glomerular capillary wall acts as a charge selective barrier to circulating molecules (Venkatachalam and Rennke, 1978; Deen *et al*, 1980), repelling anionic and attracting cationic molecules, has important theoretical implications for the pathogenesis of immune complex GN.

Spontaneous GN in animals :

Until the early 1970's, glomerulonephritis was considered to be a relatively uncommon disease in animals and comparative pathology textbooks tended to give it rather cursory attention. Indeed, in an early study of

the overall incidence of GN in 236 domesticated animals with nephritis, Langham and Hallman (1939) quoted figures for the horse as 1/40 (2.44%), cow 3/160 (1.87%), sheep 1/8 (12.5%), pig 0/5 (0%) and dog 2/22 (9.9%).

A search of the literature would seem to suggest that there is an increasing incidence of spontaneous GN in animals, the vast majority of published work being concentrated in the last few years (reviewed by Osborne et al, 1977; Slauson and Lewis, 1979; Wright and Nash, 1983). In fact, although GN is now recognized in many animal species, it is only in the dog and cat, man's closest animal associates, that a sufficiently large number of cases has been studied to allow the veterinary clinician and pathologist to establish and record the important features of the disease, and to draw comparisons with the condition as it occurs in man. Furthermore, whether or not there is a real increase in incidence is clouded by the fact that the relatively recent regular use of renal biopsy methods, immunofluorescence and electron microscopy, although in only a few laboratories throughout the world, has led inevitably to increased accuracy of diagnosis and hence a greater number of published reports.

In general, however, GN is still a rather poorly

understood disease in animals and, only recently, particularly with the introduction of renal biopsy methods in the dog and cat, has a sufficient number of follow-up studies been carried out to enable an understanding of the progression of the disease and its prognosis (Wright et al, 1981).

In other animals such as cattle (Lerner et al, 1968; Cutlip et al, 1980; Wiseman et al, 1980), horse (Fincher and Olafson, 1934; Squire, 1968; Banks and Henson, 1972; Waldvogel et al, 1983; Sabnis et al, 1984), sheep (Lerner and Dixon, 1966), lambs (Angus et al, 1973; Angus and Gardiner, 1979), goats (Lerner et al, 1968), non human primates including baboons (Brack, 1981), Owl monkeys (Chalifoux et al, 1981), Pigtailed macaques (Giddens et al, 1981), Cynomolgus monkeys (Poskitt et al, 1974), prosimian galagos (Burkholder and Bergerson, 1970; Burkholder, 1981; Boraski, 1981), where isolated reports of GN have appeared in the literature, an insufficient number of cases has been available for study to reach any meaningful conclusions as to the etiology, incidence and morphologic types of GN and its prognosis and treatment.

In the pig, reports of immune complex GN are particularly uncommon. However, Cheville et al (1970) have described a proliferative form of GN in pigs

suffering from swine fever; in these animals, proliferation of mesangial cells was accompanied by the presence of mesangial deposits of immunoglobulin and, with the electron microscope, electron dense deposits were found in the mesangial matrix. Furthermore, McGrath et al (1975) reported the presence of electron dense deposits in the glomerular mesangium and in subendothelial sites in pigs fed the pyrrolizidine alkaloid-containing plant Crotalaria spectabilis, although they did not carry out any immunofluorescence tests for immunoglobulins. In a later report, a form of necrotising GN with deposition of IgG and IgA and accompanied by electron dense deposits in subepithelial, subendothelial as well as in mesangial regions has been described in pigs fed a waste product from the industrial production of the proteolytic enzyme Alcalase (Elling, 1979). More recently, Shirota et al, (1984) have described a proliferative form of GN in 7 six month-old litter mates from a leukaemic sow. Although no immunofluorescence tests were performed, electron dense deposits were found in subepithelial, subendothelial and mesangial areas.

One of the problems encountered in the characterization of GN in animals has been the absence of investigative techniques such as immunofluorescence and electron microscopy especially in many of the earlier

studies and this has restricted the interpretation and value of some of these previously reported cases.

Due to the paucity of detailed morphologic information of animal GN, any attempt at a useful classification similar to that of man must remain in abeyance for the time being. Nevertheless, diffuse and focal proliferative forms of GN (Murray and Wright, 1974), membranous nephropathy (Farrow and Huxtable, 1971; Murray and Wright, 1974; Muller-Peddinghaus and Trautwein, 1977; Lucke, 1982), chronic exudative GN (Wright et al, 1976) and membranoproliferative (mesangiocapillary) GN (Murray and Wright, 1974; Lucke, 1982) have all been described in the dog and cat. Some forms of human glomerulopathy, however, such as minimal change nephropathy, IgA nephropathy, rapidly progressive diffuse crescentic proliferative GN and dense deposit (mesangiocapillary, Type II), disease have not so far been reported with certainty in animals.

The purpose of this Chapter of the present work was to report for the first time a form of idiopathic mesangiopathic IgA nephropathy in pigs.

Materials and methods :

A total of 130 kidney specimens, all from clinically

normal pigs and with no macroscopic lesions on visual inspection, were divided into two groups:

Group I : consisted of the kidneys from the initial 38 pigs described in Chapter 3.

Group II : A further 92 kidneys from three to five month old pigs were obtained from the Glasgow abattoir. The origin of these pigs was not known but were presumably clinically normal. They were electrically-stunned prior to exsanguination but, unlike the initial group, up to two hours had elapsed before the kidneys were available for processing. Although all of these pigs were passed at meat inspection, full necropsical data was not available.

Kidney specimens from all 130 pigs were processed for histological and ultrastructural studies as described in Chapter 2.

For immunofluorescence techniques specimens of kidney, rapidly frozen in liquid nitrogen, were trimmed to 1cm blocks and embedded on a chuck using tissue Tek II (OCT compound) embedding medium (Raymond A. Lamb, Sunbeam Road, London). The specimens were subsequently snap frozen to 70^{o}C by placing the chuck into a flask containing liquid nitrogen. Using a slee cryostat (Slee,

London) maintained at 20°C, sections 4um thick were cut and transferred onto glass slides. The sections were washed for five minutes in phosphate buffered saline (PBS pH 7.3) and subsequently fixed in acetone for a further five minutes. They were then stained for 30 minutes in a moist chamber with sheep-anti-pig IgG, sheep-anti-pig IgM and sheep-anti-pig IgA, which were all labelled with fluorescein isothiocyanate. After washing with PBS for ten minutes, the stained sections were examined using a Leitz orthoplan fluorescence microscope equipped for incident light fluorescence.

Results :

Immunofluorescence findings : These are summarised in Tables 4.1, 4.2 and 4.3

Granular deposits of IgA, either alone or together with IgG and/or IgM, were found in a high presentage of kidneys in both groups of pigs. The degree of immunoglobulin staining was graded 1+ to 3+. In all positive cases, the intensity of IgA staining was usually 1+ to 3+ while those glomeruli also staining for IgG and/or IgM were rated 1+ to 2+. In all cases, distribution of immunoglobulin was diffuse, i.e., involving all glomeruli and was mesangial in location (Figs. 4.1 and 4.2). Circumferential deposits around the capillary loops were never observed. In no instance was IgG or IgM found in the absence of IgA.

TABLE 4.1

SUMMARY OF IMMUNOFLUORESCENCE AND ULTRASTRUCTURAL FINDINGS

GROUP I : Initial 38 pigs.

Pig No.	IgG	IgM	IgA	Electron Dense Deposits
PK1	1+	1+	1+	Yes
PK2	1+	1+	2+	Yes
PK3	1+	1+	1+	Yes
PK4	1+	-	1+	Yes
PK5	-	-	-	No
PK6	1+	1+	2+	Yes
PK7	1+	1+	3+	Yes
PK8	1+	1+	2+	Yes
PK9	-	-	1+	Yes
PK10*	-	-	-	No
PK11*	-	-	-	No
PK12*	-	-	-	No
PK13*	-	-	-	No
PK14*	-	-	-	No
PK15*	-	-	-	No
PK16*	-	-	-	No
PK17*	1+	1+	2+	Yes
PK18*	-	-	-	No

TABLE 4.1 (Cont'd)

Pig No.	IgG	IgM	IgA	Electron Dense Deposits
PK19*	-	-	1+	Yes
PK39	2+	1+	2+	Yes
PK40	1+	1+	2+	Yes
PK41	-	1+	2+	Yes
PK42	-	-	1+	Yes
PK43	1+	1+	3+	Yes
PK44	-	-	1+	Yes
PK45	-	-	1+	Yes
PK46	3+	2+	3+	Yes
PK47	-	1+	2+	Yes
PK48	1+	1+	2+	Yes
PK49	-	-	1+	Yes
PK50	2+	2+	3+	Yes
PK51	1+	1+	1+	Yes
PK52	-	-	-	No
PK104**	-	-	-	No
PK105**	-	-	-	No
PK128	1+	1+	3+	Yes
PK129	-	1+	1+	Yes
PK130**	-	-	2+	Yes

* = Litter of newborn piglets
** = Adult sow

Intensity of Immunofluorescence staining rated 1+ to 3+

TABLE 4.2

SUMMARY OF IMMUNOFLUORESCENCE AND ULTRASTRUCTURAL FINDINGS

GROUP II : Abattoir Pigs.

Pig No.	IgG	IgM	IgA	Electron Dense Deposits
PK20	-	-	-	No
PK21	1+	2+	3+	Yes
PK22	-	-	-	No
PK23	-	-	1+	No
PK24	-	1+	3+	Yes
PK25	-	-	-	No
PK26	-	-	-	No
PK27	-	-	-	No
PK28	-	-	-	No
PK29	-	-	-	No
PK30	-	-	-	No
PK31	-	-	-	No
PK32	1+	1+	2+	Yes
PK33	-	1+	2+	Yes
PK34	1+	-	1+	No
PK35	-	-	-	No
PK36	-	-	-	No
PK37	-	-	1+	Yes

TABLE 4.2 (Cont'd)

Pig No.	IgG	IgM	IgA	Electron Dense Deposits
PK38	-	-	-	No
PK53	-	1+	1+	No
PK54	-	1+	1+	Yes
PK55	-	-	-	No
PK56	3+	3+	3+	Yes
PK57	-	-	-	No
PK58	1+	2+	1+	Yes
PK59	1+	1+	1+	Yes
PK60	-	1+	2+	Yes
PK61	1+	2+	3+	Yes
PK62	-	1+	2+	Yes
PK63	1+	1+	3+	Yes
PK64	-	-	-	No
PK65	-	-	-	No
PK66	-	-	-	No
PK67	-	-	-	No
PK68	-	-	-	No
PK69	-	-	-	No
PK70	-	-	-	No
PK71	-	-	-	No
PK72	-	-	-	No
PK73	-	-	-	No

TABLE 4.2 (Cont'd)

Pig No.	IgG	IgM	IgA	Electron Dense Deposits
PK74	-	-	1+	Yes
PK75	-	-	-	No
PK76	-	1+	2+	Yes
PK77	-	-	-	No
PK78	-	-	2+	Yes
PK79	-	-	-	No
PK80	-	-	-	No
PK81	-	-	1+	Yes
PK82	-	-	1+	No
PK83	-	-	1+	Yes
PK84	-	-	-	No
PK85	-	-	1+	Yes
PK86	1+	1+	2+	Yes
PK87	1+	1+	1+	Yes
PK88	-	-	-	No
PK89	-	-	-	No
PK90	-	-	2+	Yes
PK91	-	-	1+	No
PK92	-	-	-	No
PK93	-	-	-	No
PK94	-	-	-	No
PK95	-	-	-	No

TABLE 4.2 (Cont'd)

Pig No.	IgG	IgM	IgA	Electron Dense Deposits
PK96	-	-	-	No
PK97	-	-	1+	Yes
PK98	-	-	1+	Yes
PK99	-	-	-	No
PK100	-	-	-	No
PK101	-	-	1+	Yes
PK102	1+	1+	1+	Yes
PK103	-	-	-	No
PK106	-	1+	1+	Yes
PK107	-	-	-	No
PK108	-	-	-	No
PK109	-	-	-	No
PK110	-	-	1+	Yes
PK111	-	-	-	No
PK112	1+	-	2+	Yes
PK113	-	-	-	No
PK114	-	1+	2+	Yes
PK115	-	-	2+	Yes
PK116	-	1+	2+	Yes
PK117	-	-	-	No
PK118	-	-	1+	Yes
PK119	-	-	2+	Yes

TABLE 4.2 (Cont'd)

Pig No.	IgG	IgM	IgA	Electron Dense Deposits
PK120	-	-	-	No
PK121	-	-	1+	No
PK122	-	-	-	No
PK123	-	1+	3+	Yes
PK124	-	-	-	No
PK125	-	-	-	No
PK126	-	-	-	No
PK127	-	-	-	No

Intensity of immunofluorescence staining rated 1+ to 3+

TABLE 4.3

SUMMARY OF IMMUNOFLUORESCENCE FINDINGS

	INITIAL GROUP		ABATTOIR GROUP	
No. of Kidneys	38		92	
Negative	12	(31,5%)	51	(55.4%)
Positive	26	(68.4%)	41	(44.5%)
IgA Only	7/26	(26.9%)	18/41	(43.9%)
IgG + IgA	1/26	(3.8%)	2/41	(4.8%)
IgM + IgA	3/26	(11.5%)	11/41	(26.8%)
IgG + IgM + IgA	15/26	(57.6%)	10/41	(24.3%)

Total No. of Kidneys	-	130	
Negative	-	63	(48.4%)
Positive	-	67	(51.5%)

Fig. 4.1 Glomerulus showing granular deposits of IgA in mesangial stalk areas. Immunofluorescence x 400.

Fig. 4.2 Granular deposits of IgG again in mesangial areas. This case was also positive for IgA and IgM. Immunofluorescence x 400.

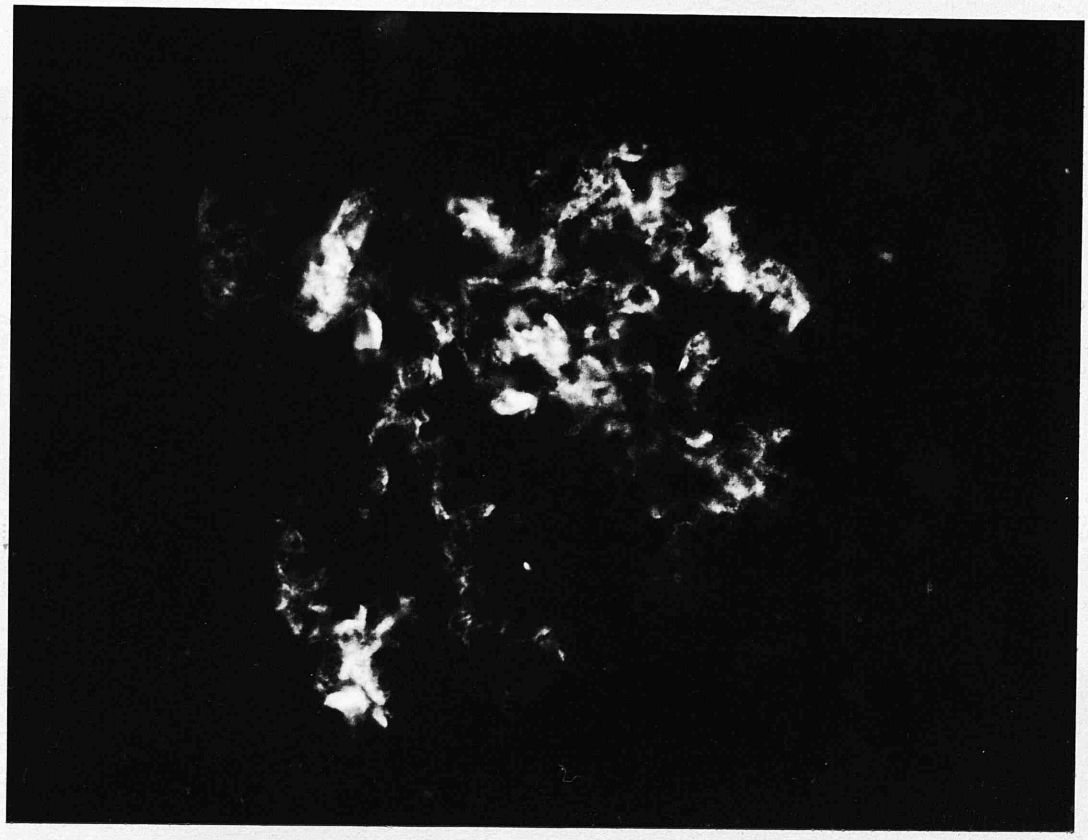

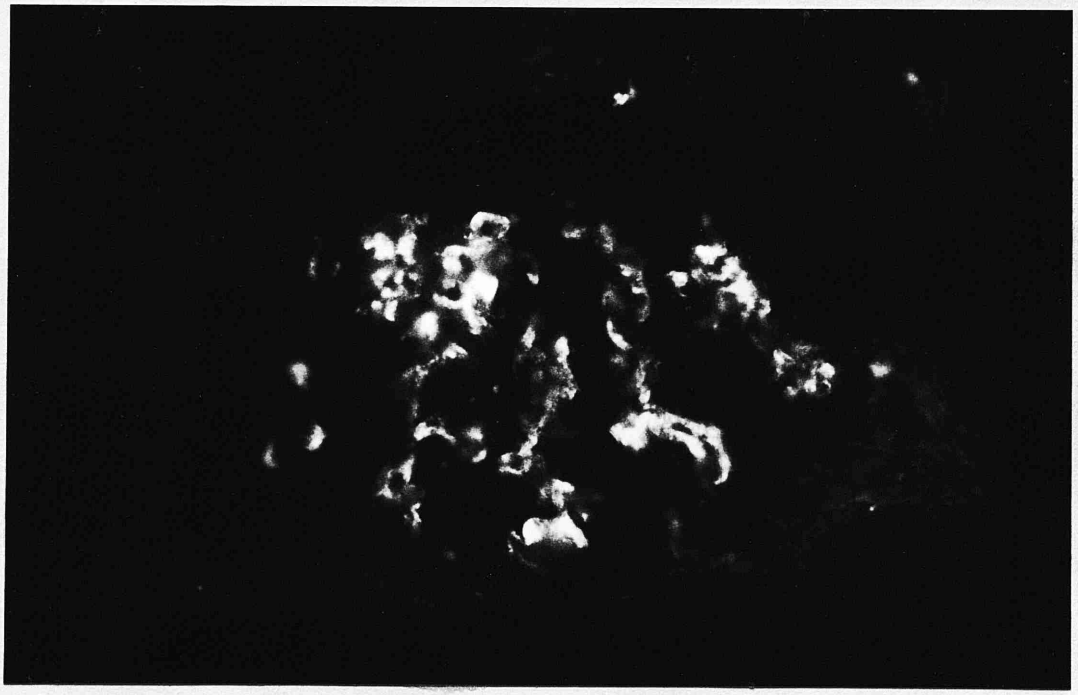

Fig. 4.3 Glomerulus showing extensive deposition of IgA in mesangial areas.
Immunofluorescence x 400.

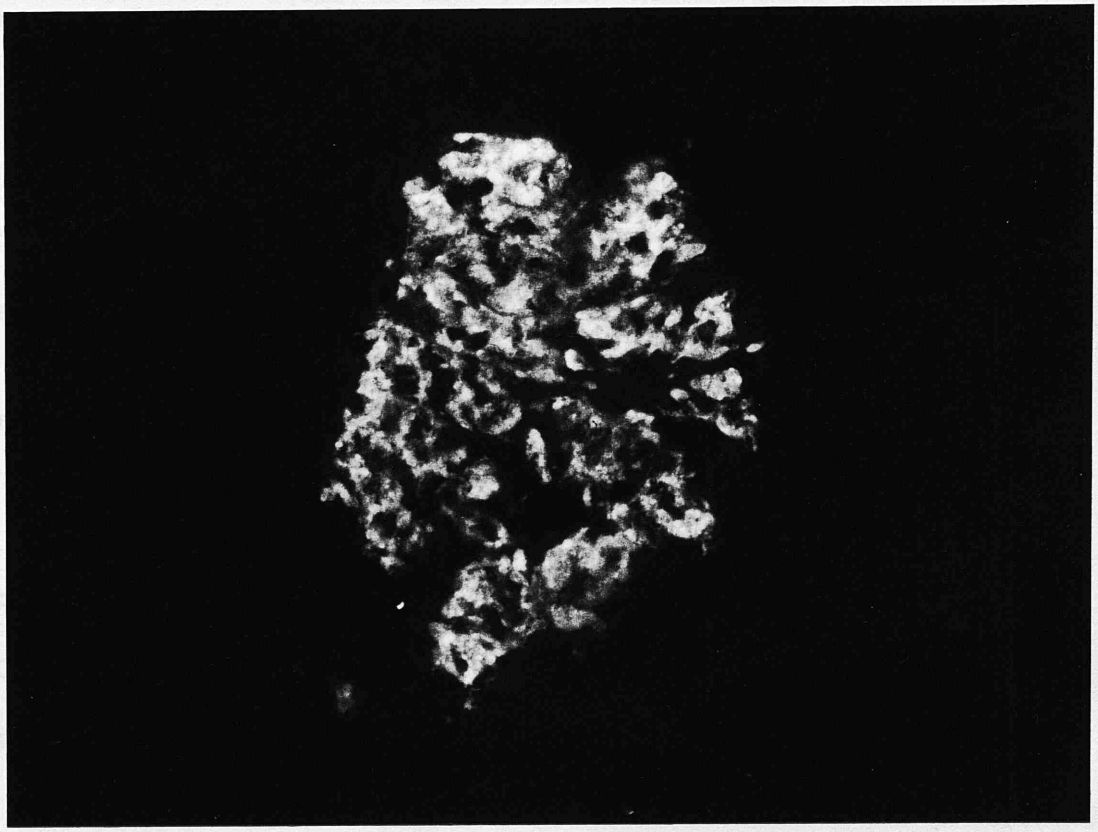

In the initial group of 38 pigs, 68.4% showed deposition of IgA. Only one of the nine piglets killed up to four weeks of age was fluorescence positive and only one of the three adult sows showed deposits of IgA. In contrast, the 92 abattoir group of kidneys showed a 44.5% incidence of IgA deposits (Fig. 4.3). Furthermore, only 24.3% of these positive kidneys showed deposition of IgA, IgG and IgM compared to the initial group where 57.6% of positive cases showed all three immunoglobulins. Like the initial group, however, none of the 92 abattoir kidneys showed deposits of IgG or IgM alone in the absence of IgA.

Histological findings :

Apart from an occasional small focal area of interstitial scarring and lymphoid cell infiltration, all 130 kidneys were histologically normal. It was only possible to assess with accuracy the glomerular morphology in the 38 freshly fixed kidneys as, in the abattoir group, up to two hours had elapsed before the kidneys were processed for histological examination and consequently autolytic mesangial swelling and nuclear pyknosis was already underway.

Excluding the ten piglets killed up to four weeks of age and in which glomerular morphogenesis was still in

Fig. 4.4 Glomerulus from an immunofluorescence negative pig. Note the prominent mesangial areas (arrows).
HE x 250.

Fig. 4.5 Glomerulus from a pig showing deposits of IgA, IgM and IgG. Note the expanded mesangial areas with mesangial cell hypercellularity (arrows).
HE x 300.

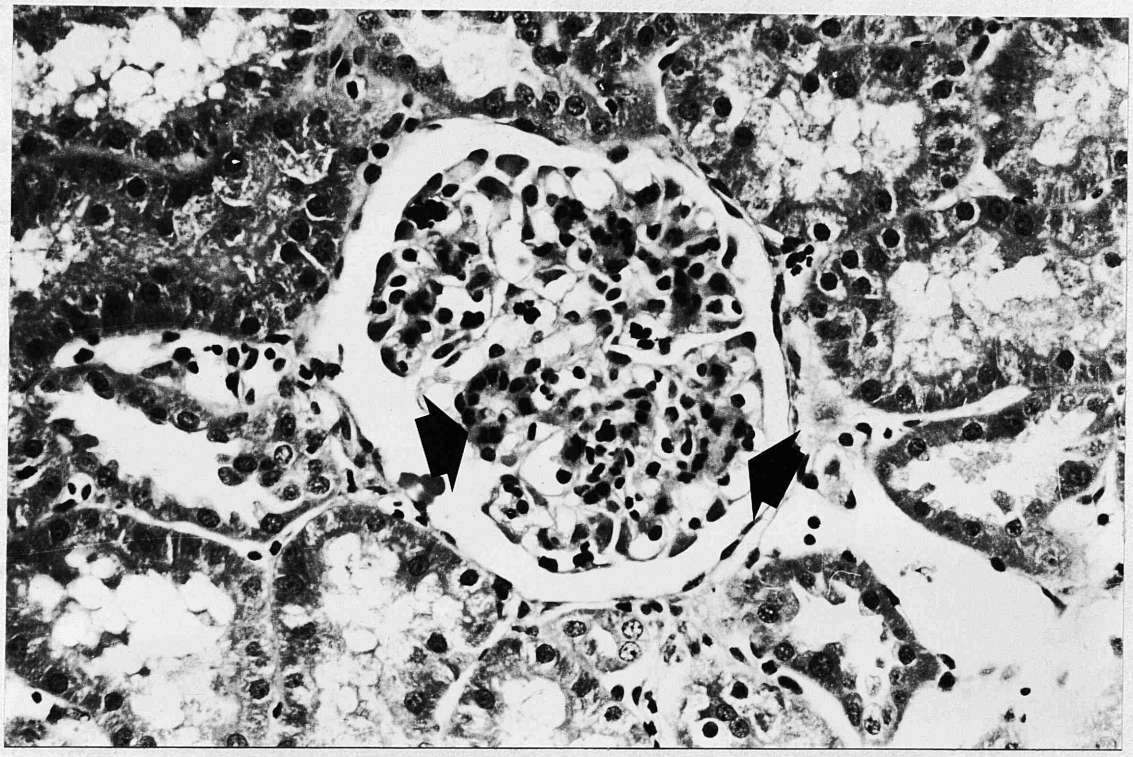

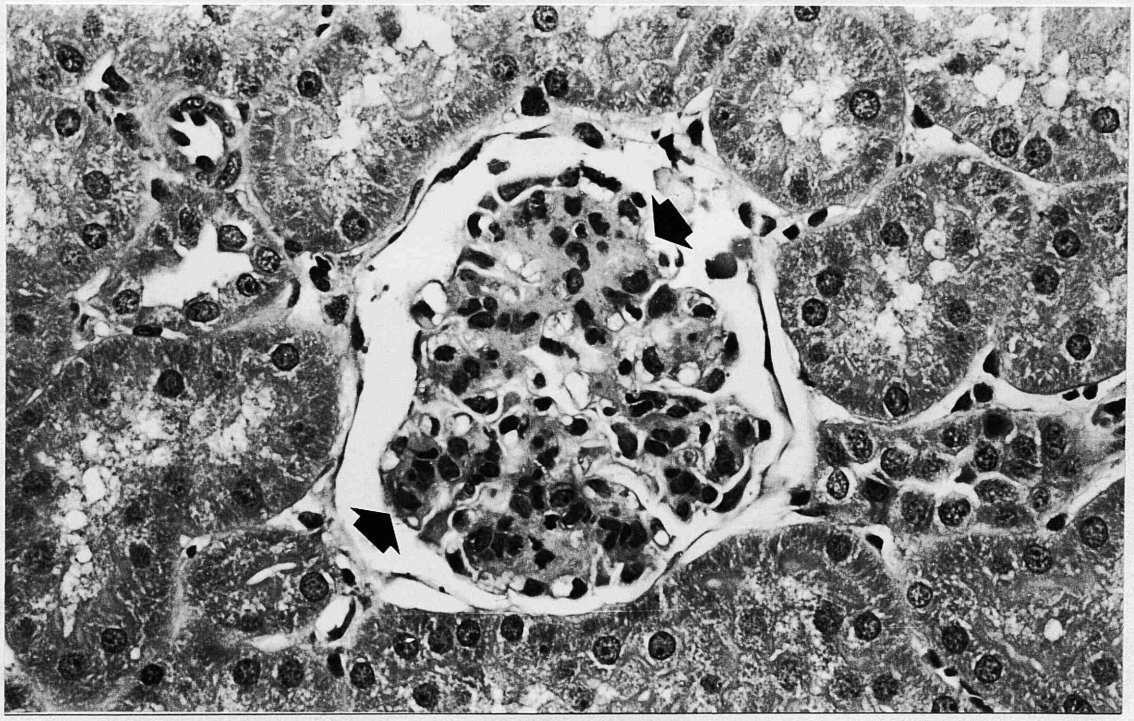

progress in the outer cortex, all the animals in this group showed histologically "normal" glomeruli with patent capillary loops. In kidneys which were immunofluorescence negative, it was not uncommon to find up to eight contiguous mesangial cells in otherwise normal glomeruli (Fig. 4.4). In the kidneys which had deposition of immunoglobulins, however, segmental mesangial expansion and hypercellularity with up to 25 contiguous mesangial cells were present in approximately 10% of glomeruli (Fig. 4.5).

In the abattoir group, autolytic changes had advanced sufficiently to preclude a clear assessment of glomerular morphology, particularly with regard to mesangial expansion.

Ultrastructural findings :

Interpretation of glomerular morphology was again best assessed in the initial group of pigs where the kidneys were fixed immediately on death. In this group, all 26 kidneys which showed deposition of IgA on immunofluorescence examination, had distinctive electron dense deposits in the mesangial area (Figs. 4.6 and 4.7). Although similar deposits were not found in subepithelial or intramembranous sites, a few axial subendothelial deposits were found in three cases (Fig. 4.8). In

Fig. 4.6 Electron micrograph of the mesangial region from a kidney which showed heavy immunofluorescence deposits of IgA and IgG. Electron dense deposits can be seen in the mesangial matrix (arrows). Mesangial cell nucleus (M). TEM x 10,000.

Fig. 4.7 Electron micrograph from the mesangial region showing extensive electron dense deposits in the mesangial matrix (arrows).
TEM x 13,400.

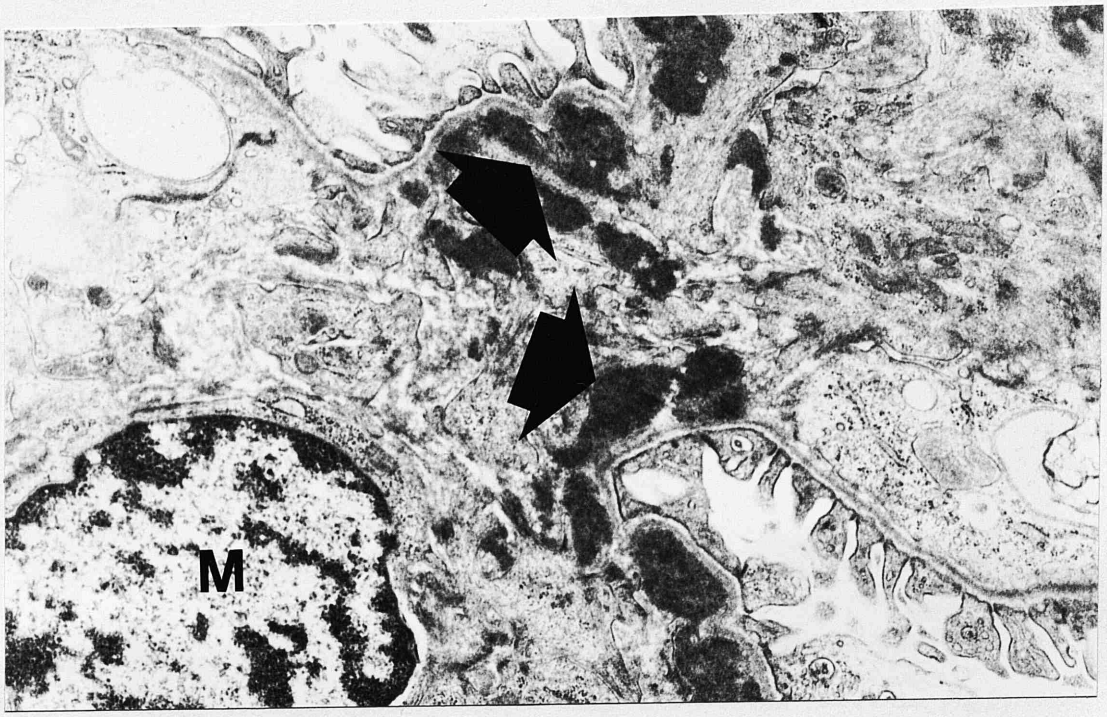
M

Fig. 4.8 Electron micrograph showing electron dense deposits in a subendothelial location (arrow).
TEM x 28,000.

Fig. 4.9 Electron micrograph showing extensive fusion of epithelial foot processes (arrows).
TEM x 13,400.

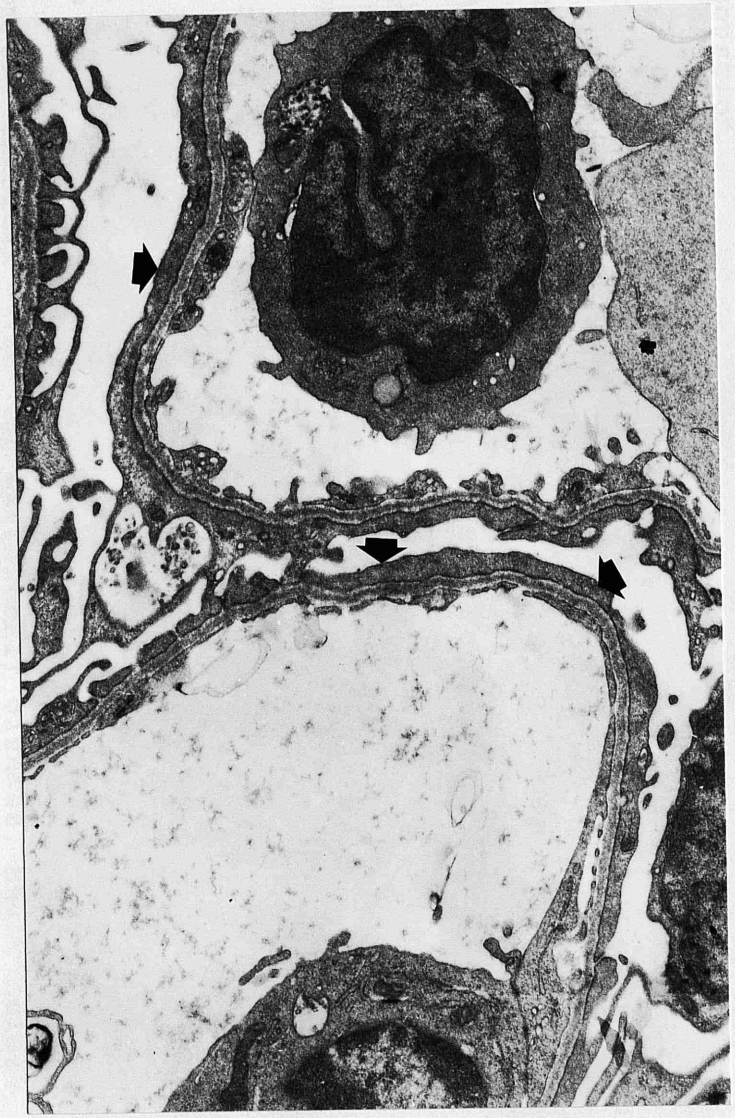

addition, affected glomeruli showed widespread effacement of epithelial foot processes (Fig. 4.9). In animals which were immunofluorescence negative, no electron dense deposits were observed in the mesangium or elsewhere.

In the 92 abattoir kidneys, autolytic changes precluded detailed ultrastructural assessment. Nevertheless, of the 41 kidneys which had deposits of IgA, 35 (85.3%) showed electron dense deposits in the glomerular mesangium (Fig. 4.10). In the remaining six kidneys, autolytic changes had advanced to a degree that ultrastructural assessment was impossible.

Discussion :

The presence of host immunoglobulins in the renal glomeruli together with electron dense deposits in the capillary walls and/or mesangium is generally accepted as evidence of immune complex formation, whether by deposition of circulating complexes (Germuth et al, 1967) or in situ localisation (Border et al, 1982).

The present study has shown that, although none of the pigs under investigation were apparently suffering from any clinical renal (or extrarenal) disease, nevertheless, an unexpectedly high number of kidneys (51.5%) showed

Fig. 4.10 Electron micrograph from an abattoir derived kidney showing well-developed autolytic changes. Nevertheless, many electron dense deposits are present in the mesangial matrix (arrows). TEM x 5,400.

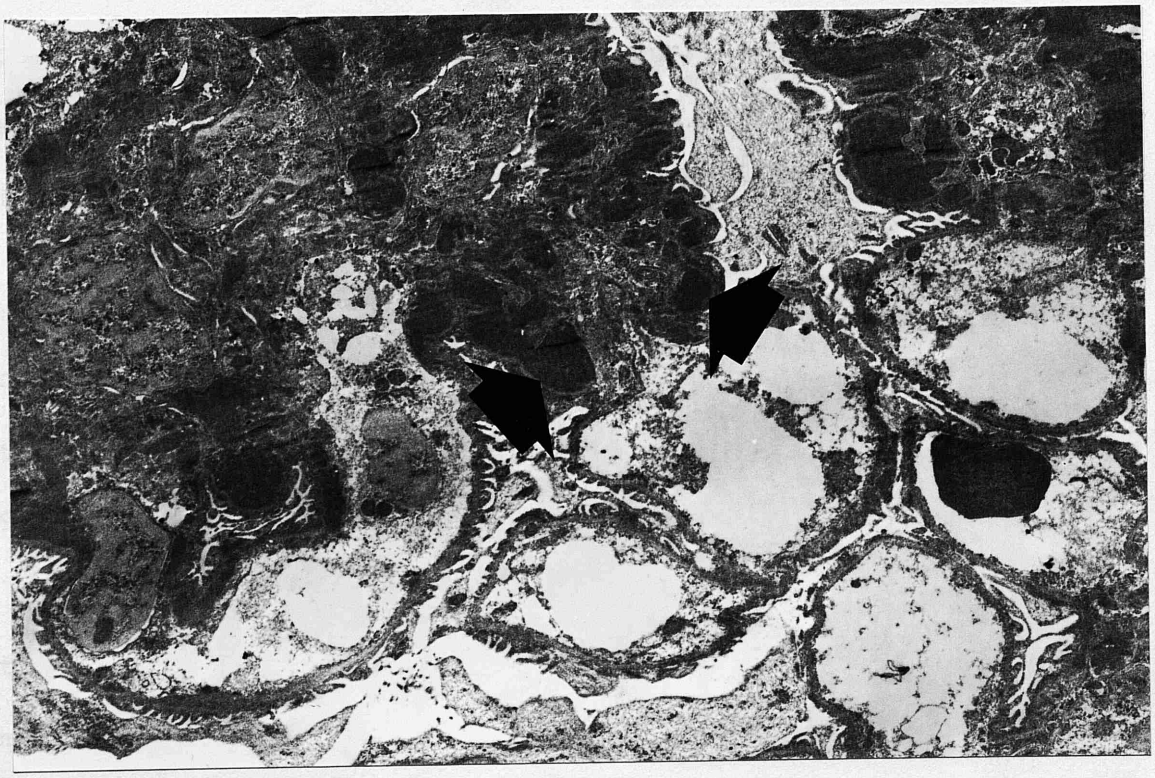

deposits of IgA and to a lesser extent IgG or IgM in the glomerular mesangium. In most of these pigs, ultrastructural examination confirmed the presence of immune complex deposition although in the 92 abattoir kidneys which were not processed for up to two hours after death the correlation between deposition of IgA and the finding of electron dense deposits was not as high as in the initial group of 38 freshly fixed kidneys. Due to the unavailability of a suitable anti-complement serum, it was unfortunately not possible to test for the presence of C3.

Although such a high incidence of spontaneously-occurring glomerular immune deposits in histologically normal kidneys is not considered usual, Sutherland et al (1974), have reported finding immune deposits (mainly IgG) in the glomeruli of 21/303 (6.9%) normal human kidneys at autopsy while Markham et al (1973) have shown that immune complex deposition, predominantly IgG, is common in normal laboratory mice.

In the present series of pigs, the occurrence of immune complex deposits did not seem to be associated with any marked glomerular alteration in glomerular morphology. It was of interest to note, however, that even in the pigs with no deposits of immunoglobulin, it was not unusual to find up to eight contiguous mesangial cells. This is in

sharp contrast to the glomeruli of man and dogs where in normal animals only one or two contiguous mesangial cells are present between adjacent capillaries (Crowell et al, 1974). In pigs with deposits of immunoglobulin, however, 10% of glomeruli showed up to 25 contiguous mesangial cells with associated expansion of mesangial matrix.

Although there were some differences in the incidence of immune complex deposition between the initial group of 38 pigs whose kidneys were available immediately for study and the 92 abattoir pigs where up to two hours had passed before the kidneys were processed, nevertheless the overall incidence of deposition of IgA was 51.5%.

In any of the domesticated animals, such a high incidence of IgA deposition in the renal glomeruli has never before been described. Indeed, to the best of the author's knowledge the prominent nature of the renal mesangium in both fluorescence negative and fluorescence positive pigs, but particularly the latter, has also never been reported.

At the present time, the pathogenetic mechanisms leading to deposition of IgA in the glomerular mesangium of normal pigs must await further study. There are,

however, distinct similarities with idiopathic mesangial IgA nephropathy in man (Berger's disease), the most common form of GN in southern Europe, Japan and Australia, but accounting for less than 10% of cases in the U.K. and U.S. (D'Amico, 1983).

Immunofluorescence deposits of IgA, and to a lesser extent IgG and IgM, associated with electron dense deposits in the glomerular mesangium and mesangial expansion and hypercellularity were first described in human patients by Berger and Hinglais (1968) and Berger (1969). In man, the disease usually presents with episodes of macroscopic or microscopic haematuria; nevertheless, approximately 25% of cases progress to renal failure. Males are affected more than females (Emancipator et al, 1985). The nephropathy occurs in the second and third decade and there appears to be a genetic predisposition (Woodroffe et al, 1982).

There is good evidence in the human patient that the IgA deposited in the glomeruli is dimeric or polymeric in nature and is therefore likely to be of mucosal origin (Cousar, 1985). Indeed, the disease sometimes follows respiratory or gastrointestinal infections (Woodroffe et al, 1982; Emancipator et al, 1985) and a similar form of mesangiopathic IgA nephropathy has been

induced in experimental mice by oral immunization with a number of different heterologous antigens (Emancipator et al, 1983).

Although it is too early to make a definitive diagnosis of IgA nephropathy in the present group of pigs, particularly as urine was not available for analysis for haematuria, data on extrarenal lesions was insufficient especially in the 92 abattoir kidneys and tests for the presence of complement (C3) were not performed, sufficient similarities exist to warrant further investigation.

Studies should now be aimed at investigating the possible initiating antigen(s) which might be present in the food, environment or indeed host antigens localised at mucosal surfaces and which might, through a mucosal IgA response, lead to deposition of IgA/antigen complexes in the renal glomeruli of pigs.

C H A P T E R 5

GENERAL SUMMARY AND CONCLUSIONS

Familiarity with the normal anatomy of the porcine kidney is an essential prerequisite to the understanding and interpretation of morphological changes which occur during kidney diseases.

Most of the morphological studies of the mammalian kidney have been carried out in the rat, mouse, rabbit and, of course, man. What may be true of the kidney of laboratory animals or man might not necessarily apply to the pig. Furthermore, recent reports of a variety of kidney diseases of the pig (Cheville et al, 1970; Elling, 1979; McGrath et al, 1975) have highlighted the importances of a real understanding of the gross, histological and ultrastructural features of the normal pig kidney and also provided a stimulus to establish for the first time the baseline morphologic parameters so necessary for the proper evaluation of future studies into porcine renal disease.

In this study, a detailed description of the morphology of the pig kidney has for the first time been reported. A total of 38 pigs of different ages were examined by light and electron microscopy in order to expand the meagre information currently limited to a single report by Yadava and Calhoun (1958) who compared the pig kidney with that of other mammals.

In the present work, the renal specimens were either perfused with fixative via the renal artery or fixed by immersion prior to processing for histological and ultrastructural studies. The advantages of perfusion fixation for light microscopy was that the glomerular capillaries were patent, relatively free of red blood cells, and the constituent epithelial, endothelial and mesangial cells were easily recognised. However, the main disadvantage of this technique was that there was often artificial dilation of the Bowman's capsule and not all glomeruli were evenly perfused. In TEM and SEM studies, there did not seem to be any differences between the two fixation methods although the visualisation of the microvilli of the proximal convoluted tubule was enhanced by perfusion fixation.

In general terms, the structure of the pig kidney was essentially similar to that of other mammals which have been investigated in detail. The main histological and ultrastructural differences recorded in this study were related to :

1) The glomerular mesangium where up to 8 contiguous cells were present in a single glomerulus, and
2) The surface microprojections (microvilli and blebs) on the surface of the visceral epithelial cells were more numerous than reported in other species.

The present work also confirmed the usefulness of SEM techniques in the study of corrosive vascular casts of the pig kidney.

Ten piglets in the present study formed the basis of a sequential study of nephrogenesis from day one up to six weeks of age using combined light microscopy, TEM and SEM.

The results showed that the nephrogenic zone which occupied a third of the cortical width of the new-born pig kidney had disappeared at four weeks but 50% of the glomeruli were still immature and nonfunctional; however, by six weeks, mature functioning glomeruli predominated.

As 68.4% of the initial group of 38 kidneys showed electron dense deposits in the mesangial matrix a further series of 92 kidneys from clinically normal animals, derived from different sources, were examined by immunofluorescence, histological and ultrastructural methods. The results have shown for the first time that, although none of the 130 pigs under investigation were apparently suffering from any clinical renal disease, nevertheless, an unexpectedly high numer of kidneys (51.5%) showed deposits of IgA and, to a lesser extent, IgG or IgM in the glomerular mesangium.

In most of these pigs, ultrastructural examination confirmed the presence of immune complex deposition. In the domesticated animals, a high incidence of IgA deposition in the renal glomeruli has never before been described. At the present time, the pathogenetic mechanisms leading to deposition of IgA in the glomerular mesangium of normal pigs must await further study. There are, however, distinct similarities with idiopathic mesangial IgA nephropathy in man.

REFERENCES

ALLEN, F. and TISHER, C.C. (1976). Morphology of the ascending thick limb of Henle. Kidney International, 9, 8-22.

ANDERSON, B.G. and ANDERSON, W.D. (1976). Renal vasculature of the trout demonstrated by scanning electron microscopy, compared with canine glomerular vessels. American Journal of Anatomy, 145, 445-458.

ANDREWS, P.M. (1975). Scanning electron microscopy of human and rhesus monkey kidney. Laboratory Investigation, 32, 610-618.

ANDREWS, P.M. (1981). Investigations of cytoplasmic contractile and cytoskeletal elements in the kidney glomerulus. Kidney International, 20, 549-562.

ANDREWS, P.M. and PORTER, K.R. (1974). A scanning electron microscopic study of the nephron. American Journal of Anatomy, 140, 81-115.

ANGUS, K.W. and GARDINER, A.C. (1979). Mesangio-capillary glomerulonephritis in Dorset-Finnish Landrace Cross Lambs. Veterinary Record, 105, 471.

ANGUS, K.W., GARDINER, A.C., SYKES, A.R. and DAVISON, A.M. (1973). A rapidly progressing mesangio-capillary glomerulonephritis in Finnish Landrace lambs. Veterinary Record, 92, 337-338.

AOKI, A. (1966). Development of the human renal glomerulus. Differentiation of the filtering membrane. Anatomical Record, 155, 339-352.

ARAKAWA, M. (1970). A scanning electron microscopy of the glomerulus of normal and nephrotic rats. Laboratory Investigation, 23, 489-496.

ARAKAWA, M. (1971). A scanning electron microscope study of the human glomerulus. American Journal of Pathology, 64, 457-463.

ARAKAWA, M. and TOKUNAGA, J. (1972). A scanning electron microscope study of the glomerulus. Further consideration of the mechanism of the fusion of podocyte terminal processes in nephrotic rats. Laboratory Investigation, 27, 366-371.

ARAKAWA, M. and TOKUNAGA, J. (1974). Further scanning electron microscopy studies of the human glomerulus. Laboratory Investigation, 31, 436-440.

ARATAKI, M. (1926). On the postnatal growth of the kidney, with special reference to the number and size of the glomeruli (albino rat).
American Journal of Anatomy, 36, 399-436.

AREY, L.B. (1954). "Developmental Anatomy". A textbook and laboratory manual of embryology, 6th edition (W.B. saunders Company, Philadelphia and London), pp. 292-312.

AUSIELLO, D.A., KREISBERG, J.I., ROY, C. and KARNOVSKY, M.S. (1980). Contraction of cultured rat glomerular cells of apparent mesangial origin after stimulation with angiotensin II and arginine vasopressin.
Journal of Clinical Investigation, 65, 754-760.

BAINTNER, K. (1970). Urinary excretion of colostral trypsin inhibitor in neonatal pigs.
Life Sciences, 9, 847-849.

BANKS, K.L. and HENSON, J.B. (1972). Immunologically medicated glomerulitis of horses. II. Antiglomerular basement membrane antibody and other mechanisms in spontaneous disease. Laboratory Investigation, 26, 708-715.

BARAJAS, L. (1970). The ultrastructure of the juxtaglomerular apparatus as disclosed by three-dimensional reconstructions from serial sections. The anatomical relationship between the tubular and vascular components.
Journal of Ultrastructure Research, 33, 116-147.

BARAJAS, L. (1971). Renin secretion. An anatomical basis for tubular control. Science, 172, 485-487.

BARAJAS, L. and LATTA, H. (1963). A three dimensional study of the juxtaglomerular apparatus in the rat. Light and electron microscopic observations.
Laboratory Investigation, 12, 257-269.

BEEUWKES, R., 111 and BONVENTRE, J.V. (1975). Tubular organization and vascular tubular relations in the dog kidney. American Journal of Physiology, 229, 695-713.

BERGELIN, I.S.S. and KARLSSON, B.W. (1973). Dehydrogenases in the kidney of the developing neonatal pigs as compared with the foetal and adult pig.
International Journal of Biochemistry, 4, 51-61.

BERGELIN, I.S.S. and Karlsson, B.W. (1974). Colostrum, serum and kidney proteins in the urine of the developing neonatal pig. International Journal of Biochemistry, 5, 885-894.

BERGELIN, I.S.S. and KARLSSON, B.W. (1975). Functional structure of the glomerular filtration barrier and the proximal tubule in the developing foetal and neonatal pig kidney. Anatomy and Embryology, 148, 223-234.

BERGER, J. (1969). IgA glomerular deposits in renal disease. Transplant Proceedings, 1, 939-944.

BERGER, J. and HINGLAIS, N. (1968). Les depots intercapillaries d' IgA-IgG. Journal Urology, 74, 694-699.

BING, J. and KAZIMIERCZAK, J. (1962). Renin content of different parts of the juxtaglomerular apparatus. Acta Pathologica et Microbiologica Scandinavica, 54, 80-95.

BING, J. and KAZIMIERCZAK, J. (1964). Renin in nephrogenic renal tissue devoid of both granular and non-granular epithoid juxtaglomerular cells. Acta Pathologica et Microbiologica Scandinavica, 60, 83-89.

BORASKI, E.A. (1981). Renal disease in prosimians. Veterinary Pathology, 18, 1-5.

BORDER, W.A., WARD, H.J., KAMIL, E.S. and COHEN, A.H. (1982). Induction of membranous nephropathy in rabbits by administration of an exogenous cationic antigen. Demonstration of a pathogenic role for electrical charge. Journal of Clinical Investigation, 69, 451-461.

BOSS, J.M.N., DLOUHA, H., KRAUS, M. and KRECEK, J. (1962). The development of the kidney in young rats. Journal of Physiology, 161, 51-52.

BOWMAN, W. (1842). On the structure and use of the malpighian bodies of the kidney, with observations on the circulation through that gland. Philosophical Transactions royal Society, London, 132, 57-80.

BOYER, C.C. (1956). The vascular pattern of the renal glomerulus as revealed by plastic reconstruction from serial sections. Anatomical Record, 125, 433-441.

BRACK, M. (1981). Renal pathology in captive baboons (papio cynocephalus). Veterinary Pathology, 18, 55-58.

BRAUS, H. (1929). Anatomie des Menschen. Springer-verlag, Berlin. (Cited by Tisher, 1981).

BRENNER, B.M., HOSTETTER, T.H. and HUMES, H.D. (1978). Molecular basis of proteinuria of glomerular origin. New England Journal of Medicine, 298, 826-833.

BULGER, R.E. (1965). The shape of rat kidney tubular cells. American Journal of Anatomy, 116, 237-256.

BULGER, R.E. and TRUMP, B.F. (1966). Fine structure of the rat renal papilla. American Journal of Anatomy, 118, 685-722.

BULGER, R.E., TISHER, C.C. MYERS, C.H. and TRUMP, B.F. (1967). Human renal ultrastructure II. The thin limb of Henle's loop and the interstitium in healthy individuals. Laboratory Investigation, 16, 124-136.

BULGER, R.E., SIEGEL, F.L. and PENDERGRASS, R.R. (1974). Scanning and transmission electron microscopy of the rat kidney. American Journal of Anatomy, 139, 433-502.

BURKHOLDER, P.M. (1981). Glomerular disease in captive galagos. Veterinary Pathology, 18, 6-22.

BURKHOLDER, P.M. and BERGERSON, J.A. (1970). Spontaneous glomerulonephritis in the prosimian primate galago. A correlative light, immunofluorescence and electron microscopic analysis. American Journal of Pathology, 61, 437-449.

BUSS, H. and KRONERT, W. (1969). Zur strukture des nierenglomerulum der ratte. Rasterelektron enmikorskopische undersuchungen. Virchows Archives, Abstract B: Cell Pathology, 4, 79-92.

CARROL, N., CROCK, G.W., FUNDER, C.C., GREEN, C.R., HAM, K.N. and TANGE, J.D. (1974). Scanning electron microscopy of the rat renal papilla. Journal of Anatomy, 117, 447-452.

CARLSSON, L.C.T., BERGELIN, I.S.S. and KARLSSON, B.W. (1974). Trypsin inhibition in urine of developing neonatal pigs and in sow's colostrum. Enzyme, 18, 176-188.

CHALIFOUX, L.V., BRONSON, R.T., SENGAL, P., BLAKE, B.J. and KING, N.W. (1981). Nephritis and haemolytic anaemia in owl monkeys (Aotus trivirgatus). Veterinary Pathology, 18, 23-37.

CHANDRA, S., HUBBARD, J.C., SKELTON, F.R., BERNARDIS, L.L. and KAMURA, S. (1965). Genesis of juxtaglomerular cell granules. Laboratory Investigation, 14, 1834-1847.

CHURG, J. and GRISHMAN, E. (1975). Ultrastructure of glomerular disease. A review.
Kidney International, 7, 254-270.

CHEVILLE, N.F., MENGELING, W.L. and ZINOBER, M.R. (1970). Ultrastructural and immunofluorescent studies of glomerulonephritis in chronic hog cholera.
Laboratory Investigation, 22, 458-467.

CLARK, S.C. (1957). Cellular differentiation in the kidneys of newborn mice studied with the electron microscope.
Journal of Biophysics and Biochemistry, 3, 349-359.

COCHRANE, C.G. and KOFFLER, D. (1973). Immune complex disease in experimental animals and man.
Advances in Immunology, 16, 185-264.

COUSER, W.G. (1985). Mechanisms of glomerular injury in immune complex disease. Kidney International, 28, 569-583.

COUSER, W.G., STEINMULLER, D.R., STILMANT, M.M., SALANT, D.J. and LOWENSTEIN, L.M. (1978). Experimental glomerulonephritis in the isolated perfused rat kidney.
Journal Clinical Investigation, 62, 1275-1287.

CROWELL, W.A., DUNCAN, D.V.M. and FINCO, D.R. (1974). Canine glomeruli. A light and electron microscopic change in biopsy, perfused and in situ autolysed kidney from normal dogs. American Journal of Veterinary Research, 35, 889-896.

CUTLIP, R.C., McCLURKIN, A.W. and CORIA, M.F. (1980). Lesions in clinically healthy cattle persistently infected with the virus of bovine viral diarrhoea-glomerulonephritis and encephalitis.
American Journal of Veterinary Research, 41, 1938-1941.

D'AMICO, G. (1983). Idiopathic mesangial IgA nephropathy in "Glomerular Injury" 300 years after Morgagni.
Eds. Bertani, T. and Remuzzi, G. pp. 2o5-228.

DEEN, W.M., SATVAT, B. amd JAMIESON, J.M. (1980). Theoretical model for glomerular filtration of charged solutes.
American Journal of Physiology, 238, 126-139.

DIXON, F.J., FELDMAN, J.D. and VAZQUEZ, J.J. (1961). Experimental glomerulonephritis. The pathogenesis of a laboratory model resembling the spectrum of human glomerulonephritis.
Journal of Experimental Medicine, 113, 899-919.

DU BOIS, A.M. (1969). The embryonic kidney in "The Kidney", Volume I. Eds. Rouiller, C. and Muller, A.F. (Academic Press, New York and London), pp. 351-447.

DUNIHUE, F.W. and BOLDOSSER, W.G. (1963). Observations on the similarity of mesangial to juxtaglomerular cell. Laboratory Investigation, 12, 1228-1240.

EDELMAN, R. and HARTROFT, P.M. (1961). Localization of renin in juxtaglomerular cells of rabbit and dog through the use of fluorescent-antibody technique. Circulation Research, 9, 1069-1077.

EDWARDS, J.G. (1951). Development of efferent arteriole in human metanephros. Anatomical Record, 109, 495-498.

ELIAS, H., HOSSMAN, A., BARTH, I.B. and SOLMOR, A. (1960). Blood flow in renal glomerulus. Journal of Urology, 83, 796-798.

ELLING, F. (1979). Nutritionally induced necrotizing glomerulonephritis and polyarteritis nodosa in pigs. Acta Pathologica et Microbiologica Scandinavica, 87, 387-392.

EMANCIPATOR, S.N., GALLO, G.R. and LAMM, E. (1983). Experiment IgA nephropathy induced by oral immunization. Journal of Experimental Medicine, 157, 572-582.

EMANCIPATOR, S.N., GALLO, G.R. and LAMM, M.E. (1985). IgA nephropathy : perspectives on pathogenesis and classification. Clinical Nephrology, 24, 161-179.

ERICSSON, J.L.E. and TRUMP, B.F. (1969). Electron microscopy of the uriniferous tubules in "The Kidney", Volume I. Eds. Rouiller, C. and Muller, A.F. (Academic Press, New York and London), pp. 351-447.

EVAN, A.P., HAY, D.A. and DAIL, W.G. (1978). Scanning electron microscopy of the proximal tubule of the adult rabbit kidney. Anatomical Record, 191, 397-414.

FARQUHAR, M.G. (1975). The primary glomerular filtration barrier-basement membrane or epithelial slits. Kidney International, 8, 197-211.

FARQUHAR, M.G. and KANWAR, V.V. (1980). Characterization of anionic sites in the glomerular basement membranes of normal and nephrotic rats. In A. Leaf, G. Giebisch, L. Bolis and S. Gorin :(Eds), Renal Pathophysiology - Recent Advances, New York : Raven, p.57.

FARQUHAR, M.G. and PALADE, G.E. (1962). Functional evidence for the existence of a third cell type in the renal glomerulus. American Journal of Pathology, 13, 55-85.

FARQUHAR, M.G., WISSIG, S.C. and PALADE, G.E. (1961). Glomerular permeability. I. Ferritin transfer across the normal glomerular capillary wall. Journal of Experimental Medicine, 113, 47-66.

FARROW, B.R.H. and HUXTABLE, C.R.R. (1971). Membranous nephropathy and the nephrotic syndrome in the cat. Journal of Comparative Pathology, 81, 436-467.

FINCHER, M.G. and OLAFSON, P. (1934). Chronic diffuse glomerulonephritis in a horse. Cornell Veterinarian, 24, 356-360.

FLEUREN, G., GROND, J. and HOEDEMAEKER, P.J. (1980). In situ formation of subepithelial glomerular immune complexes in passive serum sickness. Kidney International, 17, 631-637.

FORD, P.M. and KOSATKA, I. (1979). In situ formation of antigen-antibody complexes in the mouse glomerulus. Immunology, 38, 473-479.

FRANDSON, R.D. (1981). "Anatomy and Physiology of Farm Animals", 3rd edition, pp. 373-389. (Lea and Febiger, Philadelphia).

FRIIS, C. (1980). Postnatal development of the pig kidney : ultrastructure of the glomerulus and the proximal tubule. Journal of Anatomy, 130, 513-526.

FUJITA, T., TOKUNAGA, J. and MIYOSHI, M. (1970). Scanning electron microscopy of the podocytes of renal glomerulus. Archivum Histologicum Japonicum, 32, 99-113.

GERLACH, J. (1845). Beitrage zur strukturlehre der niere. Archiv Anatomie Physiologie Wissenchaftliche Medicin, 379. (Cited by Potter, 1965).

GERMUTH, F.G. (1953). A comparative histologic and immunologic study in rabbits of induced hypersensitivity of the serum sickness type. Journal of Experimental Medicine, 97, 257-281.

GERMUTH, F.G., SENTERFIT, L.B. and POLLACK, A.D. (1967). Immune complex disease. I. Experimental acute and chronic glomerulonephritis.
Johns Hopkins Medical Journal, 120, 225-241.

GERMUTH, F.G., SENTERFIT, L.B. and DRESSMAN, G.R. (1972). Immune complex disease. V. The nature of the circulating complexes associated with glomerular alteration in the chronic BSA-rabbit system.
Johns Hopkins Medical Journal, 131, 344-357.

GERSH, L. (1937). The correlation of structure and function in the developing mesonephros and metanephros.
Contributions to Embryology, 26, 38-58.

GETTY, R. (1975). The anatomy of the domestic animals.
5th ed. W.B. Saunders Company, Philadelphia - London - Toronto.

GIDDENS, W.E., BOYCE, J.T., BLAKLEY, G.A. and MORTON, W.R. (1981). Renal disease in the pig-tailed Macaque (Macaca nemestrina). Veterinary Pathology, 18, 70-81.

GOLBUS, S. and WILSON, C.B. (1979). Experimental glomerulonephritis induced by in situ formation of immune complexes in glomerular capillary wall.
Kidney International, 16, 148-157.

GOTTSCHALK, C.W. and MYLLE, M. (1956). Micropuncture study of pressures in proximal tubules and peritubular capillaries of the rat kidney and their relation to uretral and renal venous pressure.
American Journal of Physiology, 185, 430-439.

GRAHAM, T. (1953). The pelvis and calyces of the kidneys of some mammals.
British Veterinary Journal, 109, 51-55.

GRAHAM, R.C. and KARNOVSKY, M.J. (1966). Glomerular permeability. Ultrastructural cytochemical studies using perioxidase as protein tracers.
Journal of Experimental Medicine, 124, 1123-1133.

GROBSTEIN, C. (1957). Some transmission characteristics of the tubule influence on mouse metanephrogenic mesenchyme.
Experimental Cell Research, 13, 575-587.

GRUENWALD, P. (1952). Development of the excretory system.
Annals New York Academy Sciences, 55, 142-146.

GUTTMAN, P.H. and ANDERSON, A.C. (1968). Progressive intercapillary glomerulosclerosis in aging and irradiated beagles. Radiation Research, 35, 45-60.

HALL, B.V. (1953). Studies of normal glomerular structure. In Proceedings of the Fifth Annual Conference of the Nephrotic Syndrome, New York; National Nephrosis Foundation, pp. 1-40.

HALL, B.V. (1954). Further studies of the normal structure of the renal glomerulus. Proceedings of the 6th Annual Conference of the Nephrotic Syndrome, Cleveland, Nov. 5-6. National Nephrosis Foundation, New York, pp. 1-39.

HALL, B.V. and ROTH, L.E. (1956). Preliminary studies on development and differentiation of cells and structures of renal corpuscles. Proceedings of Stockholm Conference on Electron Microscopy, Almqvist and Wiksells International Booksellers. (Cited Potter, 1965).

HAY, D.A. and EVAN, A.P. (1979). Maturation of the glomerular visceral epithelium and capillary endothelium in the puppy kidney. Anatomical Record, 193, 1-22.

HERRING, P.T. (1900). The development of the Malpighian bodies of the kidney, and its relation to pathological changes which occur in them.
Journal of Pathology and Bacteriology, 6, 459-496.

HUCKER, H. and FRENZEL (1975). Scanning electron microscopy of the distal nephron and calyx of the human kidney. Virchows Archives B Cell Pathology, 18, 157-164.

JONES, B.D. (1963). The nature of scar tissue in glomerulonephritis. American Journal of Pathology, 42, 185-200.

JONES, B.D. (1969). Mucosubstance of the glomerulus. Laboratory Investigation, 21, 119-125.

JONES, B.D., MULLER, C.B. and MENEFEE, M. (1962). The cellular and extra-cellular morphology of the glomerular stalk. American Journal of Pathology, 41, 373-388.

JORGENSEN, F. and BENTZON, M.W. (1968). The ultrastructure of the normal human glomerulus. Thickness of glomerular basement membrane. Laboratory Investigation, 18, 42-48.

KANWAR, Y.S. and FARQUHAR, M.G. (1979). Anionic sites in the glomerular basement membrane.
Journal of Cell Biology, 81, 137-155.

KARNOVSKY, M.J. and AINSWORTH, S.K. (1972). The structural basis of glomerular filtration. Advances in Nephrology, 2, 35-60.

KARNOVSKY, M.J. and RYAN, G.B. (1975). Substructure of the glomerular slit diaphragm in freeze-fractured normal rat kidney. Journal of Cell Biology, 65, 233-236.

KAZIMIERCZAK, J. (1963). Histochemical study of oxidative enzymes in rabbit kidney before and after birth. Acta Anatomica (Basel), 55, 352-369.

KAZIMIERCZAK, J. (1971). Development of the renal corpuscle and the juxtaglomerular apparatus. A light and electron microscopic study. Acta Pathologica et Microbiologica Scandinavica, Suppl. 218, 1-115.

KAZIMIERCZAK, J. (1978). Topography and structure of vasculature in developing cortex of rat kidney. Anatomy and Embryology, 153, 213-226.

KAZIMIERCZAK, J. (1980). A study by scanning (SEM) and transmission (TEM) electron microscopy of the glomerular capillaries in developing rat kidney. Cell and Tissue Research, 212, 241-255.

KITTELSON, J.A. (1917). The postnatal growth of the kidney of the albino rat, with observations on an adult human kidney. Anatomical Record, 13, 385-408.

KURTZ, S.M. (1958). The electron microscopy of the developing human renal glomerulus. Experimental Research, 14, 355-367.

LANGHAM, R.F. and HALLMAN, E.T. (1939). The kidney in health and disease. Journal of the American Veterinary Medical Association, 95, 22-32.

LARSSON, L. (1975). The ultrastructure of the developing proximal tubule in the rat kidney. Journal of Ultrastructure Research, 51, 119-139.

LARSSON, L. and MAUNSBACH, A.B. (1975). Differentiations of the vacuolar apparatus in cells of the developing proximal tubule in the rat kidney. Journal of Ultrastructure Research, 53, 254-270.

LATTA, H. (1970). The glomerular capillary wall.
Journal of Ultrastructure Research, 32, 526-544.

LATTA, H. (1973). Ultrastructure of the glomerulus and juxtaglomerular apparatus. In Handbook of Physiology, Section 8, Renal Physiology. J. Orloff and R. Berliner, eds. William and Wilkins Company, Baltimore, pp. 1-29.

LATTA, H. and FLIGIEL, S. (1985). Mesangial fenestrations, sieving, filtration and flow.
Laboratory Investigation, 52, 591-598.

LATTA, H. and JOHNSTON, W.H. (1976). The glycoprotein inner layer of glomerular capillary basement membrane as a filtration barrier.
Journal of Ultrastructure Research, 57, 65-67.

LATTA, H., BARAJAS, L., JACKSON, J.D. and COOK, M.L. (1962). The significance of the mesangial region of glomeruli.
Fifth International Congress for Electron Microscopy.
Academic Press Inc. III. Fifth Avenue, New York, U.S.A.

LE FURGEY, A. and TISHER, C.C. (1979). Morphology of the rabbit collecting duct.
American Journal of Anatomy, 155, 111-124.

LERNER, R.A. and DIXON, F.J. (1966). Spontaneous glomerulonephritis in sheep.
Laboratory Investigation, 15, 1279-1289.

LERNER, R.A., GLASSOCK, R.J. and DIXON, F.J. (1967). The role of the anti-glomerular basement membrane antibody in the pathogenesis of human glomerulonephritis.
Journal of Experimental Medicine, 126, 989-1004.

LERNER, R.A., DIXON, F.J. and LEE, S. (1968). Spontaneous glomerulonephritis in sheep. II. Studies on natural history, occurrence in other species and pathogenesis.
American Journal of Pathology, 53, 501-512.

LJUNGQVIST, A. (1963). The intrarenal arterial pattern in the normal and diseased human kidney.
Acta Medica Scandinavica Supplements, 401, 1-38.

LOH, S.W. (1970). Studies on urinary proteins in the pig with particular reference to the immunoglobulins.
Thesis. University of Bristol, U.K.

LOH, S.W., BOURNE, F.J., and CURTIS, J. (1972). Urine protein levels in the pig. Animal Production, 15, 273-283.

LUCKE, V.M. (1982). Glomerulonephritis in the cat. Veterinary Annual, pp. 270-278. Bristol : Scientechnica.

MACHIELSEN, P. and CREEMERS, J. (1967). The structure and function of the glomerular mesangium in "Ultrastructure in Biological Systems", Volume 2. Edited by Dalton, A.J. and Haguenan, F. (New York Academic Press Inc.), pp. 57-72.

MALPIGHI, M. (1669). De viscerum structura. (Cited by Mueller and Syracuse, 1958).

MARKHAM, R.V. Jr., SUTHERLAND, J.C. and MARDINEY, M.R. Jr. (1973). The ubiquitous occurrence of immune complex localisation in the renal glomeruli of normal mice. Laboratory Investigation, 29, 111-120.

MARTINSSON, K. (1972). Studies on the proteinuria of newborn piglets with special reference to IgG fragments. Acta Veterinaria Scandinavica, 13, 87-95.

MARTIN-DUPONT, P. and CAMBER, J. (1981). Mise en evidence, dans le cortex de rein de porc, de deux populations glomerulaires distinctes par technique de tamisage. Compte Rendu Seances Societe Biologie, 175, 787-791.

MAUNSBACH, A.B. (1964). Ultrastructure of different segments within the rat renal proximal tubule. Anatomical Record, 148, 387.

MAUNSBACH, A.B. (1966). Observations on the segmentation of the proximal tubule in the rat kidney. Comparison of results from phase contrast, fluorescence and electron microscopy. Journal of Ultrastructure Research, 16, 239-258.

MAUNSBACH, A.B. (1973). Ultrastructure of the proximal tubule. In Handbook of Physiology, Section B, Renal Physiology. J. Orloff and R.W. Beriner, eds. Williams and Wilkins Company, Baltimore, pp. 31-79.

MAYER, E. and OTTELENGHI, L.A. (1947). Protrusion of the tubular epithelium into the space of Bowman's capsule in the kidneys of dogs and cats. Anatomical Record, 99, 477-509.

McCLUSKY, R.T. (1971). The value of immunofluorescence in the study of human renal disease. Journal of Experimental Medicine, 134, 242-264.

McGRATH, J.P.M., DUNCAN, J.R. and MUNNELL, J.F. (1975). Crotalaria spectabilis toxicity in swine : characterisation of the renal glomerular lesion. Journal of Comparative Pathology, 85, 185-194.

McGREGOR, L. (1929). The fine histology of the normal glomerulus. American Journal of Pathology, 5, 545-558.

McMANUS, J.F.A. (1948). Structure of the glomerulus of the human kidney. American Journal of Pathology, 24, 1259-1265.

MICHELL, A.R. (1983). Physiology of the mammalian kidney in "Veterinary Nephrology", edited by Hall, L.W. (Heinemann Veterinary Books).

MOORE, R.A. (1931). The total number of glomeruli in the normal human kidney. Anatomical Record, 48, 153.

MUELLER, C.B. and SYRACUSE, N.Y. (1958). The structure of the renal glomerulus. American Heart Journal, 55, 304-322.

MUELLER-PEDDINGHAUS, R. and TRAUTWEIN, G. (1977). Spontaneous GN in dogs. I. Classification and immunopathology. Veterinary Pathology, 14, 1-13.

MUELLER, C.B., MASON, A.D. and STOUT, D.G. (1955). Anatomy of the glomerulus. American Journal of Medicine, 18, 267-276.

MURAKAMI, T. (1972). Vascular arrangement of the rat renal glomerulus. A scanning electron microscope study of corrosion casts. Archivum Histologicum Japonicum, 34, 87-107.

MURAKAMI, T., MIYOSHI, M. and FUJITA, T. (1971). Glomerular vessels of the rat kidney with special reference to double efferent arterioles. A scanning electron microscope study of corrosion casts. Archivum Histologicum Japonicum, 33, 179-198.

MURRAY, M. and WRIGHT, N.G. (1974). A morphologic study of canine glomerulonephritis. Laboratory Investigation, 30, 210-221.

MYERS, C.H., BULGER, R.E., RISHER, C.C. and TRUMP, B.F. (1966). Human renal ultrastructure IV. Collecting duct of healthy individuals. Laboratory Investigation, 15, 1357-1394.

NASH, M.A. and EDELMANN, C.M. (1973). The developing kidney. Nephrology, 11, 71-90.

NICKEL, R., SCHUMMER, A., SEIFERLE, E. and SACK, W. (1979). The viscera of the domestic animals. 2nd edition. (Berlin Verleg Paul Parey) pp. 295-298.

NOVIKOFF, A.B. (1960). The rat kidney : Cytochemical and electron microscopic studies. In E.L. Quinn and E.H. Kass (Eds.) Henry Ford Hospital International Symposium on Biology of Pyelonephritis. Boston : Little, Brown.

OBERLING, C. and HATT, P.Y. (1960). Study of the juxtaglomerular apparatus of the rat using the electron microscope. Annales Anatomie Pathologie (Paris), 5, 441-474.

OSBORNE, C.A. and VERNIER, R.L. (1973). Glomerulonephritis in the dog and cat. A comparative review. Journal of the American Animal Hospital Association, 9, 101-127.

OSBORNE, C.A., HAMMER, R.F., STEVENS, J.B., RESNICK, J.S. and MICHAEL, A.F. (1977). The glomerulus in health and disease: A comparative review of domestic animals and man. Advances in Veterinary Sciences and Comparative Medicine, 21, 207-285.

OSVALDO-DECIMA, L. (1973). Ultrastructure of the lower nephron. In Handbook of Physiology, Section 8. Renal Physiology. J. Orloff and R.W. Beriner, eds. Williams and Wilkins Company, Baltimore.

OSVALDO, L. and LATTA, H. (1966). The thin limbs of the loop of Henle. Journal of Ultrastructure Research, 15, 144-168.

PEASE, D.C. (1955). Fine structures of the kidney seen by electron microscopy. Journal of Histochemistry and Cytochemistry, 3, 295-308.

PEASE, D.C. and BAKER, R. (1950). Electron microscopy of the kidney. American Journal of Anatomy, 87, 349-389.

PECIFFER, E.W. (1968). Comparative anatomical observations of the mammalian renal pelvis and medulla. Journal of Anatomy, 102, 321-331.

PETER, K.I. (1927). Die Nierenkanalchen des Menschen und einiger saugetiere. In : Untersuchungen Uber Bau und Entwicklung der Niere. Jenaische Zeitschrift Naturwissenschaft, pp. 1-358.

POPLEWSKI, R. (1947). Anatomic Saakow Warszawa, 4, p.195.

POSKITT, T.R., FORTWENGLER, H.P., BABROW, J.C. and ROTH, G.J. (1974). Naturally occurring immune complex glomerulonephritis in monkeys (Macaca Irus). American Journal of Pathology, 76, 145-159.

POTTER, E.L. (1965). Development of human glomerulus. Archives of Pathology, 80, 241-255.

QUIESSER, G. and DROMMER, W. (1982). Mesangium in rats after E-coli urotoxin shock: A morphometric and light microscopic analysis. Veterinary Pathology, 19, 294-304.

REINHOFF, W.F. (1922). Development and growth of metanephros or permanent kidney in chick embryos. Bulletin : Johns Hopkins Hospital, 33, 392-406.

RENNKE, H.G., GOTRAN, R.S. and VENKATACHALAM, M.A. (1975). Role of molecular charge in glomerular permeability. Tracer studies with cationized ferritins. Journal of Cell Biology, 67, 638-646.

RHODIN, J. (1955). Electron microscopy of the glomerular capillary wall. Experimental Cell Research, 8, 572-574.

RHODIN, J. (1958). Anatomy of kidney tubules. International Review of Cytology, 7, 485-534.

RHODIN, J. (1962). The diaphragm of capillary endothelial fenestrations. Journal of Ultrastructure Research, 6, 171-185.

RIBBERT, H. (1900). Ueber die Entwicklung der bleidenden Niere und Uber die Entstchung der cystenniere. Verhandlungen Deutschen Pathologischen Gesellschaft, 2, 187-203.

ROUILLER, C.H. (1969). General anatomy and histology of the kidney in "The Kidney", Volume I. Eds. Rouiller, C. and Muller, A.F. (Academic Press, New York and London), pp. 61-156.

RYAN, G.B., COGHLAN, J.P. and SCOGGINS, B.A. (1979). The granulated peripolar epithelial cell: a potential secretory component of the renal juxtaglomerular complex. Nature, 277, 655-656.

SABINS, S.G., GUNSON, D.E. and ANTONOVYCH, T.T. (1984). Some unusual features of mesangio-proliferative glomerulonephritis in horses. Veterinary Pathology, 21, 574-581.

SCHACHOWA, S. (1879). Unter suchungen uber die Nieren Dissertation, Bern, Stampli. (Cited by Le Furgey and Tisher, 1979).

SCHREINER, K.E. (1902). Uber die Entwicklung der Amniotenniere. Zeitschrift Wissenschaftliche Zoologie, 71, 1-188.

SCHREINER, G.F., COTRAN, R.S. and UNANUE, E.R. (1981). Glomerular cell types and immune function. In Proceedings of 8th International Congress on Nephrology, Athens, pp. 858-864.

SHIROTA, K., NOMURA, Y. and SAITO, Y. (1984). Spontaneous swine glomerulonephritis in littermates from a leukemic sow. Veterinary Pathology, 21, 158-163.

SIEGEL, F.L., PENDERGRASS, R. and BULGER, R.E. (1974). Kidney morphology studied by scanning electron microscopy. Laboratory Investigation, 30, 410.

SIMON, G.T. and CHATELANAT, F. (1969). Ultrastructure of the normal and pathological glomerulus in "The Kidney", Volume I. Eds. Rouiller, C. and Muller, A.F. (Academic Press, New York and London), pp. 324-336.

SISSON, S. (1975). Porcine urogenital system in Sisson and Grossman's "The Anatomy of the Domestic Animals", 5th edition. Edited by Getty, R. (W.B. Saunders Company, Philadelphia, London, Toronto), pp. 937-954.

SLAUSON, D.O. and LEWIS, R.M. (1979). Comparative pathology of glomerulonephritis in animals. Veterinary Pathology, 16, 135-164.

SMITH, J.P. (1956). Anatomical features of the human renal glomerular efferent vessel. Journal of Anatomy, 90, 290-292.

SPINELLI, F. (1974). Structure and development of the renal glomerulus as revealed by scanning electron microscopy. International Review of Cytology, 39, 345-378.

SPINELLI, F. (1976). Structure and development of the renal glomerulus as revealed by scanning electron microscopy. International Review of Cytology, 39, 345-381.

SPINELLI, F.R., WIRZ, H., BRUCHER, Ch. and PEHLING, G. (1972). Non-existence of shunts between afferent and efferent arterioles of juxtamedullary glomeruli in dog and rat kidney. Nephron, 9, 123-128.

SQUIRE, R.A. (1968). Equine infections anaemia : a model of immunoproliferative disease. Blood, 32, 157-169.

SRAER, J., FORDART, J., CHANSEL, D., MAHIEU, P. and ARDAILLOUR (1980). Prostaglandin synthesis by rat isolated glomeruli and glomerular cultured cells. International Journal of Biochemistry, 12, 203-220.

STEIN, H.D., FEDERGREEN, W., KASHGARIAN, M. and STERZEL, R.B. (1983). The role of angiotensin II - induced renal functional changes in mesangial deposition of exogenous ferritin in rats. Laboratory Investigation, 49, 270-280.

STRIKER, G.E., KILLEN, P.D. and FARIN, F.M. (1981). Mesangial matrix and inflammatory cells. In Proceedings of the 8th International Congress on Nephrology, Athens, Greece, pp. 879-887.

SUTHERLAND, J.C., MARKHAM, R.V. Jr. and MARDINEY, M.R. (1974). Subclinical immune complexes in the glomeruli of kidneys postmortem.
American Journal of Medicine, 57, 536-541.

SUZUKI, Y. (1959). An electron microscopy of the renal differentiation. II. Glomerulus. Keio.
Journal of Medicine, 8, 129-142.

SUZUKI, Y. and MOSTOFFI, F.K. (1967). Intramitochondrial filamentous bodies in the thick limb of Henle of the rat kidney. Journal of Cell Biology, 33, 605-623.

SUZUKI, Y., CHURG, J., GRISHMAN, E., MAUTNER, W. and DACHS, S. (1963). The mesangium of the renal glomerulus. Electron microscopic studies of pathologic alterations.
American Journal of Pathology, 43, 555-578.

THOENES, W. (1967). Endoplasmatisches retikulum und "Sekretkirper" im glomerulum - peithel der saugerniere. Ein morphologischer beitray zum problem der basal membran-bildung. Zeitschrift fur Zellforschung Mikrosh Anatomy, 78, 561-582.

THOENES, W. and LANGER, K.H. (1969). Relationship between cell structures of renal tubule and transport mechanisms.
In : "Renal Transport and Diuretics". K. Thuran and H. Kahmarker, eds. Springer-Velag, Berlin, pp. 37-64.

TISHER, C.C. (1981). Anatomy of the kidney in "The Kidney". Edited by Brenner, B.M. and Rector, F.C. 2nd Edition.
(W.B. Saunders Company), pp. 3-76.

TISHER, C.C., BULGER, R.E. and TRUMP, B.F. (1966). Human renal ultrastructure I. Proximal tubule of healthy individuals. Laboratory Investigation, 15, 1357-1394.

TISHER, C.C., BULGER, R.E. and TRUMP, B.F. (1968). Human renal ultrastructure III. The distal tubule.
Laboratory Investigation, 18, 655-668.

TISHER, C.C., ROSEN, S. and OSBORNE, G.B. (1969). Ultrastructure of the proximal tubule of the rhesus monkey kidney. American Journal of Pathology, 56, 469-518.

TRABUCCO, A. and MARQUEZ, F. (1952). Structure of the glomerular tuft. Journal of Urology, 67, 235-255.

TRUMP, B.F. and BENDITT, E.P. (1962). Electron microscopic studies on human renal disease. Observations of normal visceral glomerular epithelium and its modifications in disease. Laboratory Investigation, 11, 753-781.

TRUMP, B.F. and BULGER, R.E. (1968). The morphology of the kidney in "The Structural Basis of Renal Disease". Edited by Becker, E.L. and Ellis, J. (Harper, Hoebar, New York).

VAN DAMME, B.J.C., FLEUREN, G.J., BAKKER, W.W., VERNIER, R.L. and HOEDEMAEKER, P.T. (1978). Experimental glomerulonephritis in the rat induced by antibodies directed against tubular antigens: IV. Fixed glomerular antigens in the pathogenesis of hetrologous immune complex glomerulonephritis. Laboratory Investigation, 38, 502-510.

VENKATACHALAM, M.A. and RENNKE, H.G. (1978). The structural and molecular basis of glomerular filtration. Circulation Research, 43, 337-347.

VERNIER, R.L. and BIRCH-ANDERSEN, A. (1962). Studies of the human fetal kidney. I. Development of the glomerulus. Journal of Pediatrics, 60, 754-768.

VERNIER, R.L. and BIRCH-ANDERSEN, A. (1963). Studies of the human fetal kidney. II. Permeability characteristics of the developing glomerulus. Journal of Ultrastructure Research, 8, 66-88.

VIMTRUP, B.J. (1928). On the number, shape, structure and surface area of the glomeruli in the kidneys of man and mammals. American Journal of Anatomy, 41, 123-151.

WALDVOGEL, A., WILD, P. and WEGMANN, C.H. (1983). Membranoproliferative glomerulonephritis in a horse. Veterinary Pathology, 20, 500-503.

WALKER, F. (1973). The origin, turnover and removal of glomerular basement membrane. Journal of Pathology, 110, 233-244.

WALKER, A.M. and OLIVER, J. (1941). Methods for the collection of fluid from single glomeruli and tubules of the mammalian kidney. American Journal of Physiology, 134, 562-579.